

# ***Coaxial electrospinning of reversibly thermochromic fibres***

**Ilana Malherbe**

Thesis presented in partial fulfilment of the requirements for the degree of  
Master of Science (Polymer Science)



University of Stellenbosch

**Study Leaders:**

Prof. R.D. Sanderson

Dr. A.E. Smit

December 2009

## DECLARATION

By submitting this thesis electronically, I declare that the entirety of the work contained therein is my own, original work, that I am the owner of the copyright thereof (unless to the extent explicitly otherwise stated) and that I have not previously in its entirety or in part submitted it for obtaining any qualification.

Signature: .....

Date: December 2009

## ABSTRACT

---

A novel method, herein referred to as 'solvent facilitated coaxial electrospinning', was used to produce reversibly thermochromic core-shell fibres with poly(methyl methacrylate) (PMMA) as shell and a thermochromic dye composite as core. The thermochromic dye composite consisted of combinations of 1-dodecanol, bisphenol A (BPA) and crystal violet lactone (CVL). In the 'solvent facilitated coaxial electrospinning' method, the thermochromic dye composite was dissolved in a suitable 'facilitating solvent' prior to spinning, instead of being spun into the fibres from the melt as previously described in literature. A low interfacial tension between the core and shell liquids, which is beneficial to effective core entrainment, was achieved by using a correctly chosen core 'facilitating solvent'. The PMMA was dissolved to form the shell spinning liquid and by selecting the correct core and shell solvents, spinneret blockage and precipitation due to core and shell liquid interactions were eliminated. High molar mass PMMA was used to produce fibres with diameters in the range of 3–10  $\mu\text{m}$  (larger than typical electrospun fibres) in order to minimize light scattering and subsequently allow visual observation of the thermochromic transitions, unlike the fibres that were produced in literature. The fibres were analyzed using SEM, TEM, TGA and DSC to investigate fibre morphology, dye composite thermal transition and fibre composition. Physical and chemical interactions between the thermochromic dye composite and the PMMA shell were identified as possible causes of differences between the thermochromic transition temperatures of the core-shell fibres and the bulk dyes, as well as of the instability of the colour developed state of certain thermochromic fibres. The spatial confinement of the dye composite inside the fibres and the extensive volume reduction (from bulk dye to small volume inside the fibres) affected the thermochromic behaviour of the thermochromic composite once it was entrained in the fibres. An excess BPA was used in the dye composition to allow the production of reversibly thermochromic fibres with a stable colour developed state.

## OPSOMMING

---

A nuwe metode, hierin beskryf as 'oplosmiddel gefasiliteerde koaksiale elektrospinnery', is gebruik om omkeerbare termochromiese kern-skil vesels met polie(metiel metakrilaat) (PMMA) as skil en 'n saamgestelde termochromiese kleurmiddel as kern te vervaardig. Die saamgestelde termochromiese kleurmiddel het bestaan uit kombinasies van 1-dodekanol, bisfenol A (BPA) en kristal violet laktoon (CVL). Vir die 'oplosmiddel gefasiliteerde koaksiale elektrospin'-metode, is die saamgestelde termochromiese kleurmiddel opgelos in 'n gepaste 'fasiliterende oplosmiddel' voordat dit geëlektrospin is, eerder as om dit te smelt om dit sodoende in vesels te kan inspin soos beskryf in die literatuur. 'n Lae raakvlakspanning tussen die kern- en skilspinvloeistowwe, wat voordelig is vir doeltreffende kern insluiting, is bereik deur gebruik te maak van sorgvuldig verkose 'fasiliterende oplosmiddels' vir die kern. Die PMMA is opgelos om die skilspinoplossing te vorm en, deur die keuse van die korrekte kern- en skiloplosmiddels, kon spinneret blokkasie en neerslag van die polimeer as gevolg van kern- en skilvloeistofinteraksies elimineer word. Hoë molekulêre massa PMMA is gebruik om vesels te vervaardig met deursnee in die omtrek van 3–10  $\mu\text{m}$  (groter as tipiese elektrogespinde vesels) om sodoende lig-verstrooiing te verminder en daardeur visuele waarneming van die termochromiese oorgange moontlik te maak, in teenstelling met die vesels wat in die literatuur gevorm is. Die vesels is ge-analiseer met SEM, TEM, TGA en DSC om veselmorfologie, termiese omskakelinge van saamgestelde kleurmiddels en veselsamestelling te bestudeer. Fisiese en chemiese interaksies tussen die saamgestelde termochromiese kleurmiddel kern en die PMMA skil is geïdentifiseer as moontlike oorsake van verskille tussen die termochromiese oorgangstemperature van die kern-skil vesels en die kleurmiddels in grootmaat, asook van die onstabiliteit van die gekleurde toestand van sommige termochromiese vesels. Die ruimtelike inperking van die saamgestelde kleurmiddel binne in die vesels asook die beduidende volume verkleining (van grootmaat kleurmiddel tot klein volume binne in die vesels) het die termochromiese gedrag van die saamgestelde kleurmiddel binne die vesels beïnvloed. 'n Oormaat BPA is in die saamgestelde termochromiese kleurmiddel gebruik om die produksie van omkeerbaar termochromiese vesels met 'n stabiele gekleurde toestand toe te laat.



## ACKNOWLEDGEMENTS

---

I would like to express my sincere gratitude to my study leaders. Firstly, to Prof. Ron Sanderson, for taking me on as an MSc student and for every word of wisdom and encouragement. A very special thanks goes to Dr. Eugene Smit, for all his assistance, especially in editing this thesis and also for all his advice, guidance and encouragement throughout my MSc. Thank you, I have learnt so much from you.

To Miss Adine Gericke, thank you for organizing everything when I decided to return to Stellenbosch to continue my studies.

Thanks to all the staff at Polymer Science who were always willing to help when I needed anything; and also to Dr. Margie Hurndall for her assistance in the editing of this thesis.

To the electrospinning group, thank you Haydn, Abdu, Carla for your endless support. A special thanks to Haydn, for your patience in helping me get started and for all the helpful chats on our electrospinning problems.

Thanks to everyone who assisted me in the analyses of my samples, especially to Liesl Keulder for DSC and to Mohammed Jaffer (UCT) for TEM.

My gratitude goes out to the Department of Chemistry and Polymer Science, to the University of Stellenbosch and to the National Research Foundation for financial support.

A special thanks to my parents, for giving me the opportunity to study and for their support in everything I do. Thank you for your endless love, understanding and encouragement throughout my studies. To my sister, Tarien, thank you for always being willing to listen and for every bit of good advice. Thanks also to my brother and grandmother. Thank you all for being my strength.

Thanks to all my friends, especially Nadia, Elinzi, Annatjie, Eunice and Monika for listening and for being interested in the progress of my work. Thank you for believing in me and helping me to believe in myself again. Without your continuous support and loving hearts this would have been a much tougher journey.

Finally and most importantly, thanks to my heavenly Father who walks beside me and takes care of me every day of my life. All glory to God in heaven.

## TABLE OF CONTENTS

---

<i>List of Figures</i> .....	v
<i>List of Tables</i> .....	xii
<i>List of Abbreviations</i> .....	xiv
<i>List of Symbols</i> .....	xiv

---

### ***Chapter 1: Introduction and Objectives***

<b>1.1</b> Introduction.....	<b>1</b>
<b>1.2</b> Conventional electrospinning.....	<b>2</b>
<b>1.3</b> Coaxial electrospinning .....	<b>2</b>
<b>1.4</b> Thermochromic dyes.....	<b>2</b>
<b>1.5</b> Production of thermochromic core-shell fibres.....	<b>3</b>
<b>1.6</b> Aim and objectives.....	<b>4</b>
<b>1.7</b> Layout of thesis.....	<b>5</b>
<b>1.8</b> References.....	<b>6</b>

---

### ***Chapter 2: Historical and Theoretical Background***

<b>2.1</b> Thermochromic dyes.....	<b>8</b>
2.1.1 Background and introduction.....	8
2.1.2 Composition .....	9
2.1.3 Mechanistic considerations.....	11
<b>2.2</b> Electrospinning .....	<b>14</b>
2.2.1 Introduction and historical background.....	14
2.2.2 The electrospinning process.....	15
2.2.3 Solution properties.....	18
2.2.3.1 Viscosity (molecular weight and solution concentration).....	18
2.2.3.2 Surface tension .....	20
2.2.3.3 Conductivity.....	21
2.2.3.4 Dielectric effect of solvent.....	22
2.2.3.5 Vapour pressure of solvent.....	22
2.2.4 Process parameters.....	23

2.2.4.1	<i>Voltage</i>	23
2.2.4.2	<i>Feed rate</i>	24
2.2.4.3	<i>Collector</i>	24
2.2.4.4	<i>Spinneret orifice diameter</i>	25
2.2.4.5	<i>Tip-to-collector distance</i>	25
2.2.5	Ambient conditions	25
2.2.5.1	<i>Humidity</i>	25
2.2.5.2	<i>Temperature</i>	26
<b>2.3</b>	<b>Coaxial electrospinning</b>	<b>26</b>
2.3.1	Introduction and historical background	26
2.3.2	The coaxial electrospinning process	28
2.3.3	System designs	29
2.3.4	Parameter effects	31
2.3.5	Solution parameters	32
2.3.5.1	<i>Core-shell miscibility/immiscibility</i>	32
2.3.5.2	<i>Core and shell polymer and solvent compatibility</i>	33
2.3.5.3	<i>Viscosity of core and shell solutions</i>	34
2.3.5.4	<i>Concentration of the core and shell solutions</i>	35
2.3.5.5	<i>Conductivity and dielectric effect</i>	35
2.3.5.6	<i>Surface tension and interfacial tension</i>	36
2.3.5.7	<i>Solvent vapor pressure</i>	36
2.3.5.8	<i>Summary</i>	37
2.3.6	Process parameters	37
2.3.6.1	<i>Applied voltage and electric field strength</i>	37
2.3.6.2	<i>Core and shell flow rates</i>	39
2.3.6.3	<i>Core needle protrusion</i>	40
2.3.6.4	<i>Coaxial spinneret diameters</i>	40
2.3.7	Melt coaxial electrospinning	41
2.3.8	Electrospinning of thermochromic fibres	41
<b>2.4</b>	<b>References</b>	<b>42</b>

---

## **Chapter 3: Experimental**

<b>3.1</b>	<b>Preparation of core and shell solutions.....</b>	<b>51</b>
3.1.1	Core .....	51
3.1.1.1	<i>Thermochromic dye composition .....</i>	<i>51</i>
3.1.1.2	<i>Preparation method .....</i>	<i>52</i>
3.1.2	Shell .....	53
3.1.2.1	<i>Polymer systems.....</i>	<i>53</i>
3.1.2.2	<i>Preparation of solutions .....</i>	<i>55</i>
<b>3.2</b>	<b>Coaxial electrospinning .....</b>	<b>55</b>
3.2.1	Apparatus .....	55
3.2.2	Electrospinning setup and procedure .....	57
3.2.3	Collection of fibres .....	58
<b>3.3</b>	<b>Characterization techniques.....</b>	<b>59</b>
3.3.1	Viscosity.....	59
3.3.2	Surface tension.....	59
3.3.3	Electrical conductivity .....	59
3.3.4	Scanning electron microscopy (SEM) .....	59
3.3.5	Transmission electron microscopy (TEM) .....	60
3.3.6	Thermogravimetric analysis (TGA) .....	60
3.3.7	Differential scanning calorimetry (DSC) .....	60
3.3.8	Determination of thermochromic transition temperatures.....	61
<b>3.4</b>	<b>References.....</b>	<b>62</b>

---

## **Chapter 4: Results and Discussion – Part 1**

### ***Determination of Optimal Core and Shell Materials and Spinning Liquid Compositions***

<b>4.1</b>	<b>Introduction.....</b>	<b>63</b>
<b>4.2</b>	<b>Initial thermochromic dye composition and core spinning liquid.....</b>	<b>63</b>
4.2.1	Thermochromic dye composite and evaluation of its thermochromic transition .....	63
4.2.2	Core spinning liquid formulation.....	65
4.2.2.1	<i>Molten thermochromic composite as core spinning liquid .....</i>	<i>65</i>
4.2.2.2	<i>Dissolved thermochromic composite as core spinning liquid .....</i>	<i>65</i>

<b>4.3</b>	<b>Shell polymer solution composition and coaxial electrospinning.....</b>	<b>66</b>
4.3.1	Summary of polymer and solvent combinations .....	67
4.3.2	Evaluation of cellulose acetate as possible shell forming polymer .....	70
4.3.2.1	<i>CA concentration and acetone:dioxane solvent ratio studies.....</i>	<i>70</i>
4.3.2.2	<i>Proof of thermochromic composite entrainment and investigations into reasons for the absence of thermochromic transition .....</i>	<i>74</i>
4.3.3	Evaluation of poly(methyl methacrylate) as possible shell forming polymer .....	86
4.3.3.1	<i>PMMA concentration and solvent ratio studies.....</i>	<i>86</i>
4.3.3.2	<i>Investigation and elimination of the pale blue base colour.....</i>	<i>96</i>
<b>4.4</b>	<b>Optimization of thermochromic dye composition.....</b>	<b>98</b>
<b>4.5</b>	<b>Summary .....</b>	<b>101</b>
<b>4.6</b>	<b>References.....</b>	<b>102</b>

---

## **Chapter 5: Results and Discussion – Part 2**

### *Production and Analysis of Thermochromic Core-Shell Fibres*

<b>5.1</b>	<b>Introduction.....</b>	<b>104</b>
<b>5.2</b>	<b>Coaxial electrospinning of thermochromic fibres.....</b>	<b>104</b>
5.2.1	Evaluation of PMMA concentration and chloroform:ethanol solvent ratio in shell solutions .....	105
5.2.2	Evaluation of increased BPA content in thermochromic composition.....	110
<b>5.3</b>	<b>Analytical investigation of thermochromic transition .....</b>	<b>114</b>
5.3.1	Compositional analyses using TGA.....	115
5.3.2	Visual determination of thermochromic transition temperatures.....	119
5.3.3	Thermal analysis using DSC .....	121
<b>5.4</b>	<b>Summary .....</b>	<b>127</b>
<b>5.5</b>	<b>References.....</b>	<b>128</b>

---

## **Chapter 6: Conclusions and Recommendations**

<b>6.1</b>	<b>Conclusions.....</b>	<b>129</b>
<b>6.2</b>	<b>Recommendations for future work.....</b>	<b>133</b>

---

<b>Appendix.....</b>	<b>135</b>
----------------------	------------

## LIST OF FIGURES

---

### **Chapter 2**

Figure 2.1	Molecular structures of the ring-closed and ring-opened states of CVL ..	12
Figure 2.2	Basic mechanism of the thermochromic leuco dye (e.g. CVL) system .....	12
Figure 2.3	Schematic illustration of the basic electrospinning setup .....	16
Figure 2.4	Schematic illustration of the first, second and third stages of bending instability of a Taylor cone .....	17
Figure 2.5	The difference between beaded and smooth fibres due to the effect of surface tension .....	21
Figure 2.6	Flow pattern in a compound droplet attached to a core-shell spinneret (PAN solution as shell and PMMA solution dyed with malachite green as core).....	28
Figure 2.7	Coaxial electrospinning setup .....	30
Figure 2.8	Flow chart summarizing the coaxial electrospinning parameters .....	32
Figure 2.9	Schematic of the voltage dependence of core-shell fibre formation in coaxial electrospinning (A: subcritical voltage; B: critical voltage; C: supercritical voltage) .....	38

---

### **Chapter 3**

Figure 3.1	Images depicting the coaxial spinneret used in this study: (a) photograph; (b) schematic showing the coaxial capillaries; and (c) schematic of the spinneret with a luer lock attached to the shell capillary .....	56
Figure 3.2	Schematic of coaxial electrospinning setup used .....	57
Figure 3.3	Schematic of a rotating wire drum collector.....	58

---

### **Chapter 4**

Figure 4.1	Photographs showing the colour change of the 50:3:1 dodecanol:BPA:CVL (molar ratio) bulk thermochromic dye composite over a range of temperatures.....	64
Figure 4.2	SEM images of fibres produced by single electrospinning from a) 11 wt% CA in acetone:dioxane (2:1 v/v) solution; and b) 17 wt% CA in acetone:dioxane (2:1 v/v) solution .....	71

Figure 4.3	SEM images of fibres produced by coaxial electrospinning using a) a shell spinning solution of 11 wt% CA in 2:1 v/v acetone:dioxane; and b) a shell spinning solution of 17 wt% CA in 2:1 v/v acetone:dioxane. The core spinning solution, in both cases, consisted of a 50:3:1 (molar ratio dodecanol:BPA:CVL) thermochromic composite dissolved 5:2 v/v in acetone .....	72
Figure 4.4	SEM images indicating core-shell morphology in fibres produced by coaxial electrospinning using a shell spinning solution of 14 wt% CA in 2:1 v/v acetone:dioxane, and a core spinning solution of thermochromic dye composite (50:3:1 molar ratio dodecanol:BPA:CVL) in acetone (5:3 v/v).....	72
Figure 4.5	Yarn of coaxially electrospun dye composite CA core-shell fibres.....	75
Figure 4.6	Core-shell fibres with thermochromic dye composite as core material (CA shell), before and after immersion in DCM.....	76
Figure 4.7	TEM images revealing the core-shell structures of fibres produced by coaxial electrospinning using a shell spinning solution of 14 wt% CA in 2:1 v/v acetone:dioxane; and a core solution of thermochromic dye composite (100:3:1 molar ratio dodecanol:BPA:CVL) dissolved in acetone (5:3 v/v).....	77
Figure 4.8	TGA thermogram for compositional analysis of dye composite core-shell fibres (core electrospinning solution: 50:3:1 dodecanol:BPA:CVL thermochromic composite dissolved 5:3 v/v in acetone; shell electrospinning solution: 14 wt% CA in 2:1 v/v dioxane:acetone) .....	79
Figure 4.9	DSC analysis of dodecanol (-----); dodecanol CA core-shell fibres (- - -) and pure CA fibres (- - - -).....	81
Figure 4.10	DSC plot of 50:3:1 dodecanol:BPA:CVL bulk thermochromic dye composite .....	82
Figure 4.11	DSC plot of dye composite CA core-shell fibres electrospun using a thermochromic composite with a molar ratio of 50:3:1 dodecanol:BPA:CVL .....	83
Figure 4.12	DSC plot of dye composite CA core-shell fibres electrospun using a thermochromic composite with a molar ratio of 100:3:1 dodecanol:BPA:CVL .....	85
Figure 4.13	SEM images showing the surface morphology of core-shell fibres coaxially electrospun using shell solutions of different concentrations of PMMA in 2:1 v/v acetone:dioxane solutions: a) 8 wt%; b) 10 wt%; c) 12 wt%; d) 15 wt%.....	87

Figure 4.14	Graph showing the increase in solution viscosity corresponding to increased polymer concentrations for PMMA solutions in 2:1 v/v acetone:dioxane .....	88
Figure 4.15	TEM images revealing the core-shell structures of fibres produced by coaxial electrospinning using a shell solution of 8 wt% PMMA in 2:1 v/v acetone:dioxane; and a core solution of thermochromic dye composite (50:3:1 molar ratio dodecanol:BPA:CVL) dissolved in acetone (5:3 v/v) ..	89
Figure 4.16	SEM images showing cross-sections and surface morphologies of core-shell fibres coaxially electrospun using shell solutions of different concentrations of PMMA in 1:1 v/v acetone:dioxane: a) 10 wt%; b) 10 wt% cross-section; c) 11 wt%; d) 12 wt%.....	91
Figure 4.17	SEM images showing the surface morphology of core-shell fibres coaxially electrospun using shell solutions of 12 wt% PMMA in 1:1:1 v/v/v acetone:THF:dioxane.....	94
Figure 4.18	SEM images showing the surface morphology of core-shell fibres coaxially electrospun using shell solutions of 12 wt% PMMA in 2:1:2 v/v/v acetone:THF:dioxane.....	94
Figure 4.19	TEM images revealing the core-shell structures of fibres produced by coaxial electrospinning using shell solutions of: a) 12 wt% PMMA in 2:1:2 v/v/v acetone:THF:dioxane, b) 12 wt% PMMA in 1:1:1 v/v/v acetone:THF:dioxane; and core solutions of thermochromic dye composite (50:3:1 molar ratio dodecanol:BPA:CVL) dissolved in acetone (5:3 v/v).....	95
Figure 4.20	Photographs showing the colour change of different bulk thermochromic dye composites (dodecanol:BPA:CVL molar ratio, with increasing dodecanol content) over a range of temperatures.....	99

## **Chapter 5**

Figure 5.1	SEM images showing (a) surface morphology (beaded) and (b) cross-section of thermochromic core-shell fibres (shell solution: 14 wt% PMMA, 3:1 v/v chloroform:ethanol; core liquid: 100:6:1 dodecanol:BPA:CVL, 5:2 v/v dye composite:chloroform).....	107
Figure 5.2	SEM images showing (a) surface morphology and (b) surface morphology of thermochromic core-shell fibres (shell solution: 14 wt% PMMA, 3:2 v/v chloroform:ethanol; core liquid: 100:6:1 dodecanol:BPA:CVL, 5:2 v/v dye composite:chloroform).....	108



Figure 5.3	SEM images showing surface morphology of thermochromic core-shell fibres (shell solution: 16 wt% PMMA, 3:1 v/v chloroform:ethanol; core liquid: 100:6:1 dodecanol:BPA:CVL, 5:2 v/v dye composite:chloroform).....	108
Figure 5.4	SEM images showing (a) surface morphology and (b) cross-section of thermochromic core-shell fibres (shell solution: 16 wt% PMMA, 3:2 v/v chloroform:ethanol; core liquid: 100:6:1 dodecanol:BPA:CVL, 5:2 v/v dye composite:chloroform).....	108
Figure 5.5	Photographs indicating the colour of the different dye compositions (dodecanol:BPA:CVL molar ratio) in bulk, over a range of temperatures.....	111
Figure 5.6	SEM images showing (a) surface morphology and (b) cross-section of thermochromic core-shell fibres (shell solution: 16 wt% PMMA, 3:2 v/v chloroform:ethanol; core liquid: 100:20:1 dodecanol:BPA:CVL, 5:2 v/v dye composite:chloroform).....	114
Figure 5.7	SEM images showing (a) surface morphology and (b) cross-section of thermochromic core-shell fibres (shell solution: 16 wt% PMMA, 3:2 v/v chloroform:ethanol; core liquid: 100:30:1 dodecanol:BPA:CVL, 5:2 v/v dye composite:chloroform).....	114
Figure 5.8	TGA profile for compositional analysis of thermochromic core-shell fibres fabricated from 100:6:1 molar ratio dodecanol:BPA:CVL thermochromic composite and 16 wt% PMMA (3:2 v/v chloroform:ethanol) solution...	116
Figure 5.9	TGA profile for compositional analysis of thermochromic core-shell fibres fabricated from 100:20:1 molar ratio dodecanol:BPA:CVL thermochromic composite and 16 wt% PMMA (3:2 v/v chloroform:ethanol) solution...	117
Figure 5.10	TGA profile for compositional analysis of thermochromic core-shell fibres fabricated from 100:30:1 molar ratio dodecanol:BPA:CVL thermochromic composite and 16 wt% PMMA (3:2 v/v chloroform:ethanol) solution...	117
Figure 5.11	Photographs showing the colour change over a range of temperatures for thermochromic dye, paper coatings. The thermochromic dyes were composed of 100:30:1 (top), 100:20:1 (middle) and 100:6:1 (bottom) molar ratios of dodecanol:BPA:CVL.....	119
Figure 5.12	Photographs showing the colour change over a temperature range for PMMA core-shell thermochromic fibres containing 100:30:1 (top), 100:20:1 (middle) and 100:6:1 (bottom) dodecanol:BPA:CVL dye composites.....	119
Figure 5.13	DSC analysis showing melting and solidification peaks of thermochromic dye composites with varied amounts of BPA.....	122

Figure 5.14	DSC analysis showing melting and solidification peaks of thermochromic core-shell fibres produced using thermochromic dye composites with varied amounts of BPA ..... 123
Figure 5.15	Graph of melting and solidification temperatures (from DSC analysis) for thermochromic dyes and fibres with varying BPA content..... 124

---

## **Appendix**

Figure A1	Overlay of TGA thermograms for dodecanol, BPA, CVL, CA and thermochromic core-shell fibres (core electrospinning solution: 50:3:1 dodecanol:BPA:CVL thermochromic composite dissolved 5:3 v/v in acetone; shell electrospinning solution: 14 wt% CA in 2:1 v/v dioxane:acetone) ..... 135
Figure B1	SEM images of electrospun Nylon 6,6 from: a) 16 wt% solution in formic acid; b) 20 wt% solution in formic acid; c) 30 wt% solution in formic acid; d) 35 wt% solution in formic acid; e) 40 wt% solution in formic acid ..... 136
Figure B2	SEM images of electrospun PVOH from: a) 8 wt% solution in distilled water; b) 10 wt% solution in distilled water; c) 12 wt% solution in distilled water ..... 137
Figure B3	SEM images of fibres from 8wt% PAN solutions in DMF: a) single solution electrospinning; b) coaxial electrospinning with 50:1:3 molar ratio dodecanol:CVL:BPA thermochromic dye composite dissolved 1:1 v/v in DMF ..... 137
Figure B4	SEM images of PMMA fibres coaxially electrospun from a solution in 2:1 v/v acetone:dioxane: a) 15 wt% with 100:3:1 molar ratio dodecanol:BPA:CVL (5:3 v/v dye composite:acetone) as core spinning liquid; b) 8 wt% with 50:3:1 molar ratio dodecanol:BPA:CVL (5:3 v/v dye composite:acetone) as core spinning liquid ..... 138
Figure B5	SEM images of PMMA fibres coaxially electrospun from a solution in chloroform: a) 15 wt% with 100:3:1 molar ratio dodecanol:BPA:CVL (5:3 v/v dye composite:acetone) as core spinning liquid; b) 8 wt% with 50:3:1 molar ratio dodecanol:BPA:CVL (5:3 v/v dye composite:acetone) as core spinning liquid ..... 138
Figure B6	SEM image of PMMA fibres coaxially electrospun from 8 wt% solution in 1:1 v/v THF:DMF with 50:3:1 molar ratio dodecanol:BPA:CVL (5:3 v/v dye composite:acetone) as core spinning liquid ..... 139
Figure B7	SEM images of PMMA fibres coaxially electrospun from a solution in 2:1 v/v acetone:DMF: a) 15 wt% with 143:3:1 molar ratio dodecanol:BPA:CVL (5:2 v/v dye composite:acetone) as core spinning liquid; b) 8 wt% with 50:3:1 molar ratio dodecanol:BPA:CVL (5:3 v/v dye composite:acetone) as core spinning liquid ..... 139

Figure B8	SEM image of PMMA fibres coaxially electrospun from 10 wt% solution in 3:2 v/v acetone:dioxane with 50:3:1 molar ratio dodecanol:BPA:CVL (5:3 v/v dye composite:acetone) as core spinning liquid.....	140
Figure B9	SEM images of PMMA fibres coaxially electrospun from a solution in 1:1 v/v acetone:dioxane: a) 11 wt% with 50:3:1 molar ratio dodecanol:BPA:CVL (5:3 v/v dye composite:acetone) as core spinning liquid; b) 12 wt% with 50:3:1 molar ratio dodecanol:BPA:CVL (5:3 v/v dye composite:acetone) as core spinning liquid.....	140
Figure B10	SEM image of PMMA fibres coaxially electrospun from a 12 wt% solution in MEK with 50:3:1 molar ratio dodecanol:BPA:CVL (5:3 v/v dye composite:acetone) as core spinning liquid.....	141
Figure B11	SEM images of PMMA fibres coaxially electrospun from 12 wt% solutions in a) 1:1 v/v acetone:MEK with 50:3:1 molar ratio dodecanol:BPA:CVL (5:3 v/v dye composite:acetone) as core spinning liquid; b) 3:1 v/v acetone:MEK with 50:3:1 molar ratio dodecanol:BPA:CVL (5:3 v/v dye composite:acetone) as core spinning liquid.....	141
Figure B12	SEM image of PMMA fibres coaxially electrospun from a 12 wt% solution in 1:1 v/v MEK:THF with 50:3:1 molar ratio dodecanol:BPA:CVL (5:3 v/v dye composite:acetone) as core spinning liquid.....	142
Figure B13	SEM images of PMMA fibres coaxially electrospun from a solution in 2:1 v/v acetone:dioxane: a) 12 wt% with 50:3:1 molar ratio dodecanol:BPA:CVL (5:3 v/v dye composite:acetone) as core spinning liquid; b) 10 wt% with 50:3:1 molar ratio dodecanol:BPA:CVL (5:3 v/v dye composite:acetone) as core spinning liquid.....	142
Figure B14	SEM images of PMMA fibres coaxially electrospun from 12 wt% solutions in a) 2:1:2 v/v/v acetone:THF:dioxane with 50:3:1 molar ratio dodecanol:BPA:CVL (5:3 v/v dye composite:acetone) as core spinning liquid; b) 1:1:1 v/v/v acetone:THF:dioxane with 50:3:1 molar ratio dodecanol:BPA:CVL (5:3 v/v dye composite:acetone) as core spinning liquid .....	143
Figure B15	SEM images of PMMA fibres coaxially electrospun from 12 wt% solutions in a) 1:1:2 v/v/v acetone:THF:dioxane with 50:3:1 molar ratio dodecanol:BPA:CVL (5:3 v/v dye composite:acetone) as core spinning liquid; b) 1:1 v/v acetone:THF with 50:3:1 molar ratio dodecanol:BPA:CVL (5:3 v/v dye composite:acetone) as core spinning liquid.....	143
Figure B16	SEM image of PMMA fibres coaxially electrospun from a 10 wt% solution in acetone with 50:3:1 molar ratio dodecanol:BPA:CVL (5:3 v/v dye composite:acetone) as core spinning liquid.....	144

Figure B17	SEM images of PMMA fibres coaxially electrospun from a) 14 wt% solutions in 3:1 v/v chloroform:acetone with 100:6:1 molar ratio dodecanol:BPA:CVL (5:2 v/v dye composite:chloroform) as core spinning liquid; b) 16 wt% solution in 1:1 v/v chloroform:acetone with 100:6:1 molar ratio dodecanol:BPA:CVL (5:2 v/v dye composite:chloroform) as core spinning liquid .....	144
Figure B18	SEM image of PMMA fibres coaxially electrospun from a 10 wt% solution in DMF with 50:3:1 molar ratio dodecanol:BPA:CVL (5:3 v/v dye composite:acetone) as core spinning liquid.....	145
Figure B19	SEM image of PMMA fibres coaxially electrospun from a 12 wt% solution in 3:1 v/v chloroform:ethanol with 30:3:1 molar ratio dodecanol:BPA:CVL (5:3 v/v dye composite:acetone) as core spinning liquid.....	145
Figure E1	Raman spectrum of PMMA powder: the arrows from left to right indicate the peaks at 1180 $\text{cm}^{-1}$ , 1342 $\text{cm}^{-1}$ and 1822 $\text{cm}^{-1}$ .....	149
Figure E2	Raman spectrum of PMMA fibres: the arrows from left to right indicate the peaks at 1180 $\text{cm}^{-1}$ , 1342 $\text{cm}^{-1}$ and 1822 $\text{cm}^{-1}$ .....	149
Figure E3	Raman spectrum of thermochromic PMMA core-shell fibres (core composition of 100:6:1 molar ratio dodecanol:BPA:CVL): the arrows from left to right indicate the peaks at 1180 $\text{cm}^{-1}$ , 1342 $\text{cm}^{-1}$ and 1822 $\text{cm}^{-1}$ .....	150
Figure E4	Raman spectrum of dodecanol .....	150
Figure E5	Raman spectrum of BPA.....	151
Figure E6	Raman spectrum of CVL .....	151

## LIST OF TABLES

---

### **Chapter 2**

Table 2.1	Core and shell (sheath) solution properties required for successful coaxial electrospinning .....	37
-----------	---	----

---

### **Chapter 3**

Table 3.1	Polymers and solvents used in this study.....	54
Table 3.2	Properties of solvents used in this study.....	55

---

### **Chapter 4**

Table 4.1	Summary of notable results for the selected polymer–solvent systems.....	68
Table 4.2	The effects of different acetone:dioxane v/v ratios in coaxial electrospinning experiments .....	73
Table 4.3	Comparison of average fibre diameters for single and core-shell fibres according to polymer concentration .....	75
Table 4.4	Approximate temperatures for onset of decomposition of core-shell fibre components .....	78
Table 4.5	TGA heating profile for compositional analysis of electrospun core-shell fibres .....	78
Table 4.6	Solution properties for a range of PMMA concentrations in 2:1 v/v acetone:dioxane .....	88
Table 4.7	Results of varying the dodecanol:CVL molar ratio of the thermochromic composite, while keeping the BPA:CVL molar ratio (3:1) constant .....	99
Table 4.8	Results of varying the dodecanol:CVL molar ratio of the thermochromic composite, while keeping the dodecanol:BPA molar ratio (50:3) constant ..	100

---

### **Chapter 5**

Table 5.1	Thermochromic composite and core spinning solution composition and properties .....	105
Table 5.2	PMMA shell solution combinations, properties and resulting core-shell fibre morphologies.....	105

Table 5.3	Process parameters for coaxial electrospinning experiments with PMMA (chloroform:ethanol) shell solutions .....	106
Table 5.4	Thermochromic dye compositions and spinning solution properties .....	112
Table 5.5	Process parameters for coaxial electrospinning experiments with thermochromic composites of increasing BPA content.....	113
Table 5.6	TGA heating profile for compositional analysis of core-shell thermochromic fibres .....	115
Table 5.7	Summary of TGA results (% weight loss) for thermochromic core-shell fibres .....	116

---

### ***Appendix***

Table C1	PMMA (weight percentages) and solvent combinations used as shell spinning solutions during coaxial electrospinning experiments .....	146
Table C2	Process and solution parameters of coaxial electrospinning experiments performed during PMMA concentration and solvent ratio studies .....	147
Table D1	Weight percentages of dye composite in the core spinning solutions.....	148

## LIST OF ABBREVIATIONS

---

BPA	Bisphenol A
CA	Cellulose acetate
CVL	Crystal violet lactone
DMF	Dimethylformamide
DSC	Differential scanning calorimetry
MEK	Methyl ethyl ketone
PAN	Polyacrylonitrile
PCM	Phase change material
PVOH	Poly(vinyl alcohol)
PMMA	Poly(methyl methacrylate)
rH	Relative humidity
SEM	Scanning electron microscopy
TEM	Transmission electron microscopy
TGA	Thermal gravimetric analysis
THF	Tetrahydrofuran
wt%	Weight percentage

## LIST OF SYMBOLS

---

$c$	Mass of polymer per unit volume
$\gamma$	Surface tension (mN/m)
kV	Kilovolt
$m$	Mass (g)
$M_e$	Molecular weight between entanglement points
$M_w$	Weight average molecular weight
$\rho$	Static resistivity ( $\Omega$ m)
$\rho$	Density (g/mL)
$\sigma$	Conductivity ( $\mu$ S/cm)
V	Volume (ml)

# ***Chapter 1***

## ***Introduction and Objectives***

### **1.1 Introduction**

The process of electrospinning, as well as the modified process of coaxial electrospinning, is important in the development of various new applications in a wide range of fields. Conventional electrospinning has been around for over a 100 years but renewed interest, in the form of both fundamental and applied research, have only come to the fore over the past 15 years or so (since the early 1990s).<sup>1</sup> Electrospinning has become a widely studied process. The process of coaxial electrospinning (to produce fibres with core-shell morphology), on the other hand, is relatively new and not that widely studied. Only a few established electrospinning groups, including that of Y. Xia (USA), G.C. Rutledge (USA), E. Zussman (Israel), S. Ramakrishna (Singapore) and J.H. Wendorff & A. Greiner (Germany) currently focus on this intricate technique. The focus of coaxial electrospinning projects in our group is mainly application oriented.

The coaxial electrospinning process is expected to have a significant impact for many applications in the future. Therefore, the development and better understanding of this process is important. Any study that would provide new insights into the process, especially with regard to interactions between core and shell electrospinning solutions, can be of value.

The inclusion into coaxially electrospun fibres, of compounds that are able to reversibly change colour in response to temperature (thermochromic effect) would be useful in terms of temperature sensing applications.<sup>2</sup> Thermochromic fibre based products are used for product labelling; medical and security applications; safety and quality control applications; and novelty applications such as stress testers, forehead thermometers and battery testers.<sup>3</sup>



## 1.2 Conventional electrospinning

Conventional electrospinning is a technique that produces ultrafine fibres, often referred to as nanofibres, by subjecting a polymer melt or solution to an electric field. Due to the small diameters (tens of nanometres to a few micrometres)<sup>4</sup> of electrospun fibres, both the surface area to volume ratio and the length to diameter ratio are greatly increased compared to that of conventional fibres.<sup>5,6</sup> These characteristics make nanofibres the material of choice in a variety of applications, including medical products, speciality textiles, composite-fibre-reinforcements, optics, microelectronics and filtration media.

## 1.3 Coaxial electrospinning

The process of coaxial electrospinning, as opposed to conventional electrospinning where a single needle and solution is used, enables the formation of fibres from separate and usually different core and shell materials. In this process concentric capillaries are used to produce fibres where a core material is entrained inside a shell material, along the length of the fibre.<sup>7</sup> These fibres are typically referred to as core-shell fibres.

Coaxial or core-shell electrospinning increases the options when it comes to adding and entraining substances into electrospun fibres. Coaxial electrospinning makes it possible to functionalize electrospun fibres by including functional molecules or objects into the core of the fibre structure, or by using different layers of materials that each provides a different property to the fibres.<sup>1,7</sup> Coaxial electrospinning is a useful technique for producing compound nanofibres with core materials that cannot be electrospun directly.<sup>8,9</sup>

## 1.4 Thermochromic dyes

In the manufacturing of thermochromic textile products, leuco type dyes are typically used. These dyes, in combination with other necessary components, are able to give reversibly thermochromic effects. The separate components that form part of the thermochromic dye composite have to be entrained together inside a protective shell. The shell or capsule forms a closed system that allows the reversible, thermochromic mechanism to be effective.<sup>10</sup>

In textile applications, thermochromic dyes are typically encapsulated in microcapsules and applied to the surface of textile substrates like pigments in a resin binder.<sup>3,11</sup> A downfall of microencapsulated thermochromic textile coatings is the poor wash colourfastness. This renders the thermochromic effect temporary.<sup>11</sup> A method that would allow direct entrainment of thermochromic dyes into fine fibres could provide a valuable alternative.

## 1.5 Production of thermochromic core-shell fibres

One way of isolating and directly entraining thermochromic dyes into fine fibres would be to mix the microcapsules with the spin melt and so incorporate it into conventional melt spun fibres.<sup>3</sup> The inclusion of microcapsules into the body of the fibres in this way, with the microcapsules dispersed in between the polymer molecules would, however, act like defects and weaken the fibres.<sup>12</sup> Inclusion of the thermochromic dye as core material in fibres with a solid polymer shell could be more appropriate. If these core-shell fibres were produced by electrospinning it could provide ultrathin fibres with increased surface to volume ratios. The increased surface area available for heat transfer, would increase the sensitivity and rate of colour switching.<sup>2</sup>

The small size of electrospun fibres means that commercially available, microencapsulated thermochromic dyes can not be incorporated into these fibres. The diameters of the microcapsules, varying in a batch between 1 and 50  $\mu\text{m}$ ,<sup>13</sup> are mostly larger than the typical size (around 100 nm to 1  $\mu\text{m}$ )<sup>14</sup> of electrospun fibres. The size of the microcapsules in a particular batch are not all the same, but vary between a certain range of values.<sup>13</sup> The components that make up the thermochromic dye, instead of being microencapsulated, would have to be directly entrained into the core of the electrospun fibres. The shell of the fibre would then form the layer that protects and keeps the components together.

Coaxial electrospinning provides the possibility of direct entrainment of the thermochromic dye composite into fibres. Melt coaxial electrospinning,<sup>15</sup> a type of coaxial electrospinning where the core material is kept in a molten state and the shell material is a polymer solution, has been used to produce ultrafine core-shell fibres with a thermochromic dye composite as

core material. However, the nanoscale diameters of these fibres resulted in light scattering, which made the colour change effect unobservable.<sup>2</sup>

Fibres of slightly larger diameter would be more suitable. Fibres with diameters of 1–10  $\mu\text{m}$  can be expected to eliminate the light scattering phenomenon whilst still giving a rapid colour switching response time.

In this study a novel method of producing core-shell thermochromic fibres by coaxial electrospinning is investigated wherein all dye components are dissolved in a suitable solvent to form a core liquid that does not need to be melted. This process is referred to as solvent facilitated coaxial electrospinning.

## **1.6 Aim and objectives**

The aim of this research project was to develop reversibly thermochromic core-shell fibres by using the coaxial electrospinning process. The main focus was on developing a solvent facilitated method. Emphasis was placed on selecting the appropriate electrospinning setup, selecting appropriate core and shell spinning compositions, investigating the process limiting parameters and analyzing the thermochromic effect of the thermochromic core-shell fibres.

The following objectives were set out at the start of this study:

- a) Select the suitable components and produce a reversibly thermochromic dye composite that can be used as core material in the coaxial electrospinning of thermochromic core-shell fibres
- b) Explore options and determine the most suitable composition for the core liquid that will be used in the coaxial electrospinning process
- c) Find a suitable polymer–solvent system from which the shell of the core-shell fibres can be formed
- d) Determine the most suitable polymer concentration and solvent ratio for the shell spinning liquid

- e) Produce core-shell fibres with reversibly thermochromic functionality by coaxial electrospinning, using a suitable setup and processing conditions, of the selected core and shell liquids
- f) Characterize the fibres in terms of fibre morphology and fibre composition
- g) Analyze the thermochromic behaviour of the core-shell fibres

## 1.7 Layout of thesis

This thesis consists of six chapters.

Chapter 1 introduces the topic of the study and the aim and objectives are laid out.

Chapter 2 gives an overview of the literature on the relevant fields including thermochromic dyes, conventional electrospinning, and coaxial electrospinning.

Chapter 3 describes details of the materials used and the experiments conducted to produce the fibres, as well as the analytical methods used to characterize the fibres in terms of morphology, composition and thermochromic behaviour.

The results and discussions are spread out over two separate chapters (Chapters 4 and 5).

Chapter 4 focuses on experiments performed to formulate appropriate core and shell spinning solution compositions, and the optimal thermochromic dye composition. The results of the experiments are discussed along with analyses of the thermochromic dyes and fibres that were produced.

Chapter 5 builds on Chapter 4 by further evaluating the optimal core and shell solutions as summarized at the end of Chapter 4. The process parameters like flow rates, ambient conditions, spinneret diameters, and core needle protrusion are discussed; and the morphology, composition and thermochromic transitioning of the thermochromic core-shell fibres are characterized using various analytical methods.

Chapter 6 concludes the study and contains recommendations for future work.

## 1.8 References

1. Greiner, A. and Wendorff, J.H., *Electrospinning: A fascinating method for the preparation of ultrathin fibers*. Angewandte Chemie International Edition, 2007, **46**:5670-5703.
2. Li, F., Zhao, Y., Wang, S., Han, D., Jiang, L. and Song, Y., *Thermochromic core-shell nanofibers fabricated by melt coaxial electrospinning*. Journal of Applied Polymer Science, 2009, **112**:269-274.
3. Nelson, G., *Application of microencapsulation in textiles*. International Journal of Pharmaceutics, 2002, **242**:55-62.
4. Li, D. and Xia, Y., *Electrospinning of nanofibers: Reinventing the wheel?* Advanced Materials, 2004, **16**(14):1151-1170.
5. Ramakrishna, S., Fujihara, K., Teo, K.E., Lim, T.C. and Ma, Z., *An introduction to electrospinning and nanofibers*. 2005, World Scientific Publishing: Singapore.
6. Doshi, J. and Reneker, D.H., *Electrospinning process and applications of electrospun fibers*. Electrostatics, 1995, **35**:151-160.
7. Moghe, A.K. and Gupta, B.S., *Co-axial electrospinning for nanofiber structures: Preparation and applications*. Polymer Reviews, 2008, **48**(2):353-377.
8. Yu, J.H., Fridrikh, S.V. and Rutledge, G.C., *Production of submicrometer diameter fibers by two-fluid electrospinning*. Advanced Materials, 2004, **16**(17):1562-1566.
9. Sun, Z., Zussman, E., Yarin, A.L., Wendorff, J.H. and Greiner, A., *Compound core-shell polymer nanofibers by co-electrospinning*. Advanced Materials, 2003, **15**(22):1929-1932.
10. Periyasamy, S. and Khanna, G. *Thermochromic colors in textiles*. [Article] [cited 2009 12 August]; Available from: <http://www.fibre2fashion.com/industry-article/9/804/thermochromic-colors-in-textiles1.asp>.
11. Lam Po Tang, S. and Stylios, G.K., *An overview of smart technologies for clothing design and engineering*. International Journal of Clothing Science and Technology, 2006, **18**(2):108-128.
12. Papkov, S.P., *Theory of the preparation of superstrong polymer fibres*. Fibre Chemistry, 1981, **13**(4):212-216.

13. Stahl, K.D., Koenig, D.W., Wenzel, S.W., Ribble, B.F., Cunningham, C.T., MacDonald, J.G. and Archart, K.D., *Color changing cleansing composition, US Patent 0142263 A1*, 2007.
14. Huang, Z.-M., Zhang, Y.Z., Kotaki, M. and Ramakrishna, S., *A review on polymer nanofibers by electrospinning and their applications in nanocomposites*. Composites Science and Technology, 2003, **63**:2223-2253.
15. McCann, J.T., Marquez, M. and Xia, Y., *Melt coaxial electrospinning: A versatile method for encapsulation of solid materials and fabrication of phase change nanofibers*. Nano Letters, 2006, **6**(12):2868-2872.

# **Chapter 2**

## ***Historical and Theoretical Background***

### **2.1 Thermochemical dyes**

#### **2.1.1 Background and introduction**

Thermochromism is a reversible change of colour exhibited by a compound upon heating or cooling. This colour change is quite noticeable and often dramatic and it usually occurs over a small temperature interval.<sup>1</sup>

Thermally induced colour changing compounds, or thermochemical dyes, have many possible applications, for example: aesthetic purposes in the fashion or mass-market garment industry;<sup>2</sup> functional purposes in polymer fibres and textiles (such as product labelling and security applications);<sup>3</sup> chameleon-type building coatings;<sup>4</sup> and other novelty applications.<sup>3</sup>

Materials that can be used as thermochemical dyes include: organic compounds, inorganic compounds,<sup>1</sup> polymers,<sup>5</sup> and sol-gels (e.g. pH indicator dyes incorporated in a transparent hydrogel matrix).<sup>6-8</sup> In the manufacturing of thermochemical textile products, the organic compounds are preferred. It has the advantage of sharp colour changes and the colour transition temperature can be altered by making changes to the composition (discussed in Section 2.1.2) of these dyes.<sup>1</sup>

The mechanism responsible for thermochromism of organic compounds varies with molecular structure of the compound. The colour change is due to equilibrium changes, either between two molecular species (e.g. acid-base, keto-enol or lactim-lactam tautomerism); or between different crystal structures; or between stereoisomers. The latter is ruled out for most thermochemical applications because these compounds typically exhibit colour change behaviour only at temperatures in excess of 150 °C.<sup>1</sup> Thermochemical dyes and pigments that exhibit the other two types of mechanisms (e.g. leuco dyes and liquid crystals) have many applications and offer great potential in the area of so-called 'smart' and

functional textiles ('smart' refers to the ability to react in response to stimuli from the environment).<sup>1,9</sup>

In liquid crystals a change in temperature leads to thermal expansion, resulting in a change in layer adhesion and pitch, which induces the corresponding change in colour. Liquid crystals give fine coloured images, but have the disadvantage of high cost and low colour density. These materials are typically used to manufacture thermochromic printing inks and are not the preferred option for textile applications.<sup>1</sup>

Thermochromic dyes of the leuco type are able to exhibit thermally induced colour changes by means of molecular rearrangements induced by a change in temperature; alteration of solvent polarity; or by a change in the pH of the system. The molecular rearrangement, arising from tautomerism, leads to an increase in the conjugation of the molecule, resulting in the formation of a new chromophore. In the case of a pH dependent chromism, temperature dependence of the acid-base equilibrium means that pH-sensitivity can result in thermochromic behaviour.<sup>1</sup>

In order to create a reversible thermochromic effect for the leuco type dyes the dye composites generally have to contain at least three components (as discussed in the next section).<sup>10-14</sup> These separate components have to be protected and contained in one space to maintain the reversibility of the effect. For this reason the dyes are encapsulated into microcapsules.<sup>2,3</sup>

In textile applications, the microencapsulated thermochromic dyes are typically applied to textile surfaces like pigments in a resin binder.<sup>2,3</sup> The thermochromic effect on the textiles generally survive up to 20 laundry cycles; the longevity of the finish is even less when high temperatures or bleaches are used.<sup>2,3</sup>

### **2.1.2 Composition**

The focus of this discussion is on the components required for reversibly thermochromic, leuco type dye systems. As mentioned, the reversible thermochromic effect requires at least



three main components and these components must stay in contact. The components include a leuco dye (colour former), a colour developer, and a phase change solvent.<sup>10-14</sup>

The main component of the thermochromic composite is the colour former or leuco dye. Examples include spirolactones such as fluorans, crystal violet lactone (CVL) and other phthalide dyes e.g. RED-40;<sup>8</sup> spiropyrans; and fulgides.<sup>10,12</sup> CVL (a type of phthalide dye)<sup>11,13</sup> is a well studied colour changing compound that is often used in thermochromic dye composites. In the dye composite CVL exhibits a reversible and distinct colour change across a small temperature range. This change occurs between blue and colourless.<sup>12</sup>

A colour developer is required to enable the colour formation. Colour developers are weak acids that act as proton donors to induce the coloured state of the leuco dye components that act as weak organic bases.<sup>10,12</sup> Examples of colour developers include: bisphenol A (BPA); octyl p-hydroxybenzoate; methyl p-hydroxybenzoate; 1,2,3-triazoles; 4-hydroxycoumarin derivatives;<sup>10</sup> laurylgallate; ethylgallate; p-hydroxybenzoic acid methyl ester;<sup>12</sup> and various other phenols, aromatic amines, carboxylic acids and Lewis acids.<sup>13</sup> Ethylgallate (EG) has been shown to give very high absorbance i.e. an intense colour in the coloured state of CVL-EG-1-octadecanoic acid methyl ester composites. The same study showed that, of the developers tested for this type of composite, BPA provided the second most intense colour.<sup>12</sup> An investigation into the ageing of thermochromic dye composites revealed that compositions containing BPA as developer, remained intensely coloured over long periods of time while many other formulations exhibited quick colour loss.<sup>14</sup>

A phase change material (PCM), in the context of thermochromic dyes frequently referred to as the solvent (referred to as PCM-solvent from here on), is added to enable reversibility of the thermochromic functionality. It provides a medium in which the colour former and developer are soluble (when the PCM-solvent is in its molten state).<sup>10-14</sup> The melting point of the PCM-solvent is the main contributing factor in the determination of the colour switching temperature of the dye composite.<sup>13,14</sup> The PCM-solvent should be a relatively low-melting hydrophobic compound and it typically has a long chain aliphatic character (chain length affects colour intensity).<sup>10,14</sup> It may be a fatty alcohol, lipid, ester, ketone, ether, carbonic acid or amide.<sup>10,13,14</sup> Examples include lauryl alcohol (1-dodecanol, or dodecanol), cetyl

alcohol (1-hexadecanol), methyl stearate, butyl stearate<sup>10</sup>, 1-octanoic acid methyl ester,<sup>12</sup> and stearic acid<sup>13</sup>.

Additional components can be added to the thermochromic composite. Stabilizers can be added to enhance the light fastness of the colour formers.<sup>15</sup> Regular textile dyes can be added to create a base colour and thereby a thermochromic transition, between this base colour and the combined colour (of the base colour and the coloured leuco dye), can be attained.<sup>10</sup>

Production of the thermochromic composite, for research purposes, is achieved by mixing and heating the components to a temperature significantly above the melting point of the selected PCM-solvent and stirring it at that temperature for a certain amount of time, or until a homogeneous mixture is obtained. Subsequent cooling to room temperature results in a solidified coloured composite. The composite prepared in this way can be used for further experimentation.<sup>13,14</sup>

### 2.1.3 Mechanistic considerations

The thermochromic dye composites that are formed by combining the required components, as discussed above, typically change from a coloured to a colourless state when the temperature is increased. Subsequent cooling will allow restoration of the coloured state.<sup>14</sup> The colour transformation occurs over a temperature range that is specific to each composite.<sup>15</sup>

The colour change observed for CVL is pH-sensitive and in a dye-developer-solvent system (with a PCM solvent) this pH-sensitivity is made temperature dependent.<sup>1,14</sup> The PCM-solvent provides a medium wherein the CVL and the developer can interact<sup>14</sup> and undergo molecular rearrangements that leads to colour changes.

The basic mechanism of thermochromism in CVL dyes is a reversible ring-opening/ring-closing reaction (Figure 2.1).<sup>11-14,16</sup> When the dye-developer-solvent system experiences a temperature below the melting point of the PCM-solvent, dye-developer interactions prevail. The CVL is protonated by the developer and assumes its ring-opened state. This

conformation of CVL absorbs light in the visible region (608 nm) and therefore it exhibits a blue colour.<sup>11,14</sup> The ring-opened state is stabilized by complex formation, via hydrogen bonding, between CVL and the developer. The coordination number of dye to developer in the composite depends on the tendency of the developer to form hydrogen bonds, as well as on steric effects.<sup>12,16,17</sup> Above the melting point of the PCM-solvent, solvent-developer interactions begin to dominate. Subsequently, CVL is deprotonated and assumes its ring-closed state, which absorbs in the UV region (276 nm), and is colourless (Figure 2.2).<sup>11,13,14</sup>

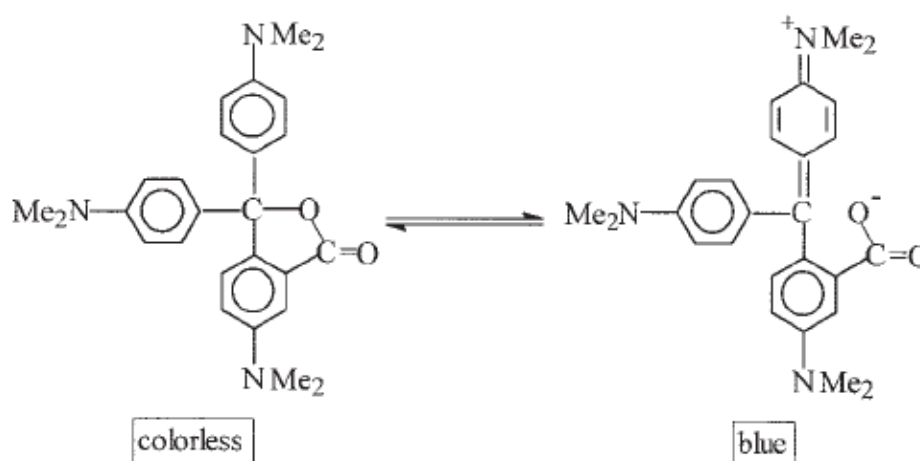


**Figure 2.1** Molecular structures of the ring-closed and ring-opened states of CVL.<sup>11</sup>

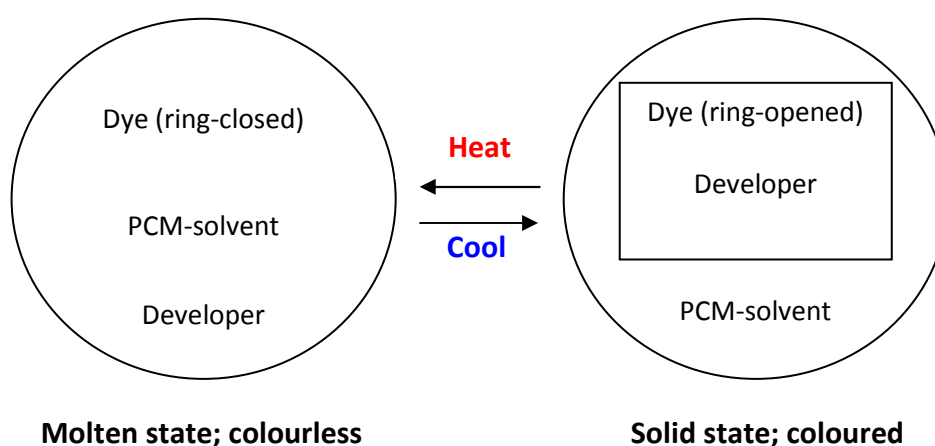


**Figure 2.2** Basic mechanism of the thermochromic leuco dye (e.g. CVL) system.

The temperature driven phase change mechanism implies that it is important to have the appropriate balance between the solubilities and solvating powers of the components in the composite, as well as the correct balance between the acidity (tendency to donate a proton)

of the developer and basicity (tendency to accept a proton) of the dye. It is important that the developer possesses just enough solubility in the molten PCM-solvent to cause complete dissolution (full developer-solvent interaction) and yet have a poor enough solubility in the cooled composition to maximize phase separation of the developer and PCM-solvent so that developer-dye interactions prevail. The dye should have sufficient solubility in the PCM-solvent, as well as the correct basicity to give colour formation with high contrast. Furthermore, the dye must be compatible (give good association) with the developer, otherwise phase separation of these two components, in the solid, colour developed state, could occur and result in the loss of colour over time.<sup>14</sup>

In some studies it has been proposed that the intensity of the coloured state is dependent on the acidity of the proton donating developer. When the developer had a stronger acidic property the colour intensity of the developed state was deeper, and a higher value of energy was required for thermal transition.<sup>13</sup> On the other hand, it has also been shown that the acidity of the system is not the dominating factor for the colour development and therefore the simple model of a pH-dependent equilibrium between the ring-opened and ring-closed structures of the leuco dye is not sufficient to explain the colour development in a dye-developer-solvent system. These studies showed that the molecular structure of the developer, including the length of its alkyl chain and the specific dye-developer interaction for each specific dye-developer-system, determines the intensity of the thermochromic colour.<sup>12,14</sup>

The different theories on the thermochromic mechanism indicates that for each type of thermochromic composite a specific leuco dye-developer-solvent system is built up, and each system has a different effect on the final colour intensity, because all three components have an influence on each of the others. In addition to the previously explained stabilization of the ring-opened structure (through dye-developer complex formation via hydrogen bonding) as dominating force for the colour development, it has been shown that the developer does not interact with the leuco dye as a single molecule. In the first step, developer-developer complexes are formed by intermolecular interactions, which then, in a second step, interact with the leuco dye. In this way complexes and large clusters can be built up. The complex formation between leuco dye and developer molecules indicates that a developer with strong developer-developer interactions (via hydrogen bonding) should be

preferable to trigger the ring-opening mechanism of the leuco dye, and to stabilize the whole complex. According to this model steric factors (of the leuco dye and the developer), as well as the tendency and ability to form and stabilize hydrogen bonds are important factors in determining which developer will give the highest colour intensity with a specific leuco dye.<sup>12</sup>

Based on the fact that colour development in reversible, thermochromic systems depends on the competition between dye–developer and solvent–developer interactions, it has been shown that, depending on the developer, the solvent as well as the polymer matrix and other additives can all have a strong influence on the colour intensity of the system.<sup>12</sup>

In addition to the various interactions described above, interactions between the components of a thermochromic dye and the polymer matrix can also be expected when embedding a thermochromic composite in a polymer matrix. When non-reactive polymer matrices, such as polyolefins, were used it was shown that the interactions between the components of the thermochromic composite were stronger than the interactions between the polymer and the thermochromic composite.<sup>11,12</sup> It can be expected that polymers with reactive side groups will be more likely to interact with the components of the thermochromic dye composite.

## **2.2 Electrospinning**

### **2.2.1 Introduction and historical background**

Extremely thin polymer fibres can be produced when using the electrospinning process. The fibres that are produced vary in size from a few micrometres to as small as three nanometres, but are typically in the sub-micron (100-800 nm)<sup>18</sup> range. It is from this size characteristic that the term ‘nanofibres’, which is commonly used to refer to electrospun fibres, is derived.

Nanofibres have several characteristics that make them superior to conventional fibres. These include very large surface area to volume ratios and increased length to diameter ratios. High surface to volume ratios increase the availability of functional groups and give

the nanofibres enhanced properties over conventional, larger fibres with similar surface functionalities.<sup>19,20</sup>

The superior properties of nanofibres have led to its application in: biomedical and biotechnological applications (e.g. wound dressings, tissue scaffolding and materials for controlled drug release);<sup>21,22</sup> protective clothing;<sup>23</sup> thermo- and photochromic fabrics;<sup>24,25</sup> insulative materials;<sup>26</sup> filtration and membrane applications;<sup>27-30</sup> composite-fibre-reinforced products;<sup>18</sup> and sensors and electrodes for use in optics and microelectronics;<sup>31,32</sup> to name a few.

The history of electrospinning dates back to the work of Cooley and Morton, who patented devices that sprayed liquids under the influence of an electrical charge, in 1902–1903.<sup>33-35</sup> In 1929, Hagiwaba et al.<sup>36</sup> described the fabrication of artificial silk through the application of an electric charge. Some years later (1934–1944), a series of patents was published by Formhals.<sup>37-41</sup> Formhals described an apparatus for the production of polymer filaments, by taking advantage of the electrostatic repulsions between surface charges.<sup>37</sup> Up until the early 1990s, this technique had been known by the term ‘electrostatic spinning’, and besides Formhals there was very little interest and only a few publications dealing with the use of this technique in the manufacturing of thin fibres.<sup>42,43</sup>

In the early 1990s the process gained substantial academic interest from various groups.<sup>43</sup> The revived interest was mainly triggered by the activities of the Reneker group.<sup>20</sup> During this time the term electrospinning became popular and is now widely used in literature to describe the process.<sup>42</sup> Research in the field includes both fundamental and application-oriented projects from different science and engineering disciplines.<sup>43</sup> Since the beginning of the revived interest, the number of publications in the field, including journal papers and patents, has been growing exponentially.<sup>43</sup>

### **2.2.2 The electrospinning process**

Electrospinning is a process whereby fine polymer fibres are produced by applying a high voltage and electrostatic field to a polymer solution or melt.<sup>42</sup> The process is mostly and most easily performed on polymer solutions. This enables the fabrication of fibres with

extremely thin diameters but the productivity of the process is very low. Another problem is that if the solvent volatility is too low, wet fibres may be deposited on the collector and this can result in filming and destruction of the evolved fibres.<sup>43</sup> The use of toxic and dangerous solvents is not always suitable for the end use, but often required. Many polymers are hard to dissolve and some cannot be dissolved at all. Electrospinning from the melt is an alternative but the process is more difficult to control and it usually results in fibres with larger overall diameters and a broader distribution of diameters. This is due to the high melt viscosities of the often high melting polymers.<sup>44</sup> The remainder of the discussion is focused on electrospinning of polymer solutions.

The basic setup for electrospinning consists of three major components: a high voltage power supply, a spinneret (a capillary tube with a pipette or needle with a small orifice diameter), and a metallic collector. A syringe pump can be included if a controlled flow rate is desired. Figure 2.3 gives a graphic representation of the general electrospinning setup, which can be placed either horizontally or vertically. The spinneret is connected to a syringe that contains the polymer solution or melt. In the vertical setup gravity is sometimes employed to feed the solution, but typically, for any setup, a syringe pump is used to feed the solution to the spinneret at a constant and controllable rate.<sup>42</sup> One electrode from the power supply (usually positively charged) is attached to or inserted into the spinning solution and the other is attached to the collector. In most cases the collector is grounded, but it can also be negatively charged. Hence, the fibres are electrospun either from a positive to a zero potential<sup>18</sup> or from a positive to negative potential.<sup>45</sup>

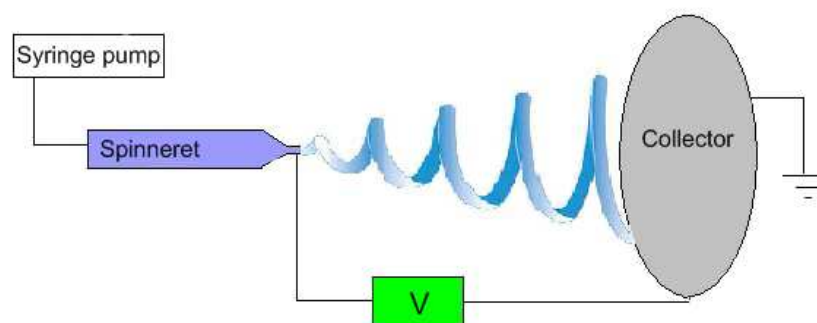


**Figure 2.3** Schematic illustration of the basic electrospinning setup.

The power supply is the source of high voltage, usually in the range of 1–30 kV. On application of this high voltage, the pendant drop at the tip of the spinneret becomes highly electrified. The induced charges are evenly distributed over the surface. The result of this is

that the drop experiences the force of the electrostatic repulsion between the surface charges, as well as the coulombic force exerted by the external electric field. Under the influence of these forces, the drop is transformed into a conical shape known as the Taylor cone. At a certain threshold value of electric field strength, the critical voltage is reached where the electrostatic forces overcome the surface tension of the polymer solution and a liquid jet is ejected from the Taylor cone.<sup>42</sup>

As the electrified jet is accelerated toward the grounded collector, it undergoes a whipping and stretching process known as bending instability. Bending instability occurs in three stages, as shown in Figure 2.4. The continuous elongation and thinning of the liquid jet, due to the bending instability, and the simultaneous evaporation of solvent as the jet moves toward the collector, enables the formation of extremely fine fibres.<sup>42</sup> The fibres are commonly deposited on aluminium foil in the form of randomly orientated, non-woven webs but several other collection methods, including methods used to align fibres, have been proposed and studied.<sup>46-51</sup>

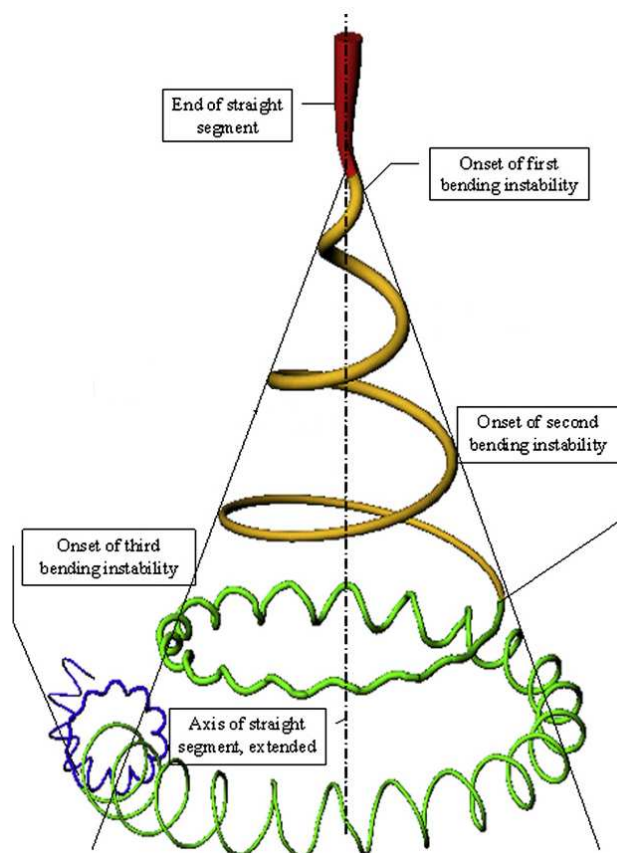


**Figure 2.4** Schematic illustration of the first, second and third stages of bending instability of a Taylor cone.<sup>52</sup>



The electrospinning mechanism, as opposed to the rather simple electrospinning setup, is rather complicated.<sup>42</sup> It is important to gain a better understanding of the electrospinning process and its mechanism, in order to predict outcomes and enable planning of desired end products. In order to explain bending instability, Reneker et al.<sup>49</sup> have proposed a general electrohydrodynamic model of the electrified jet accelerated by an external electric field. Such mathematical models, once fully validated with experimental data, can be used for better control and optimization of the electrospinning process.<sup>53</sup> The complexity of the electrospinning process makes it difficult and often impossible to experimentally vary one parameter, while keeping the others constant, without impeding the electrospinning process.

Under certain experimental conditions, polymer fibres with controllable diameters and without beads can be obtained. The presence of beads in electrospun nanofibres is a common problem. Several groups<sup>42,20,27</sup> have investigated this phenomenon in order to eliminate bead formation.

The various parameters that affect the formation and final morphology and diameter of the electrospun fibres can be broadly classified into three categories. These include solution properties, processing parameters and ambient conditions.<sup>20</sup> It is not possible to make recommendations for the exact experimental conditions required for successful electrospinning of specific spinning solutions, because the ideal values of the parameters vary considerably for each polymer–solvent system. The parameters that influence the electrospinning process and the morphology of electrospun fibres are discussed in the following sections.

### **2.2.3 Solution properties**

#### *2.2.3.1 Viscosity (molecular weight and solution concentration)*

The viscosity of a polymer in solution is influenced by the molecular weight of the polymer and the concentration of the polymer in solution, or more fundamentally, by the extent of polymer chain entanglements. In electrospinning a limiting concentration and viscosity exists

for every polymer–solvent combination, below which the solution is too dilute to form a stable jet. In such cases the jet will break and droplets, instead of fibres, will form.<sup>20</sup>

The phenomenon of jet breakup, due to insufficient resistance to the electrostatic field, is termed Rayleigh instability. At a certain solution concentration, determined by the molecular weight of the polymer, the number of entanglements per polymer chain will be sufficient to subdue Rayleigh instability to the extent that a stable, continuous jet is formed and smooth fibres are produced.<sup>54-56</sup> Stable jet and smooth fibre formation occur at 2.5 or more entanglements per chain.<sup>55</sup> In cases where some entanglements are present but it is below the critical value, Rayleigh instability is not completely eliminated and beaded fibres are formed.<sup>54-56</sup> A short explanation of polymer chain entanglements follows.

The molecular weight between entanglement points ( $M_e$ ) will differ along a polymer chain as the mass of polymer per unit volume ( $c$ ), i.e. the concentration, is changed.

$$M_e = \frac{\text{the molecular weight of a chain}}{\text{number of entanglements}}$$

If highly entangled polymer molecules are diluted, the concentration will eventually be decreased to the point where the molecules do not overlap anymore and no polymer chain entanglements are present ( $M_e = \infty$ ). The opposite is also true and  $M_e$  will decrease as the concentration increases. The number of entanglements per polymer chain is proportional to the mass of polymer per unit volume.<sup>57</sup>

$$M_e \approx \frac{1}{c}$$

and  $M_e c = \text{constant}$

Increasing the polymer chain concentration in a solution will increase the number of entanglements and also increase the solution viscosity because viscous flow is related to the number of entanglements per chain.

The viscosity range in which a polymer solution is spinnable is different for every polymer–solvent combination,<sup>18</sup> and is usually achieved with polymer (in solvent) concentrations of 5–30 wt%.<sup>53</sup> Appropriate solvent viscosities range from tens to hundreds of millipascals per second (mPa/s).<sup>43</sup> Above a certain limiting concentration and viscosity it becomes difficult to form fibres due to drying of the solution at the capillary tip. A higher force is required to form a jet from a more viscous solution and above a certain concentration, the viscosity becomes too high and a stable jet cannot be formed.<sup>20</sup>

Viscosity is one of the main parameters influencing the diameter of electrospun fibres.<sup>27</sup> An increase in viscosity increases the force that opposes the coulombic force that works to pull and stretch the solution into fibres. The increase in this opposing viscoelastic force leads to larger fibre diameters.<sup>20,32</sup> Therefore the higher the polymer concentration or polymer molecular weight (i.e. higher viscosity), the larger the resulting fibre diameter will be. Deitzel et al.<sup>27</sup> showed that the average fibre diameter increases with increasing polymer concentration and that it happens according to a power law relationship. Solutions with higher viscosities generally result in more uniform fibres with more cylindrical shapes and fewer beads.<sup>29,58,59</sup> At lower viscosities and concentrations increasingly thinner fibres with more beads are formed.<sup>43</sup>

#### 2.2.3.2 *Surface tension*

The surface tension ( $\gamma$ ) of a polymer solution has a significant effect on the morphology of the electrospun fibres. By reducing the surface tension of a polymer solution, beads can be eliminated from electrospun fibres.<sup>20</sup>

Ramakrishna et al.<sup>19</sup> explained the effect of surface tension on fibre morphology as follows. The initiation of electrospinning requires the charged solution to overcome its surface tension. Surface tension decreases the surface area per unit mass of a fluid. When the concentration of solvent molecules is high they have a greater tendency to congregate and take on a spherical shape. This happens as a result of the surface tension and will lead to the formation of beads in the electrospun fibres. Bead formation is driven by the tendency towards minimization of surface area, thus high surface tension drives the solvent molecules, and therefore the dissolved polymer molecules, into spherical droplets forming

beads rather than fibres. At higher viscosities, there is a greater interaction between solvent and polymer molecules. When such a solution is stretched under the influence of the external charges, the solvent molecules will tend to spread over the entangled molecules of the polymer and so reduce the tendency of the solvent molecules to come together under the influence of surface tension and form beaded morphologies. This is shown in Figure 2.5 below.

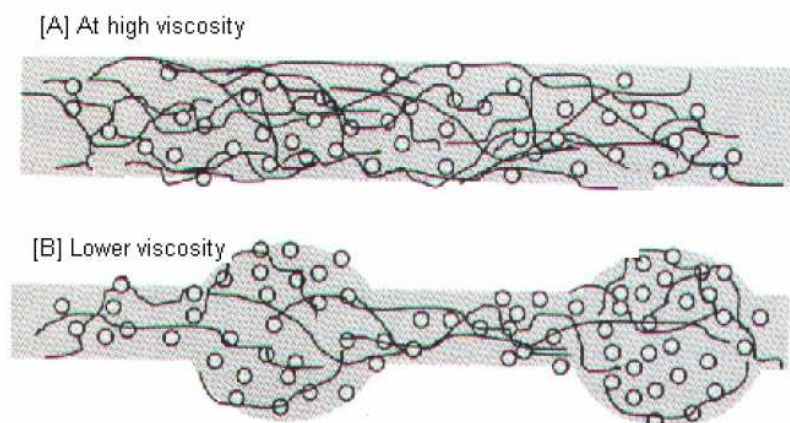


**Figure 2.5 The difference between beaded and smooth fibres due to the effect of surface tension.<sup>19</sup>**

Solvents and solvent ratios (when using combined solvent systems) can be changed to adjust the surface tension for a specific polymer in solution. The technique must be applied with caution because a change in the solvent or solvent ratio affects the other solution parameters (e.g. viscosity, conductivity, dielectric constant and vapour pressure) as well, and these also influence jet formation and fibre morphology.<sup>30</sup> The addition of a suitable surfactant to a polymer solution will also lower the surface tension. This effect can be used to promote the formation of bead free fibres.<sup>60,61</sup>

### 2.2.3.3 Conductivity

The conductivity ( $\sigma$ ) of a solution is an indication of the ability of that solution to carry an electric charge and is mainly a property of the solvent. Electrical conductivities in organic solvents typically range from nano-Siemens to micro-Siemens per centimetre ( $\mu\text{S}/\text{cm}$ ).<sup>43</sup> Addition of ions to the solution can increase the solution conductivity.<sup>29</sup> Fluids with high conductivity have high surface charge density.<sup>62</sup>

Bead formation is typical when the conductivity of a solution used for electrospinning is too low. Beads form because, due to the lack of surface charges, the polymer solution is not stretched sufficiently. The addition of small amounts of an ionic salt provides more ions that can carry electric charge. This results in a higher charge density on the surface of the electrospinning jet. As the charges carried by the jet increase, the jet experiences higher elongational forces under the applied electrical field due to the self repulsion of the excess charges on the surface. This inhibits Raleigh instability, enhances whipping and results in more uniform, less beaded fibres.<sup>29,62</sup> The addition of a polyelectrolyte can also increase the charge density of the solution and lead to fibres without beads.<sup>63</sup> It is important to note that enhanced whipping is a solution conductivity effect and does not necessarily imply that a higher applied electrical field will result in smoother fibres with fewer beads.

The effects that lead to increased conductivity and enhance the formation of bead free fibres also lead to the formation of fibres with thinner diameters. Finer fibres are formed due to the enhanced whipping effect as discussed in the previous paragraph.<sup>29,62,63</sup> The effect of conductivity on fibre diameter might be limited above a critical value because the average diameter of electrospun fibres is not only related to the magnitude of the conductivity.<sup>63</sup>

#### 2.2.3.4 *Dielectric effect of solvent*

The dielectric constant is a measure of the polarity of the solvent. Charges induced on a solution have a much greater effect when polar solvents, as opposed to non-polar solvents, are used. Solvents with higher dielectric constants have higher net charge densities in solution. Therefore a solution made using a solvent with a high dielectric value will generally form thinner and smoother fibres without beads.<sup>63</sup> Increasing the dielectric constant of the solution can enhance electrospinning and fibre formation. A low dielectric constant is not conducive to successful electrospinning.<sup>58</sup>

#### 2.2.3.5 *Vapour pressure of solvent*

A relatively slow evaporating solvent allows for longer stretch times before the jet solidifies and therefore results in thinner fibres.<sup>53</sup> The solvent must have a sufficiently high volatility

(low boiling point/high vapour pressure) to enable enough evaporation for the fibres to dry before reaching the collector. The solvent must not have such a high volatility that the polymer solution dries at the syringe tip and inhibits fibre formation. If the solvent is highly volatile and evaporates very quickly, the orifice of the spinneret can become blocked. The high viscosity and low charge density brought on by the early evaporation of highly volatile solvents, often leads to insufficient flow to maintain a fully developed jet for electrospinning.<sup>30,53</sup>

Highly volatile solvents, like tetrahydrofuran (THF) and acetone, can give rise to pores, surface roughness or microstructure when fibres are spun from polymer solutions containing these solvents. With decreasing solvent volatility the surface features diminish and disappear to leave smooth fibre surfaces.<sup>64</sup>

## **2.2.4 Process parameters**

### *2.2.4.1 Voltage*

Electrospinning is usually achieved by applying a positive potential to the spinning liquid and grounding the collector. Fibres can however be electrospun from both positive and negative electrode potentials.<sup>20,65</sup> The diameters of the fibres electrospun from a negative potential have been found to be larger than those obtained by electrospinning from a positive potential.<sup>65</sup> The use of direct current is the norm, but both direct and alternating current have been used.<sup>43</sup> Alternating current has been shown to result in the formation of finer fibres, with a higher degree of fibre alignment in the electrospun mats.<sup>66</sup>

The electrospinning process produces fibres only if the applied voltage is above the given limiting value required to overcome the surface tension of the solution. The fibres transport charge across the gap between the spinneret and the grounded collector to complete the circuit. Above a certain critical voltage an electrified jet is ejected from the Taylor cone. When the voltage is increased too much, the jet can become unstable and multiple jets can form.<sup>20</sup>

The influence of electrospinning voltage on fibre diameter is poorly established. Some studies have shown a decrease in fibre diameter with increasing voltage, while others have shown the opposite.<sup>42</sup> The voltage required to successfully spin a given polymer solution and form fibres without beads largely depends on the solution properties and on other electrospinning parameters.<sup>27,29,42</sup>

Electrospinning induces orientation and crystallisation within fibres. Crystallinity is increased with increasing voltage as long as there is enough time during the flight of the jet for crystallization to take place. If there is not enough time for crystallization to take place, crystallinity will be decreased as the time of jet flight is shortened by increased voltage.<sup>67</sup>

#### 2.2.4.2 *Feed rate*

The feed rate is defined as the rate at which the spinning solution is supplied, by means of a syringe pump, to the tip of the spinneret. The speed at which the electric field carries the solution away from the spinneret tip will determine the feed rate necessary to maintain a stable Taylor cone. An increased feed rate leads to larger fibre diameters and the formation of beads, whereas a lower feed rate leads to the formation of thinner fibres.<sup>29</sup>

#### 2.2.4.3 *Collector*

Several different types of collectors have been used to either randomly collect or attempt to align electrospun fibres.<sup>51</sup> The nature of the collector affects the morphology as well as the packing of the fibres. A non-conductive collector, such as paper, results in fibres with smooth surfaces, more uniform sizes and few defects. The fibres are deposited in the form of a loosely packed fibrous network structure. Fibres collected on conductive collectors such as aluminium foil and water are more varied in size and the fibres are tightly packed, forming a thick membrane structure.<sup>30</sup> Crystallization and orientation of the polymer chains within fibres are enhanced in the case of conductive collectors that create a greater electrostatic field effect.<sup>29,30,67</sup> A rotating wire drum can be used to collect electrospun fibres in the form of relatively uniform, aligned fibre mats.<sup>68</sup>

#### 2.2.4.4 *Spinneret orifice diameter*

The size of the orifice where the jet initiates affects the size of the initial jet radius, which in turn has a pronounced effect on the final fibre diameter. The effect of orifice size on fibre diameter has not been widely studied<sup>53</sup> but it has been shown that the average fibre diameter decreases with decreasing orifice size.<sup>22</sup> The final fibre diameter depends heavily on the initial jet radius but this is also significantly affected by applied voltage. The effect of orifice size on fibre diameter can therefore not be considered as a fully independent parameter when the applied voltage changes.<sup>53</sup>

#### 2.2.4.5 *Tip-to-collector distance*

A variation in the tip-to-collector distance has a direct influence on the strength of the electric field and on the time of flight of the polymer jet. It follows that this distance has an influence on the morphology and diameter of electrospun fibres.<sup>16,26,69</sup>

When the distance is too small, there is insufficient time for stretching and efficient solvent evaporation and thus wet fibres and/or fibres with beads are obtained on the collector.<sup>20,59</sup> Deposition of wet fibres on the collector can cause fibres to merge and form junctions.<sup>59</sup> More uniform and bead free fibres are formed as the distance between tip and collector is increased.<sup>69</sup>

As the tip-to-collector distance is increased, fibres with smaller diameters tend to form.<sup>70</sup> The fibre diameters decrease with increasing distance up to a certain point, beyond which there is no significant effect of distance on fibre diameter.<sup>71</sup>

### 2.2.5 **Ambient conditions**

#### 2.2.5.1 *Humidity*

The amount of moisture in the air affects the surface morphology of electrospun fibres. Above a certain relative humidity, pores may form on the surface of fibres. The number of pores, the pore diameter, and the pore size distribution for a specific polymer solution all



increase with increasing humidity.<sup>64,72</sup> The formation of pores at high humidity is explained by the evaporative cooling effect.<sup>73</sup> As solvent evaporates, the jet surface is cooled and water condenses on the jet surface. Later evaporation of the water droplet leaves a pore-like imprint on the fibre. Evaporation of left over solvent will also create pores. The effect is more intense at higher humidity.<sup>64,72,73</sup>

The humidity of the surrounding air determines the rate of solvent evaporation from the polymer jet. At very low humidity, volatile solvents evaporate very rapidly.<sup>64,72</sup> This means that the results for two experiments that have identical values for all other parameters, may not be the same when the humidity changes.

Fibre diameters are influenced by the interaction between humidity and solvent evaporation because it affects the distribution of electric charges on the surface of the electrospinning jet. At lower humidity thinner fibres are produced because the electric charge density on the polymer jets are higher.<sup>74</sup>

#### 2.2.5.2 *Temperature*

The influence of ambient temperatures on the electrospinning process is associated with the dependencies of other parameters, especially that of solution properties, on temperature. A change in temperature for example, affects the solution viscosity and vapour diffusivity,<sup>53</sup> which in turn affects the fibre morphology and diameter.

## 2.3 Coaxial electrospinning

### 2.3.1 Introduction and historical background

The process of coaxial electrospinning is a versatile method for producing nanofibres with core-shell structures.<sup>75</sup> Conventional (single capillary) electrospinning has also been used to produce core-shell nanofibres, but only from polymer blends<sup>76,77</sup> (containing two polymers that will phase separate upon solvent evaporation) and from immiscible solutions<sup>78</sup>. Due to the limitations of the single capillary process with regard to the formation of core-shell fibres, the focus of this section is on the process of coaxial electrospinning. In this process

two concentric capillaries are employed to produce compound core-shell fibres from separate core and shell liquids.

The need often arises to functionalize electrospun fibres through the inclusion of functional molecules or objects into the fibre structure, or by the use of different layers of materials that each provides a different property to the fibres. Inclusion of such molecules or objects and the need to produce fibres from low molecular weight materials exposes the limitations of conventional electrospinning and therefore the use of coaxial electrospinning (also called co-electrospinning or core-shell electrospinning) has become popular in various fields.<sup>32,43</sup>

Reasons for using this process include: producing fibres by electrospinning from liquids that are difficult to process or do not form fibres by themselves;<sup>75,79</sup> producing fibres with even smaller diameters than by conventional electrospinning (by selective removal of the shell after fibre formation);<sup>79</sup> isolating an unstable component to protect it from decomposition under a highly reactive environment with high electric fields;<sup>43,80</sup> forming fibres that can give controlled release of a substance over time;<sup>32,80</sup> surrounding a less biocompatible polymer by a more biocompatible material;<sup>81</sup> functionalizing the surfaces of fibres without affecting the core material;<sup>80</sup> or producing hollow fibres.<sup>82</sup> In the manufacture of hollow fibres (or 'nanotubes') the core is selectively removed after electrospinning, either by selective solvents<sup>82,83</sup> or by heat treatment.<sup>84,85</sup>

Coaxial electrospinning is an especially useful technique for the production of compound nanofibres with core materials that cannot be electrospun directly.<sup>75,79</sup> Examples of such non-electrospinnable core materials include: low viscosity fluids and low molecular weight polymers;<sup>43</sup> liquids with low electrical conductivities; and long-chain hydrocarbon melts.<sup>26</sup> Coaxial electrospinning allows for these materials to be stretched into thin filaments and entrained inside the shell materials as part of core-shell fibres. The shell fluid serves as a processing aid for the core fluid, allowing it to be electrospun into fibre form and encapsulated inside the shell of the fibre.<sup>16,79</sup>

Examples of novel functional nanofibres that have been produced by coaxial electrospinning include: luminescent nanofibres;<sup>86</sup> fluorescent nanofibres;<sup>87</sup> conductive core-shell nanofibres;<sup>77</sup> hollow nanofibres with functionalized inner and outer surfaces;<sup>88</sup> hollow

core-shell microtubes;<sup>89</sup> biodegradable double-layer nanofibres for tissue scaffolds (with inherent potential of controlled drug release or controlled degradation rate);<sup>81</sup> core-shell fibres for sustained drug delivery;<sup>90</sup> core-shell functionalized nanofibres with increased mechanical properties;<sup>81</sup> and phase change (temperature regulating)<sup>26</sup> and thermochromic nanofibres by melt coaxial electrospinning.<sup>24</sup>

### 2.3.2 The coaxial electrospinning process

The coaxial electrospinning process usually employs a coaxial, two capillary spinneret, which is used to simultaneously electrospin a core and a shell solution. Generally both the core and shell liquids are polymer solutions or a combination of polymer solution and melt or some other compound which may be dissolved in a solvent. If the right combination of liquids and operating conditions are chosen, a compound droplet is formed at the tip of the coaxial spinneret. The typical pattern of the coaxial electrospinning process close to the core-shell spinneret is shown in Figure 2.6. The core liquid experiences an increase in diameter as it exits the capillary tube. This is similar to the die swell effect that is seen when polymers exit an extruder. Below the point of maximum swelling, the outer solution forms a thin shell that attaches to the core polymer stream.<sup>84</sup>

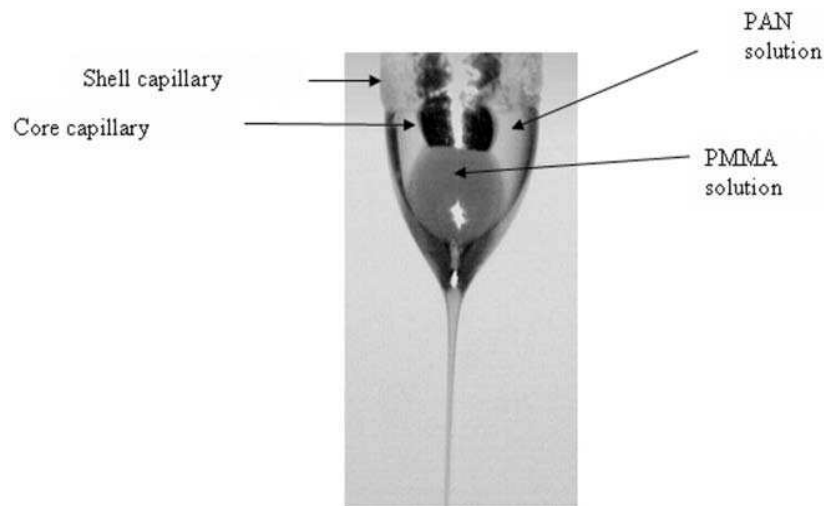


**Figure 2.6** Flow pattern in compound droplet attached to a core-shell spinneret (PAN solution as shell and PMMA solution dyed with malachite green as core).<sup>84</sup>

When both the core and shell materials are polymer solutions, a compound droplet is formed at the tip of the coaxial spinneret and under the influence of the electric field (supplied by the high voltage source) the compound droplet is pulled into a compound

Taylor cone due to charge repulsion.<sup>91</sup> Electrospinning is initiated once the charges induced by the high voltage source on the shell solution together with the electric field, overcome the surface tension. The core solution is dragged along into the jet by the shell solution if the requirements for interfacial tension and other parameters are met.<sup>42</sup> As in the conventional electrospinning process, the jet is pulled by the electric field and stretched by the bending instability due to repulsions between the charges on the jet surface.<sup>82</sup> The charges accumulate predominantly on the surface of the shell liquid flowing from the outer capillary and not on the core liquid.<sup>32</sup>

In the case of core liquids which do not form fibres when electrospun on their own, the shell liquid forms a sheath around the core fluid and entrains the latter. This entrainment stabilizes the core liquid against Rayleigh instability.<sup>79</sup> The stresses generated in the shell exert a viscous dragging effect on the core solution. A compound Taylor cone is developed and the non-spinnable core phase is elongated along with the shell into a compound coaxial jet by the mechanism of viscous dragging.<sup>82</sup> On its way to the collector, the compound jet undergoes bending instability and solidifies as the solvents evaporate.<sup>75</sup> In this way core-shell nanofibres, that contain a core material that could not be electrospun on its own, can be formed.<sup>32</sup>

A common problem experienced during fibre formation is that the shell (outer part) of the compound droplet is sometimes transformed into a jet, while the core (inner part) of the compound droplet is not. This happens mainly because all electrostatic surface charges (Maxwell stresses) accumulate on the surface of the outer droplet and no surface charges from electrostatic forces occur on the inner droplet. The ability of the core material to be electrospun and entrained by the shell is primarily dependent on the viscous forces imposed on the core droplet by the shell droplet. If these forces are insufficient to form the compound jet, core-shell fibres are not formed.<sup>43,84,91</sup>

### **2.3.3 System designs**

The general setup for coaxial electrospinning is very similar to what is used for conventional electrospinning. The only real difference in the design of the setup is the modification that is made to the spinneret. A smaller (inner) capillary is fitted concentrically inside the bigger

(outer) capillary to make a coaxial configuration (refer to Figure 2.6). The arrangement can be either horizontal or vertical. Feeding rates are usually controlled by metering pumps<sup>79</sup> but air pressure<sup>75</sup> has also been used. The simplest type of design consists of two concentric needles, each attached to a pump for flow rate control, a high voltage power supply, and a grounded collector. One such design is shown in Figure 2.7. Coaxial electrospinning has also been conducted using a molten core material together with a conventional polymer solution as shell material. In these examples a heating system surrounds and heats the reservoir (see Section 2.3.7).<sup>24,26</sup>

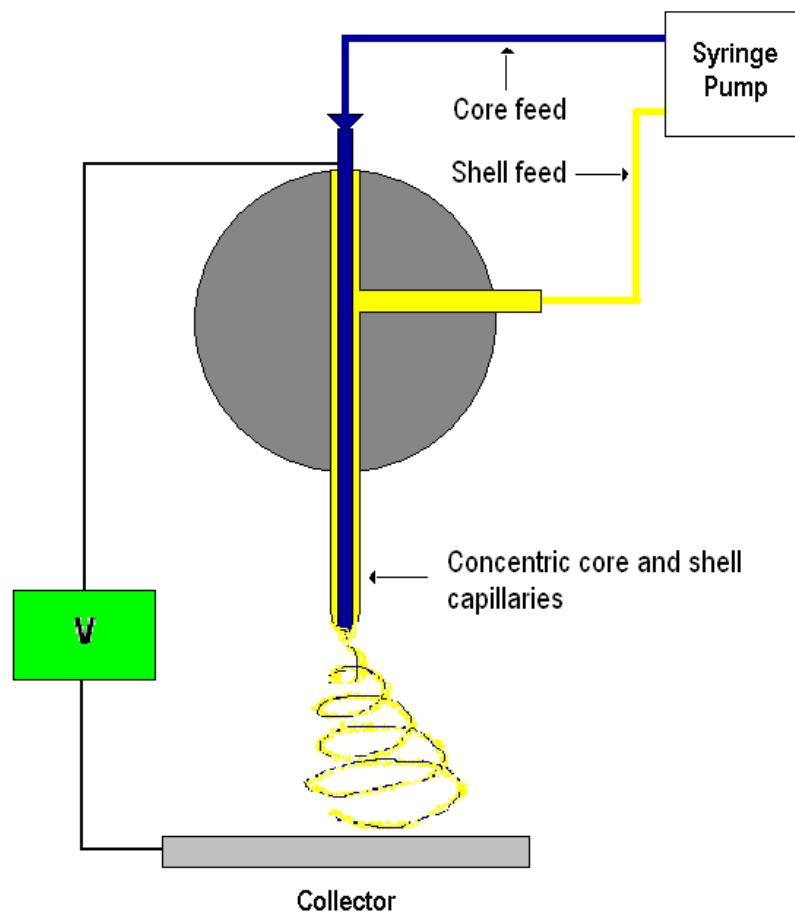


**Figure 2.7** Coaxial electrospinning setup.<sup>92</sup>

The design and manufacturing of the coaxial spinneret can be a difficult and tedious task, especially when it can only be used once and has to be repeated for every experiment. In a study by Wang et al.<sup>85</sup> a slightly different and much simpler setup, which eliminates the need to insert one capillary into another, was reported. The design consisted of two separate syringes with different sized capillaries, with the smaller one inserted from the outside into

the Taylor cone of the other to create a 'L' shaped source from which a compound core-shell Taylor cone could be generated.

#### **2.3.4 Parameter effects**

The same parameters, as for conventional electrospinning, need to be considered with regard to the coaxial electrospinning process. Additionally, the interactions between the core and shell spinning liquids are important to take notice of because these solutions are in contact during the spinning process and have to undergo the same bending instability and whipping motion. The degree of dissimilarity between the core and shell solutions, in terms of composition, and physical and rheological properties, plays an important role in the formation of the compound fibres.<sup>32</sup> The formation of a compound jet, the stability of the process and the formation of core-shell fibres are all strongly affected by the solution and processing parameters.<sup>82</sup> The selection of the appropriate values for all parameters is vital to the successful formation of coaxially electrospun core-shell fibres.

Discussions on the solution and process parameters applicable to coaxial electrospinning follow. The focus is on the interrelated influences and effects of the core and shell variables. The review should be interpreted with the parameter effects of conventional electrospinning in mind. Some parameters, for which the same rules apply as for conventional electrospinning, are not discussed again. Figure 2.8 summarizes the important coaxial electrospinning parameters.

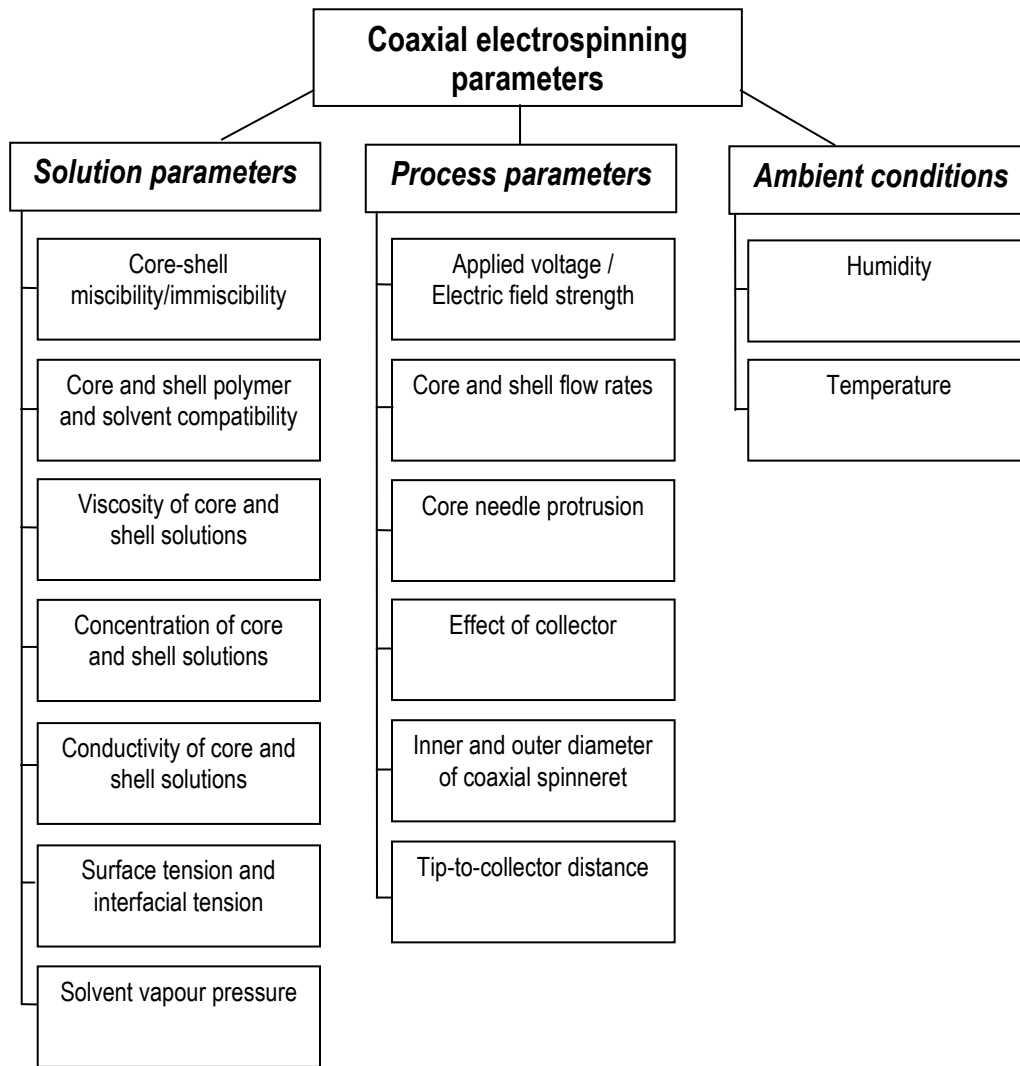


**Figure 2.8** Flow chart summarizing the coaxial electrospinning parameters.

### 2.3.5 Solution parameters

#### 2.3.5.1 Core-shell miscibility/immiscibility

There is much divergence in the opinions of researchers on the topic of miscibility of core and shell solutions and the effect that this has on fibre formation and morphology. Xia and co-workers<sup>42,82,83,88</sup> have repeatedly demonstrated that the core and shell liquids (particularly the solvents) must be immiscible in order to prevent interfacial mixing and enable effective electrospinning. This is true when producing hollow fibres, where the immiscibility of core and shell liquids is crucial to the formation of continuous and uniform hollow fibres,<sup>82</sup> and also when nanofibres with well defined core-shell structures and

boundaries are desired.<sup>83,89</sup> Immiscibility however, is not a prerequisite to the formation of solid core-shell structures by coaxially electrospinning.

Various groups have demonstrated that core-shell polymeric nanofibres can in fact be fabricated by the coaxial electrospinning of two polymer solutions that contain miscible solvents.<sup>75,79</sup> The choice of miscible core and shell fluids, even using a common solvent,<sup>79,80,93</sup> serves to reduce the interfacial tension between the core and shell liquids. A low interfacial tension enables an increase in the viscous stresses imparted by the shell liquid on the core liquid.<sup>79</sup>

Different but miscible solvents (where the shell polymer was also soluble in the core solvent) have been used to prevent precipitation of the shell material where it exits the spinneret and comes into contact with the core solution. The solvent miscibility also serves to enhance the cohesive forces (by lowering the interfacial tension) between the shell and core solutions. In these experiments core-shell fibres were successfully produced but the boundaries were unclear.<sup>87</sup> When the core and shell solutions are miscible, some interfacial mixing can be expected. This results in core-shell structures with less defined boundaries and less uniformity than in the case of completely immiscible solutions.<sup>75,89</sup>

When miscible core and shell solvents are used but the core and shell forming polymers are immiscible, sharp boundaries are still obtained. On the other hand, when both the solvents and the polymers are miscible, the boundaries are not well defined.<sup>94</sup>

#### *2.3.5.2 Core and shell polymer and solvent compatibility*

It is important that the solvent used for one polymer or material (core or shell) does not precipitate the other polymer or material (shell or core) very quickly i.e. in the case of polymer solutions, the polymers must not precipitate at the liquid interface near the exit of the coaxial spinneret.<sup>79</sup> It has been observed that in such cases, the coaxial electrospinning process is interrupted by precipitation and agglomeration of polymer at the tip of the coaxial capillaries.<sup>95</sup>



### 2.3.5.3 Viscosity of core and shell solutions

When the shell liquid has to facilitate electrospinning of the core liquid, the viscosity of the shell solution is critical. The polymer–solvent system selected for the shell liquid should at least have a sufficiently high viscosity to be electrospinnable by itself. An increase in the polymer concentration of the shell solution, to increase the viscosity, is useful to better stabilize the core fluid against break up due to Rayleigh instability.<sup>79</sup>

In some cases, a shell polymer solution which can be directly electrospun on its own, does not form a coaxial jet when co-electrospun with a non-electrospinnable core solution.<sup>82</sup> Highly viscous core liquids can make the entrainment process very difficult. It is important that the shell liquid has a high enough viscosity to impart sufficient viscous stress on the core liquid to overcome the interfacial tension between the two solutions and form a stable compound Taylor cone jet.<sup>45,84,91</sup> If the shell viscosity is much lower than the core viscosity (more than 5x lower)<sup>91</sup> then the viscous forces of the shell on the core at the interface may be too weak to create entrainment of the core liquid.<sup>91</sup>

An increase in the viscosity of the shell liquid can enhance the transmission of viscous stresses onto the surface of core liquid during the electrospinning process. This can improve the stability of the compound jets and enhance core-shell fibre formation. Increased viscosity is achieved by using a higher molecular weight polymer, increasing the polymer concentration, or by mixing in an additive.<sup>96</sup>

The viscosity and electrospinnability of the core is not as critical because the jet breakup of the core fluid is prevented by the shell to some extent.<sup>79</sup> Breakup of the core jet is still observed<sup>26,45</sup> in cases where the viscosity of the core is extremely low.

If it is to be continuously entrained by the shell, the core liquid should possess a certain minimum viscosity. When the viscosity of the core liquid ejected through the inner capillary is reduced below a certain level, it is not possible to stretch the core into a continuous thin thread within the shell.<sup>82</sup> If the viscosity is extremely low, the compound fibres that are produced could still show core-shell structure but with a beads-on-a-string morphology and a discontinuous core structure. Above a certain viscosity compound core-shell fibres of

constant morphology are obtainable.<sup>95</sup> It was found that a very low core viscosity (10x less than the shell viscosity), under the experimental conditions used, made successful core-shell formation less likely.<sup>91</sup> The spinnability of compound droplets with non-spinnable cores can also be significantly enhanced by adding small amounts of a compatible polymer solution to the core liquid.<sup>96</sup>

#### *2.3.5.4 Concentration of the core and shell solutions*

The concentration of the core solution plays a role in determining the final fibre diameter. An increase in the core concentration leads to the formation of fibres with larger core and overall average diameters and vice versa.<sup>80,81,86</sup> A higher concentration of core solution also leads to a thinner shell thickness and a larger amount of core material entrained inside the shell.<sup>80</sup>

Similarly when the shell solution concentration is increased, an increase in the overall fibre diameter is observed due to an increase in the shell thickness.<sup>90,93</sup> Furthermore, it has been shown that a higher polymer concentration in the shell solution leads to the production of thinner cores and thicker shells. When the shell solution concentration is increased there is a resultant increase in viscous stresses imposed on the core that have to be compensated for by adjusting the core flow rate, in order to avoid producing an undesirably thin core.<sup>85</sup>

#### *2.3.5.5 Conductivity and dielectric effect*

It has been shown that all charges imposed on a core-shell droplet quickly accumulate at the outer surface of the shell droplet. Electric forces (Maxwell stresses) that initiate jet formation and subsequent electrospinning therefore only act on the outer surface of the compound droplet. This means that even if the core liquid has good conductivity and is electrospinnable on its own, it will not necessarily be successfully entrained inside a core-shell jet and fibre because no electric charges are imposed on the surface of the core solution.<sup>91</sup>

Electrical conductivity plays a role in the size of the core diameter, the shell thickness and the total fibre diameter of coaxially electrospun fibres in a similar way that it does for single

solution electrospinning. An increase in solution conductivity produces fibres with smaller diameters because it enhances the whipping action.<sup>56,62</sup>

The dielectric constant of the shell solvent is an important parameter. If the shell solvent has a low dielectric constant, electrospinning becomes unlikely because charges are not able to effectively accumulate at the tip of the Taylor cone.<sup>97</sup>

#### *2.3.5.6 Surface tension and interfacial tension*

In order to allow viscous interaction and viscous forces at the core-shell interface (to develop a stable Taylor cone and form core-shell compound fibres) it is important that the interfacial tension between the core and shell liquids is as low as possible.<sup>45,91</sup> For large values of interfacial tension the viscous forces that the shell liquid exerts on the surface of the core liquid will be unable to overcome the cohesive force of the core liquid's surface tension and will be unable to stretch the core into a cone. In this situation no double, compound Taylor cone will be developed. The problem can be resolved by adjusting the surface tension of either the core or shell liquid or both in order to obtain similar surface tensions for both liquids and in so doing reduce the core-shell interfacial tension. It will then be possible for the shell liquid to pull the core meniscus into a steady jet.<sup>45</sup>

The surface tension of a polymer solution that is used in electrospinning will be close to that of its solvent,<sup>98</sup> therefore surface tension can be adjusted by changing the solvent composition and also by addition of suitable surfactants.

#### *2.3.5.7 Solvent vapour pressure*

The type of solvent used, particularly the solvent for the core solution, can have a significant effect on the morphology of the resulting core-shell structure. The formation of ribbon-like structures has been reported when a rapidly evaporating solvent, such as chloroform or acetone, was used for the core solution. The explanation given is that due to the rapid evaporation of the core solvent, a thin layer is created at the core-shell interface and this leads to a triple-layered structure. The interfacial layer that forms creates a barrier that traps the residual interior solvent and makes it diffuse out more slowly. When this residual solvent

fully leaves the semi-solidified structure it creates a vacuum that causes the core structure to collapse under atmospheric pressure, transforming the fibre morphology from a round to a ribbon-like configuration.<sup>86</sup>

The use of highly volatile solvents for shell solutions is not advised, because fast evaporation may produce unstable Taylor cones and multiple jets.<sup>99</sup> Unstable Taylor cones can lead to the formation of irregular core-shell structures and result in separate fibres from the core and shell solutions.<sup>32</sup>

#### 2.3.5.8 Summary

Table 2.1 gives a summary of the material parameter requirements for successful coaxial electrospinning and core-shell fibre formation.<sup>32</sup>

**Table 2.1**

**Core and shell (sheath) solution properties required for successful coaxial electrospinning<sup>32</sup>**

- Electrospinnable sheath solution
- Higher sheath solution viscosity
- Low interfacial tension between the sheath and the core solutions
- Use of low vapour pressure solvents
- Higher sheath solution conductivity

#### 2.3.6 Process parameters

##### 2.3.6.1 Applied voltage and electric field strength

Applied voltage is critical in the formation of core-shell fibres. The forces induced by the electric field, along with surface tension forces, are the main forces driving and influencing the flow patterns of electrospun liquids. It is only possible to maintain a stable Taylor cone

above a certain minimum field strength. If the field strength is high enough, the effect of surface tension pulling the liquids back into spherical form is mostly eliminated and only the electric field strength has a dominant effect on the flow patterns.<sup>100</sup> Higher electric fields will result in shorter Taylor cones.<sup>99</sup> It is only possible to produce nanofibres of constant and continuous core-shell composition within a certain critical voltage range above the minimum electric field strength. The critical voltage range will depend on the combination of spinning liquids and experimental conditions.<sup>99,100</sup>

Studies conducted by Gupta et al.<sup>32,93</sup> showed that, for a given pair of polymer solutions with given flow rates, only a small range of applied voltage existed in which a stable compound Taylor cone could be formed (Figure 2.9 B). This range varied with the type of polymers used. Below the critical voltage range, dripping was observed and no fibres were formed. Increasing the voltage to just below the minimum critical voltage resulted in an intermittent shell jet (Figure 2.9 A) with occasional core incorporation. At the critical voltage, both solutions formed Taylor cones and a coaxial composite jet emerged and uniform fibres were formed. Voltages above the critical range caused the strength of the electric field to exceed that required for the particular systems, and Taylor cones tended to recede and jets to emanate from inside the capillaries. This resulted in separate and discontinuous jets emanating from the shell and core capillaries (Figure 2.9 C), leading to the formation of separate single fibres instead of compound core-shell fibres. For the core-shell systems that were evaluated, it was found that effective core-shell formation was only possible at specific voltages, within a range as small as 1 kV of each other, when using a 15 cm tip-to-collector distance.<sup>32,93</sup>

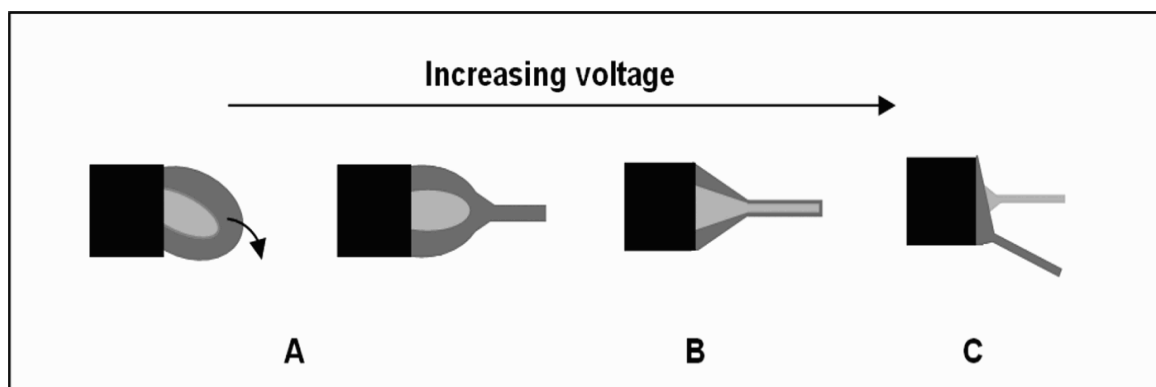


**Figure 2.9** Schematic of the voltage dependence of core-shell fibre formation in coaxial electrospinning (A: subcritical voltage; B: critical voltage; C: supercritical voltage).<sup>32,93</sup>

The voltage applied to the solutions must be set so that the electrical force does not pull the fluids too quickly or too slowly from the spinneret tip.<sup>79</sup> The strength of the electric field influences the diameters of core-shell fibres. Both the core and shell diameters have been found to decrease upon increasing the electrical field strength.<sup>82</sup>

### 2.3.6.2 Core and shell flow rates

The flow rates of both the core and the shell solutions are important controlled variable parameters. Both solutions should be pumped at appropriate individual as well as relative flow rates in order to produce continuous and uniform core-shell fibres.<sup>82</sup> In general, the core flow rate should be lower than the shell flow rate. The relative core flow rate must be high enough to prevent segmentation of the core material and also be low enough to prevent break up of the shell fluid, which will disrupt encapsulation.

When determining the appropriate flow rate for core-shell fibres, it is important to take the electrical conductivity of the core and shell solutions into account. The flow rates have to be adjusted according to the electrical conductivity, due to the influence of conductivity on the fibre diameter.<sup>89</sup>

Failure to find the correct relative core and shell flow rates results in fibres that are not efficiently encapsulated because the encapsulation process is broken down by mixing. It was shown that as the relative core to shell flow rates were increased, the compound meniscus grew until a point was reached where the liquids in the compound cone started to mix. Mixing occurred when the core and shell flow rates were more or less equal.<sup>45</sup>

The flow rate used for the core material in coaxial electrospinning plays an important role in determining the structure and diameter of the final core-shell fibres.<sup>82</sup> At a very low core flow rate, solid nanofibre segments are generated because the axial pressure of the core is then insufficient to balance the viscous stress of the shell material and produce a continuous core-shell fibre structure. The core flow rate needs to be adjusted according to the increased viscous stress caused by the increased shell polymer concentration, which will stretch the core into a thinner strand.<sup>85</sup> Below a certain limiting core flow rate, continuous core-shell

fibres will not form and the core material will at most be segmented along the fibre length. Above this rate, continuous core-shell structures with relatively uniform core and shell thickness become attainable.<sup>82</sup> An excessively high core flow rate (compared to shell flow rate) on the other hand, could cause the core fluid jet to disrupt the process by breaking up the compound jet.<sup>79</sup>

The shell flow rate is important because if it is too low, there will be insufficient material to wrap the inner solution. This could lead to the core and shell materials being electrospun separately.<sup>95</sup> If the shell flow rate is too high the core material will not be continuous within the fibres.<sup>79</sup>

Increasing the core flow rate, while keeping the shell rate constant, leads to larger core diameters and thinner shell structures.<sup>82</sup> Decreasing the core flow rate leads to thinner fibres.<sup>86</sup> In general, an increase in the flow rate of either solution gives an increase in the average total fibre diameter.<sup>93</sup>

#### 2.3.6.3 *Core needle protrusion*

Jetting from the tip of a compound droplet does not necessarily mean that compound jets and subsequent core-shell fibres are being formed. The likelihood of forming compound jets and core-shell nanofibres is greatly increased when the core capillary protrudes outside the shell capillary by the appropriate distance. Both experimental and theoretical results have shown that the optimal core capillary protrusion, for core-shell nanofibre formation, is found at 50% of the radius of the shell capillary.<sup>84,91</sup> If the core capillary protrudes too far out of the shell orifice, a corona-like effect is created. This results in the emergence of jets from the side of the droplet, as well as the formation of multiple and unstable jets.<sup>101</sup> The optimal protrusion distance is dependent on several factors including the viscosity ratio of the liquids, the interfacial tension, and the feeding rates of the inner and the outer liquids.<sup>84,91</sup>

#### 2.3.6.4 *Coaxial spinneret diameters*

The use of a small ratio of core to shell capillary (inner) diameters is able to confine the core material more effectively. This encourages encapsulation of the core material.<sup>102</sup>

### 2.3.7 Melt coaxial electrospinning

Xia and co-workers<sup>26</sup> demonstrated a method based on melt coaxial electrospinning for fabricating phase change nanofibres consisting of long-chain hydrocarbons cores and composite shells. This method allows non-polar solids such as paraffins to be electrospun and encapsulated in a single step. They combined melt electrospinning with a coaxial spinneret to encapsulate a solid as the core material inside a composite or polymer matrix shell to generate nanofibre-based phase change materials. They produced thermally stable, PCM core-shell nanofibres. The fibres displayed novel segmented core morphologies due to rapid solidification of the hydrocarbons, driven by evaporative cooling of the shell carrier solution. This same melt coaxial process was also used by Li et al.<sup>24</sup> to produce thermochromic core-shell nanofibres.

### 2.3.8 Electrospinning of thermochromic fibres

Thermochromic fibres have been produced using the melt coaxial electrospinning process. This process requires the core material to be kept above the melting temperature of the thermochromic composite during the entire electrospinning process. If the temperature is not kept sufficiently high the needle will become blocked. Based on fluorescence studies these fibres had good thermochromic reversibility but the coloured state was not actually visibly perceivable. The effect was explained by the sub-micron core and shell thicknesses of the fibres. The core diameters (200–400 nm) and shell thicknesses (200–500 nm) were in the range of the wavelength of visible light (400–800 nm) and this gave rise to the Mie light scattering phenomenon which masked the blue colour of CVL (in the solid state of the dye composite) and made the fibres appear white. The total average diameters of these fibres were between 500 nm and 2  $\mu\text{m}$ .<sup>24</sup>



## 2.4 References

1. *Thermochromism*. [cited 11 April 2008]; Available from: [http://infochem.hanyang.ac.kr/researches/researches\\_thermo\\_english.html](http://infochem.hanyang.ac.kr/researches/researches_thermo_english.html).
2. Lam Po Tang, S. and Stylios, G.K., *An overview of smart technologies for clothing design and engineering*. International Journal of Clothing Science and Technology, 2006, **18**(2):108-128.
3. Nelson, G., *Application of microencapsulation in textiles*. International Journal of Pharmaceutics, 2002, **242**:55-62.
4. Ma, Y., Zhang, X., Zhu, B. and Wu, K., *Research on reversible effects and mechanism between the energy-absorbing and energy-reflecting states of chameleon-type building coatings*. Solar Energy, 2002, **72**(6):511-520.
5. Seeboth, A. and Löttsch, D., *Thermochromic phenomena in polymers*. 2008, Smithers Rapra: UK.
6. Seeboth, A., Kriwanek, J. and Vetter, R., *The first example of thermochromism of dyes embedded in transparent polymer gel networks*. Journal of Materials Chemistry, 1999, **9**(10):2277-2278.
7. Seeboth, A., Kriwanek, J. and Vetter, R., *Novel chromogenic polymer gel networks for hybrid transparency and color control with temperature*. Advanced Materials, 2000, **12**(19):1424-1426.
8. Seeboth, A., Kriwanek, J., Löttsch, D. and Patzak, A., *Chromogenic polymer gels for reversible transparency and color control with temperature at a constant volume*. Polymers for Advanced Technologies, 2002, **13**(7):507-512.
9. Christie, R.M., Robertson, S. and Taylor, S., *Design concepts for a temperature-sensitive environment using thermochromic colour change*. Colour: Design & Creativity, 2007, **1**.
10. MacDonald, J.G., Schorr, P., Archart, K.D., Brown, T.S., Linton, L.A. and Oslund, S.G., *Thermochromic compositions for skin application, US Patent 0026105 A1*, 2008.
11. Seeboth, A., Yin, C., Kriwanek, J., Löttsch, D. and Schäper, R., *Thermochromic polyolefin foils*. Journal of Applied Polymer Science, 2005, **96**:1789-1792.
12. Seeboth, A., Löttsch, D., Potechius, E. and Vetter, R., *Thermochromic effects of leuco dyes studied in polypropylene*. Chinese Journal of Polymer Science, 2006, **24**(4):363-368.

13. Zhu, C.F. and Wu, A.B., *Studies on the synthesis and thermochromic properties of crystal violet lactone and its reversible thermochromic complexes*. *Thermochimica Acta*, 2005, **425**(1-2):7-12.
14. Burkinshaw, S.M., Griffiths, J. and Towns, A.D., *Reversibly thermochromic systems based on pH-sensitive spirolactone-derived functional dyes*. *Journal of Materials Chemistry*, 1998, **8**:2677-2683.
15. Periyasamy, S. and Khanna, G. *Thermochromic colors in textiles*. [Article] [cited 2009 12 August]; Available from: <http://www.fibre2fashion.com/industry-article/9/804/thermochromic-colors-in-textiles1.asp>.
16. Luthern, J. and Peredes, A., *Determination of the stoichiometry of a thermochromic color complex via Job's method*. *Journal of Materials Science Letters*, 2000, **19**:185-188.
17. MaLaren, D.C. and White, M.A., *Dye-developer interactions in the crystal violet lactone-lauryl gallate binary system: implications for thermochromism*. *Journal of Materials Chemistry*, 2003, **13**:1695-1700.
18. Huang, Z.-M., Zhang, Y.Z., Kotaki, M. and Ramakrishna, S., *A review on polymer nanofibers by electrospinning and their applications in nanocomposites*. *Composites Science and Technology*, 2003, **63**:2223-2253.
19. Ramakrishna, S., Fujihara, K., Teo, K.E., Lim, T.C. and Ma, Z., *An introduction to electrospinning and nanofibers*. 2005, World Scientific Publishing: Singapore.
20. Doshi, J. and Reneker, D.H., *Electrospinning process and applications of electrospun fibers*. *Electrostatics*, 1995, **35**:151-160.
21. Zhang, Y., Lim, C.T., Ramakrishna, S. and Huang, Z.-M., *Recent development of polymer nanofibers for biomedical and biotechnological applications*. *Journal of Materials Science: Materials in Medicine*, 2005, **16**:933-946.
22. Katti, D.S., Robinson, K.W., Ko, F.K. and Laurencin, C.T., *Bioresorbable nanofiber-based systems for wound healing and drug delivery: Optimization of fabrication parameters*. *Journal of Biomedical Materials Research, Part B: Applied Biomaterials*, 2004, **70B**(2):286-296.
23. Schreuder-Gibson, H.L., Gibson, P., Senecal, K., Sennet, M., Walker, J. and Yeomans, W., *Protective textile materials based on electrospun nanofibers*. *Journal of Advanced Materials*, 2002, **34**(3):44-55.

24. Li, F., Zhao, Y., Wang, S., Han, D., Jiang, L. and Song, Y., *Thermochromic core-shell nanofibers fabricated by melt coaxial electrospinning*. Journal of Applied Polymer Science, 2009, **112**:269-274.
25. Rabolt, J.F. and Bianco, A., *Active and adaptive photochromic fibers, textiles and membranes*, Patent WO/2005/090654, 2005.
26. McCann, J.T., Marquez, M. and Xia, Y., *Melt coaxial electrospinning: A versatile method for encapsulation of solid materials and fabrication of phase change nanofibers*. Nano Letters, 2006, **6**(12):2868-2872.
27. Deitzel, J.M., Kleinmeyer, J., Harris, D. and Beck Tan, N.C., *The effect of processing variables on the morphology of electrospun nanofibers and textiles*. Polymer, 2001, **42**:261-272.
28. Veleirinho, B. and Lopes-da-Silva, J.A., *Application of electrospun poly(ethylene terephthalate) nanofiber mat to apple juice clarification*. Process Biochemistry (in press), 2008.
29. Zong, X., Kim, K., Fang, D., Ran, S., Hsiao, B.S. and Chu, B., *Structure and process relationship of electrospun bioabsorbable nanofiber membranes*. Polymer, 2002, **43**:4403-4412.
30. Liu, H. and Hsieh, Y.-L., *Ultrafine fibrous cellulose membranes from electrospinning of cellulose acetate*. Journal of Polymer Science, Part B: Polymer Physics, 2002, **40**:2119-2129.
31. Zhou, F.-L. and Gong, R.-H., *Review - Manufacturing technologies of polymeric nanofibres and nanofibre yarns*. Polymer International, 2008, **57**:837-845.
32. Moghe, A.K. and Gupta, B.S., *Co-axial electrospinning for nanofiber structures: Preparation and applications*. Polymer Reviews, 2008, **48**(2):353-377.
33. Cooley, J.F., *US Patent 692,631*, 1902.
34. Morton, W.J., *US Patent 705,691*, 1902.
35. Cooley, J.F., *US Patent 745,276*, 1903.
36. Hagiwaba, K., Oji-Machi, O. and Ku, K., *Jpn Patent 1,699,615*, 1929.
37. Formhals, A., *US Patent 1,975,504*, 1934.
38. Formhals, A., *US Patent 2,160,962*, 1939.
39. Formhals, A., *US Patent 2,187,302*, 1940.
40. Formhals, A., *US Patent 2,323,025*, 1943.
41. Formhals, A., *US Patent 2,349,950*, 1944.

42. Li, D. and Xia, Y., *Electrospinning of nanofibers: Reinventing the wheel?* Advanced Materials, 2004, **16**(14):1151-1170.
43. Greiner, A. and Wendorff, J.H., *Electrospinning: A fascinating method for the preparation of ultrathin fibers.* Angewandte Chemie International Edition, 2007, **46**:5670-5703.
44. Lyons, J., Li, C. and Ko, F., *Melt-electrospinning part I: processing parameters and geometric properties.* Polymer, 2004, **45**(22):7597-7603.
45. Diaz, J.E., Barrero, A., Marquez, M. and Loscertales, I.G., *Controlled encapsulation of hydrophobic liquids in hydrophilic polymer nanofibers by co-electrospinning.* Advanced Functional Materials, 2006, **16**(16):2110-2116.
46. Teo, W.E., Gopal, R., Ramaseshan, R., Fujihara, K. and Ramakrishna, S., *A dynamic liquid support system for continuous electrospun yarn fabrication.* Polymer, 2007, **48**:3400-3405.
47. Yang, Y., Jia, Z., Hou, L., Li, Q., Wang, L. and Guan, Z., *Controlled deposition of electrospinning jet by electric field distribution from an insulating material surrounding the barrel of the polymer solution.* IEEE Transactions on Dielectrics and Electrical Insulation, 2008, **15**(1):269-276.
48. Li, D., Wang, Y. and Xia, Y., *Electrospinning nanofibers as uniaxially aligned arrays and layer-by-layer stacked films.* Advanced Materials, 2004, **16**(4):361-366.
49. Li, D., Wang, Y. and Xia, Y., *Electrospinning of polymeric and ceramic nanofibers as uniaxially aligned arrays.* Nano Letters, 2003, **3**(8):1167-1171.
50. Yee, W.A., Nguyen, A.C., Lee, P.S., Kotaki, M., Liu, Y., Tan, B.T., Mhaisalkar, S. and Lu, X., *Stress-induced structural changes in electrospun polyvinylidene difluoride nanofibers collected using a modified rotating disk.* Polymer, 2008, **49**(19):4196-4203.
51. Teo, W.E. and Ramakrishna, S., *A review on electrospinning design and nanofibre assemblies.* Nanotechnology, 2006, **17**:R89-R106.
52. Reneker, D.H. and Yarin, A.L., *Electrospinning jets and polymer nanofibers.* Polymer, 2008, **49**:2387-2425.
53. Thompson, C.J., Chase, G.G., Yarin, A.L. and Reneker, D.H., *Effects of parameters on nanofiber diameter determined from electrospinning model.* Polymer, 2007, **48**:6913-6922.

54. McKee, M.G., Wilkes, G.L., Colby, R.H. and Long, T.E., *Correlations of solution rheology with electrospun fiber formation of linear and branched polyesters*. *Macromolecules*, 2004, **37**(5):1760-1767.
55. Shenoy, S.L., Bates, W.D., Frisch, H.L. and Wnek, G.E., *Role of chain entanglements on fiber formation during electrospinning of polymer solutions: good solvent, non-specific polymer-polymer interaction limit*. *Polymer*, 2005, **46**:3372-3384.
56. Fong, H., Chun, I. and Reneker, D.H., *Beaded nanofibers formed during electrospinning*. *Polymer*, 1999, **40**:4585-4592.
57. Bueche, F., *Physical Properties of Polymers*. 1979, Robert E. Krieger Publishing Company: New York.
58. Lee, K.H., Kim, H.Y., Bang, H.J., Jung, Y.H. and Lee, S.G., *The change of bead morphology formed on electrospun polystyrene fibers*. *Polymer*, 2003, **44**:4029-4034.
59. Buchko, C.J., Chen, L.C., Shen, Y. and Martin, D.C., *Processing and microstructural characterization of porous biocompatible protein polymer thin films*. *Polymer*, 1999, **40**:7397-7407.
60. Yao, L., Haas, T.W., Guiseppi-Elie, A., Bowlin, G.L., Simpson, D.G. and Wnek, G.E., *Electrospinning and stabilization of fully hydrolyzed poly(vinyl alcohol) fibers*. *Chemical Materials*, 2003, **15**(9):1860-1864.
61. Kriegel, C., Kit, K.M., McClements, D.J. and Weiss, J., *Electrospinning of chitosan-poly(ethylene oxide) blend nanofibers in the presence of micellar surfactant solutions*. *Polymer*, 2009, **50**(1):189-200.
62. Hohman, M.M., Shin, M., Rutledge, G. and Brenner, M.P., *Electrospinning and electrically forced jets. II. Applications*. *Physics of Fluids*, 2001, **13**(8):2221-2236.
63. Son, W.K., Youk, J.H., Lee, T.S. and Park, W.H., *The effects of solution properties and polyelectrolyte on electrospinning of ultrafine poly(ethylene oxide) fibers*. *Polymer*, 2004, **45**:2959-2966.
64. Megelski, S., Stephens, J.S., Chase, D.B. and Rabolt, J.F., *Micro- and nanostructured surface morphology on electrospun polymer fibers*. *Macromolecules*, 2002, **35**:8456-8466.
65. Supaphol, P., Mit-uppatham, C. and Nithitanakul, M., *Ultrafine electrospun polyamide-6 fibers: effects of solvent system and emitting electrode polarity on morphology and average fiber diameter*. *Macromolecular Materials and Engineering*, 2005, **290**:933-942.

66. Kessick, R., Fenn, J. and Tepper, G., *The use of AC potentials in electrospaying and electrospinning processes*. Polymer, 2004, **45**(9):2981-2984.
67. Zhao, S., Wu, X., Wang, L. and Huang, Y., *Electrospinning of ethyl-cyanoethyl cellulose/tetrahydrofuran solutions*. Journal of Applied Polymer Science, 2004, **91**:242-246.
68. Katta, P., Alessandro, M., Ramsier, R.D. and Chase, G.G., *Continuous electrospinning of aligned polymer nanofibers onto a wire drum collector*. Nano Letters, 2004, **4**(11):2215-2218.
69. Ojha, S.S., Afshari, M., Kotek, R. and Gorga, R.E., *Morphology of electrospun nylon-6 nanofibers as a function of molecular weight and processing parameters*. Journal of Applied Polymer Science, 2008, **108**:308-319.
70. Liu, Y., Chen, J., Misoska, V. and Wallace, G.G., *Preparation of novel ultrafine fibers based on DNA and poly(ethylene oxide) by electrospinning from aqueous solutions*. Reactive and Functional Polymers, 2007, **67**(5):461-467.
71. Gomes, D.S., da Silva, A.N.R. and Morimoto, N.I., *Characterization of an electrospinning process using different PAN/DMF concentrations*. Polímeros: Ciência e Tecnologia, 2007, **17**(3):206-211.
72. Casper, C.L., Stephens, J.S., Tassi, N.G., Chase, D.B. and Rabolt, J.F., *Controlling surface morphology of electrospun polystyrene fibers: Effect of humidity and molecular weight in the electrospinning process*. Macromolecules, 2004, **37**:573-578.
73. Srinivasarao, M., Collings, D., Philips, A. and Patel, S., *Three-dimensionally ordered array of air bubbles in a polymer film*. Science, 2001, **292**(5514):79-83.
74. Kim, G.-T., Lee, J.-S., Shin, J.-H., Ahn, Y.-C., Hwang, Y.-J., Shin, H.-S., Lee, J.-K. and Sung, C.-M., *Investigation of pore formation for polystyrene electrospun fiber: Effect of relative humidity*. Korean Journal of Chemical Engineering, 2005, **22**(5):783-788.
75. Sun, Z., Zussman, E., Yarin, A.L., Wendorff, J.H. and Greiner, A., *Compound core-shell polymer nanofibers by co-electrospinning*. Advanced Materials, 2003, **15**(22):1929-1932.
76. Wei, M., Mead, J. and Sung, C., *Phase morphology of electrospun nanofibers from polybutadiene (PB) /polycarbonate (PC) blends*. Polymer Preprints (American Chemical Society, Division of Polymer Chemistry), 2003, **44**(2):79-80.

77. Wei, M., Lee, J., Kang, B. and Mead, J., *Preparation of core-sheath nanofibers from conducting polymer blends*. Macromolecular Rapid Communications, 2005, **26**:1127-1132.
78. Bazilevsky, A.V., Yarin, A.L. and Megaridis, C.M., *Co-electrospinning of core-shell fibers using a single-nozzle technique*. ACS Journal of surfaces and colloids, 2007, **23**(5):2311-2314.
79. Yu, J.H., Fridrikh, S.V. and Rutledge, G.C., *Production of submicrometer diameter fibers by two-fluid electrospinning*. Advanced Materials, 2004, **16**(17):1562-1566.
80. Zhang, Y., Huang, Z.-M., Xu, X., Lim, C.T. and Ramakrishna, S., *Preparation of core-shell structured PCL-r-gelatin bi-component nanofibers by coaxial electrospinning*. Chemistry of Materials, 2004, **16**(18):3406-3409.
81. Huang, Z.-M., Zhang, Y. and Ramakrishna, S., *Double-layered composite nanofibers and their mechanical performance*. Journal of Polymer Science Part B: Polymer Physics, 2005, **43**(29):2853-2861.
82. Li, D. and Xia, Y., *Direct fabrication of composite and ceramic hollow nanofibers by electrospinning*. Nano Letters, 2004, **4**(5):933-938.
83. McCann, J.T., Li, D. and Xia, Y., *Electrospinning of nanofibers with core-sheath, hollow, or porous structures*. Journal of Materials Chemistry, 2005, **15**:735-738.
84. Zussman, E., Yarin, A.L., Bazilevsky, A.V., Avrahami, R. and Feldman, M., *Electrospun polyacrylonitrile/poly(methyl methacrylate)-derived turbostratic carbon micro-/nanotubes*. Advanced Materials, 2006, **18**(3):348-353.
85. Wang, M., Jing, N., Su, C.B., Kameoka, J., Chou, C.-K., Hung, M.-C. and Chang, K.-A., *Electrospinning of silica nanochannels for single molecule detection*. Applied Physics Letters, 2006, **88**:33106(1-3).
86. Li, D., Babel, A., Jenekhe, S.A. and Xia, Y., *Nanofibers of conjugated polymers prepared by electrospinning with a two-capillary spinneret*. Advanced Materials, 2004, **16**(22):2062-2066.
87. Zhao, Q., Xin, Y., Huang, Z., Liu, S., Yang, C. and Li, Y., *Using poly[2-methoxy-5-(2'-ethyl-hexyloxy)-1,4-phenylene vinylene] as shell to fabricate the highly fluorescent nanofibers by coaxial electrospinning*. Polymer, 2007, **48**:4311-4315.
88. Li, D., McCann, J.T. and Xia, Y., *Use of electrospinning to directly fabricate hollow nanofibers with functionalized inner and outer surfaces*. Small, 2005, **1**(1):83-86.

89. Dror, Y., Salalha, W., Avrahami, R., Zussman, E., Yarin, A.L., Dersch, R., Greiner, A. and Wendorff, J.H., *One-step production of polymeric microtubes by co-electrospinning*. *Small*, 2007, **3**(6):1064-1073.
90. He, C.-L., Huang, Z.-M., Han, X.-J., Liu, L., Zhang, H.-S. and Chen, L.-S., *Coaxial electrospun poly(l-lactic acid) ultrafine fibers for sustained drug delivery*. *Journal of Macromolecular Science, Part B: Physics*, 2006, **45**:515-524.
91. Reznik, S.N., Yarin, A.L., Zussman, E. and Bercovici, L., *Evolution of a compound droplet attached to a core-shell nozzle under the action of a strong electric field*. *Physics of Fluids*, 2006, **18**:062101-062110.
92. Khalaf, A., *Production of hollow fibers by co-electrospinning of cellulose acetate*. MSc Thesis, University of Stellenbosch: Stellenbosch, March 2009.
93. Gupta, B.S., *Electrospun core-sheath fibers for soft tissue engineering*. 2006, NC State University.
94. Xin, Y., Huang, Z., Li, W., Jiang, Z., Tong, Y. and Wang, C., *Core-sheath functional polymer nanofibers prepared by co-electrospinning*. *European Polymer Journal*, 2008, **44**:1040-1045.
95. Sun, B., Duan, B. and Yuan, X., *Preparation of core/shell PVP/PLA ultrafine fibers by coaxial electrospinning*. *Journal of Applied Polymer Science*, 2006, **102**:39-45.
96. Yarin, A.L., Zussman, E., Wendorff, J.H. and Greiner, A., *Material encapsulation and transport in core-shell micro/nanofibers, polymer and carbon nanotubes and micro/nanochannels*. *Journal of Materials Chemistry*, 2007, **17**:2585-2599.
97. Andradý, A.L., *Science and technology of polymer nanofibers*. 2008, Wiley-Interscience: Hoboken, New Jersey.
98. Theron, S.A., Zussman, E. and Yarin, A.L., *Experimental investigation of the governing parameters in the electrospinning of polymer solutions*. *Polymer*, 2004, **45**:2017-2030.
99. Larsen, G., Spretz, R. and Velarde-Ortiz, R., *Use of coaxial gas jackets to stabilize Taylor cones of volatile solutions and to induce particle-to-fiber transitions*. *Advanced Materials*, 2004, **16**(2):166-1169.
100. Hu, Y. and Huang, Z.-M., *Numerical study on two-phase flow patterns in coaxial electrospinning*. *Journal of Applied Physics*, 2007, **101**(8).



101. Fridrikh, S.V., Yu, J.H., Brenner, M.P. and Rutledge, G.C., *Controlling the fiber diameter during electrospinning*. Physical Review Letters, 2003, **90**(14):144502/1-144502/4.
102. Chan, K.H.K. and Kotaki, M., *Fabrication and morphology control of poly(methyl methacrylate) hollow structures via coaxial electrospinning*. Journal of Applied Polymer Science, 2008, **111**:408-416.

# **Chapter 3**

## **Experimental**

This chapter gives an overview of the materials used in this study, and also describes the methods used to prepare the spinning liquids from these materials. Experimental techniques and equipment that were used to determine the most suitable spinning liquids and processing conditions, and to produce the reversibly thermochromic core-shell fibres are described. This is followed by a description of the analytical techniques that were used to analyze the fibres.

### **3.1 Preparation of core and shell solutions**

#### **3.1.1 Core**

##### *3.1.1.1 Thermochromic dye composition*

The thermochromic dye composite was comprised of varying ratios of the following materials (the selection is explained below):

- 1-Dodecanol
- Bisphenol A
- Crystal violet lactone

Dodecanol ( $\geq 95\%$  pure) and BPA ( $>99\%$  pure) was obtained from Sigma-Aldrich, South Africa and CVL was obtained from Leapchem, China. All materials were used as received from the supplier.

Not all phase change materials are suitable PCM-solvents for all types of dyes and developers used in thermochromic dye-developer-solvent systems. The selection had to be carefully considered. In order to enable the use of the thermochromic core-shell fibres in temperature sensing applications, colour changes around ambient or body temperatures were desired. Therefore PCMs with melting temperatures around or just above such temperatures would be most appropriate. Dodecanol and methyl stearate were selected as

possible PCM-solvents. Methyl stearate has a melting temperature of 39 °C. For colour changes at lower temperatures, dodecanol, which melts around 24–27 °C, is more suitable. It was later discovered experimentally that methyl stearate in combination with BPA and CVL was very hard to work with. The dye composite crept out of the container and did not dissolve in the type of solvents that were required or preferred for solvent facilitated coaxial electrospinning in this project. Therefore the PCM-solvent of choice for this study was dodecanol.

According to Luthern and Peredes,<sup>1</sup> the most commonly used weight ratio of BPA to CVL is about 2 to 1 (approximate molar ratio = 3.6:1 BPA:CVL). Their study on the stoichiometric relationship between BPA and CVL showed that maximum absorbance i.e. the deepest, most intense colour occurred at a BPA:CVL molar ratio of approximately 4:1. Based on the reviewed literature,<sup>1-3</sup> a molar ratio of 50:3:1 was initially chosen for the solvent:developer:dye (dodecanol:BPA:CVL) composition. Due to various problems, this ratio was changed as explained in Chapters 4 and 5.

#### 3.1.1.2 Preparation method

The preparation of the thermochromic dye composite was done by first melting and weighing off the required amount of dodecanol into a flask with a tight fitting lid. The dodecanol was then heated to 80 °C by immersing the preparation flask in an oil bath on a heated stirrer. The appropriate amounts of CVL and BPA that were required for the specific molar ratio of the dye composite, to be prepared, were weighed off. The CVL and BPA were added to the molten dodecanol at 80 °C. Stirring was continued at this temperature, in the closed flask, on the heated stirrer for another 6–12 hours until all components were dissolved and a clear, homogeneous mixture was obtained. The mixture was then slowly cooled to room temperature. The dye composites that were formed in this manner gave fully reversible, thermochromic transitions and could be used over several weeks.

In this project the thermochromic dye composite had to be coaxially electrospun as core material together with a shell solution of a suitable polymer–solvent system. The dye composite had to be in liquid form for coaxial electrospinning. The thermochromic dye composite was therefore either melt electrospun (melt coaxial electrospinning) at a

temperature above its melting temperature or dissolved in a solvent and electrospun from this liquid (solvent facilitated coaxial electrospinning).

During preparation for melt coaxial electrospinning, the thermochromic dye composite was heated to a temperature significantly above its melting point (40–60 °C) and held at that temperature until a homogeneous solution was obtained. It was attempted to maintain a temperature of at least 30 °C during melt coaxial electrospinning in order to keep the dye composite from precipitating. This was done by using an infrared lamp to heat the surrounding atmosphere.

During preparation for solvent facilitated coaxial electrospinning the thermochromic dye composite was dissolved in a suitable solvent. Prior to solvent addition, the thermochromic dye composite was heated in an oil bath, on a heated stirrer until a homogeneous solution was obtained. The dye composite was subsequently cooled (if necessary, depending on boiling point of additional solvent) to approximately 10 °C below the boiling point of the solvent to be added. At the appropriate temperature the solvent was added to the dye composite and the mixture was stirred while being cooled to room temperature. A homogeneous solution was obtained in this manner. This was used as core spinning solution.

### **3.1.2 Shell**

#### *3.1.2.1 Polymer systems*

A range of polymers was experimented with in order to find the polymer–solvent combination that could most effectively be used as the shell spinning liquid (in coaxial electrospinning), in combination with the selected core spinning liquid, to form core-shell fibres with a reversibly thermochromic effect. Conventional electrospinning of the polymer solutions was performed first, in order to determine the spinnability of the polymer solutions and to find the appropriate range of solution concentrations from which smooth, bead free fibres could be produced. Once suitable polymer–solvent combinations and suitable concentration ranges were determined, the solutions were used in coaxial electrospinning experiments to determine the compatibility of these solutions with the selected core spinning liquid. Adjustments were made until the most suitable

polymer–solvent system for the coaxial electrospinning of reversibly thermochromic fibres was determined. The following polymers were used: nylon 6,6; poly(vinyl alcohol) (PVOH); polyacrylonitrile (PAN); cellulose acetate (CA); and poly(methyl methacrylate) (PMMA). The polymers and solvents that were experimented with are tabulated in Table 3.1.

**Table 3.1****Polymers and solvents used in this study**

Polymer	Solvent
Nylon 6,6	Formic acid
PVOH ( $M_w = 85000 - 124000$ g/mol, 98-99% hydrolyzed)	Water (distilled) / Ethanol
PAN ( $M_w = 200\,000$ g/mol)	DMF
CA ( $M_w = \pm 163\,000$ g/mol <sup>4</sup> , acetal content = 39.9%)	Acetone / Dioxane
PMMA ( $M_w = 350\,000$ g/mol)	Acetone / Dioxane / Chloroform / Ethanol / THF / MEK / DMF

PVOH and PMMA were supplied by Sigma-Aldrich, SA; Nylon 6,6 was supplied by SANS, RSA; PAN was supplied by Acordis Kelheim GmbH, Germany; and CA was supplied by Eastman Kodak, USA. All polymers were used as received. Formic acid and dimethylformamide (DMF) were sourced from Sigma-Aldrich, RSA; acetone, ethanol and methyl ethyl ketone (MEK) from Sasol, RSA; 1,4-dioxane from British Drug House, England; and tetrahydrofuran (THF) and chloroform from KIMIX, RSA. All solvents were used as received, without further purification. Relevant solvent properties are tabulated in Table 3.2.

**Table 3.2****Properties of solvents used in this study**

Solvent	Surface tension at 20 °C (mN/m)	Dielectric constant at $\pm 25$ °C	Electrical conductivity at $\pm 20$ °C ( $\mu\text{S}/\text{cm}$ )	Vapour pressure at 20 °C (kPa)	Boiling point (°C)	Density (g/ml)
1,4-Dioxane	33	2.2	$\leq 3$	3.9	101	1.033
Acetone	25.2	20.7	0.02	30	56	0.786
Chloroform	27.5	4.8	0.02	30	61	1.489
DMF	37.1	38.3	$\leq 2.5$	0.3	153	0.944
Ethanol	22.39	24	0.0013	9	78	0.772
Formic Acid	37	58	5500	5.4	101	1.22
MEK	24.6	18.5	0.1	10.3	79	0.805
THF	26.4	7.58	$\approx 0$	19.3	64	0.886
Water	72	80.4	0.04	2.4	100	0.998

*3.1.2.2 Preparation of solutions*

Different polymers, solution concentrations and solvent combinations were used in this study. In each case the correct weight percentage (wt %) of polymer was weighed out and dissolved in the appropriate solvent. The mixture was stirred on a magnetic stirrer plate for 12 hours until a homogeneous solution was obtained. When homogeneous solutions could not be obtained at room temperature, the mixtures were heated in an oil bath, on a heated magnetic stirrer. In order to prevent boiling and evaporation of the solvent the mixtures were never heated to more than 10 °C below the boiling point of the solvent. Polymer solutions were used within 48 hours of preparation in order to eliminate evaporative loss of solvent and subsequent change in solution concentration.

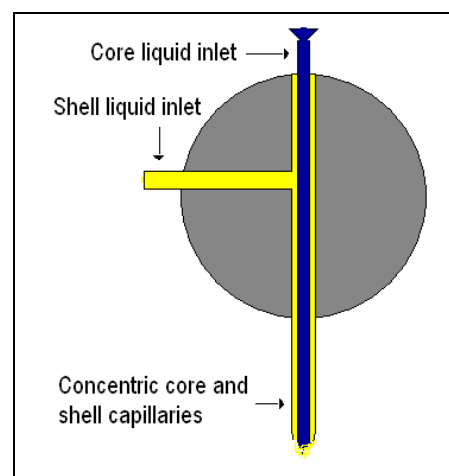
**3.2 Coaxial electrospinning****3.2.1 Apparatus**

A 30 kV high voltage supply, custom built by the Electrical Engineering Department (Stellenbosch University, RSA), was used to supply the electric field needed for the electrospinning process. A 33 dual syringe pump obtained from Harvard Apparatus (USA)

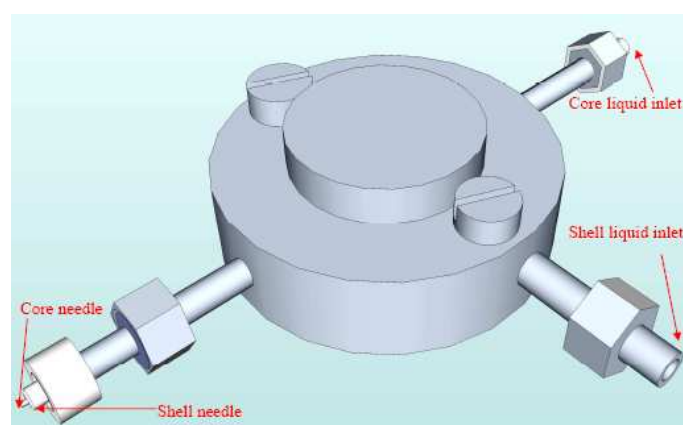
was used to supply the core and shell solutions at controlled feed rates. The solution reservoirs each consisted of a 5 ml syringe and polypropylene tubing (1.5 mm inner diameter, approximately 10 cm in length) to transport the core and shell solutions to the coaxial spinneret. The spinneret (Figure 3.1 (a)) assembled from standard HPLC components from VICI AG International (Switzerland) was fitted with a core capillary to create two concentric metal capillaries (Figure 3.1 (b)) which brought the core and shell solutions together at the spinneret tip for electrospinning. The inner (core) capillary was a needle with a blunt tip and inner diameter of 0.3 mm. The outer capillary was formed by the spinneret opening with an inner diameter of 2.0 mm or by a luer lock fitted onto the spinneret opening (Figure 3.1 (c)) to decrease the diameter to 1.2 mm.



(a)



(b)



(c)

**Figure 3.1** Images depicting the coaxial spinneret used in this study: (a) photograph; (b) schematic showing the coaxial capillaries; and (c) schematic<sup>4</sup> of the spinneret with a luer lock attached to the shell capillary.

### 3.2.2 Electrospinning setup and procedure

A schematic representation of the electrospinning setup is given in Figure 3.2. The positive electrode was attached, by an alligator clip, to the core capillary of the coaxial spinneret and the grounded electrode was attached, also by an alligator clip, to the collector. The core capillary was inserted through the top of the coaxial spinneret and subsequently the core feed entered the coaxial spinneret from the top. The shell capillary was formed by the opening around the core capillary inside the coaxial spinneret. The shell solution entered from the side of the coaxial spinneret. Shell and core solutions came together at the spinneret exit.

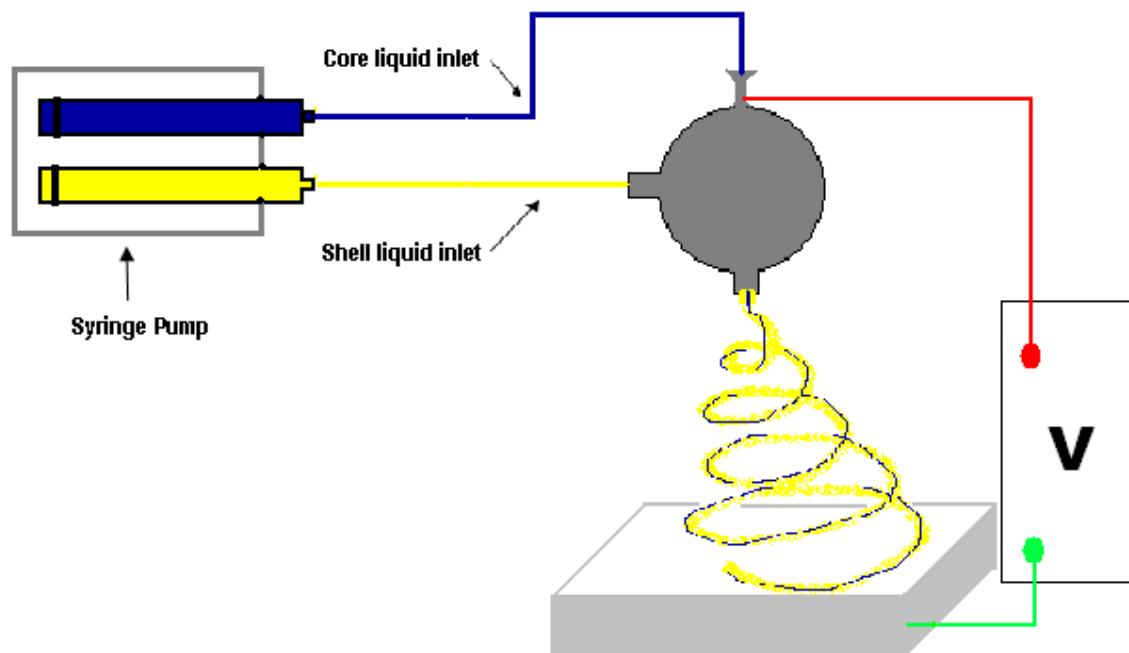


**Figure 3.2** Schematic of coaxial electrospinning setup used.

The polymer (shell) and thermochromic dye (core) solutions were added to individual 5 ml syringes (acting as reservoirs), which were attached to the polypropylene tubes and placed in the dual syringe pump. The opposite ends of the tubes were attached to their specific entry points on the coaxial spinneret (refer to Figure 3.1 (b) and Figure 3.2). The dual syringe pump was set to the required feed rates for the core and shell solutions and the spinneret was set at the required distance from the collector. To start the process, the syringes were



pushed by hand until the solutions reached the tip of the spinneret and then the pump was switched on.

As soon as the compound droplet (composed of core and shell solution) was formed, the high voltage source was switched on and set to the required voltage. A potential of 10–23 kV was applied to electrospin the range of spinning liquids that were investigated. Electrospun fibres were collected either on aluminium foil or on a rotating wire drum collector.

### 3.2.3 Collection of fibres

As mentioned, the fibres were electrospun onto a grounded collector. The collector consisted either of aluminium foil on a flat plate or of a rotating drum<sup>5</sup> composed of parallel metal wires (Figure 3.3), approximately 1 cm apart. Pieces of the fibre mats were removed at intervals during electrospinning and placed in the freezer ( $\pm 6$  °C) to test for thermochromic effect and ensure that the process was effective. After electrospinning, the fibre mats were removed from the collector, sealed in plastic bags and stored in the freezer until further analysis.

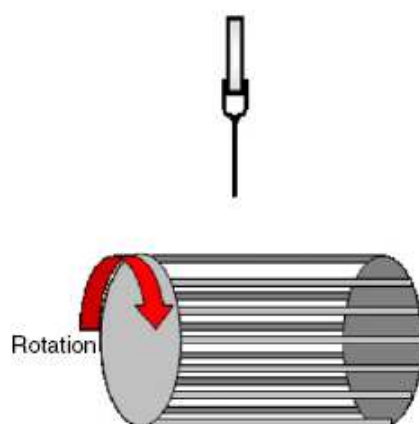


**Figure 3.3** Schematic of a rotating wire drum collector.<sup>5</sup>

### 3.3 Characterization techniques

#### 3.3.1 Viscosity

Viscosity measurements were performed using a Brookfield Digital Viscometer. The measurements were performed at 20 °C and the viscometer was set to 100 rpm. All samples gave stable readings after 1 minute, and these readings were recorded.

#### 3.3.2 Surface tension

The surface tensions of shell and core solutions were measured with a Krüss K6 Tensiometer. For each solution to be measured a 15 ml sample was prepared and added to the measuring vessel. The tests were performed at room temperature (20 °C) and the values adjusted according to the table of measured value against sample density in the Krüss manual. The density was determined by weighing the known volume of sample in the measuring vessel and calculating the density ( $\rho = m/V$ ) prior to surface tension measurement.

#### 3.3.3 Electrical conductivity

The electrical conductivities ( $\sigma$ ) of shell and core spinning solutions were determined by measuring the static resistivity ( $\rho$ ) of the solutions with a Fluke Multimeter. The resistivity (measured in ohm-metres,  $\Omega$  m), was calculated from the value measured across a 2 cm gap. The conductivity of the solution was calculated from this value, using the following equation:

$$\sigma = (1/\rho)$$

Conductivity is the inverse of resistivity. The conductivity values are given in micro-Siemens per centimetre ( $\mu\text{S}/\text{cm}$ ).

#### 3.3.4 Scanning electron microscopy (SEM)

Scanning electron microscopy was used to characterize electrospun fibres based on surface and cross-section morphology and to compare the average outer diameter of fibres. SEM analyses were performed using a Leo® 1430VP scanning electron microscope. Prior to

imaging all samples were cut from electrospun fibre mats and mounted on stubs with double sided tape. Samples were then sputter coated with a thin layer of gold in order to make the sample surface electrically conducting. The accelerating voltage was 5–7kV and the beam current was 1.5 nA, with a working distance of 13 mm and a spot size of 150.

### **3.3.5 Transmission electron microscopy (TEM)**

Transmission electron microscopy was used to examine the internal structure of fibres and to prove the existence of separate core and shell structures where possible. A Leo® Omega 912 Transmission Electron Microscope operating at 120 kV was used to obtain high-resolution images. Electrospun fibre samples were mounted on TEM grids. The grids were loaded into the chamber of the TEM apparatus. Photographs were taken using a Proscan CCD camera.

### **3.3.6 Thermogravimetric analysis (TGA)**

The relative weight percentages of dodecanol, BPA and PMMA in electrospun thermochromic fibres were determined by the use of TGA. A Perkin Elmer Pyris TGA 7 instrument was used. The samples were placed in standard aluminium pans, weighed accurately and placed in the TGA chamber. All TGA measurements were conducted under a nitrogen atmosphere. The heating rates for different samples are given in the results section (Chapter 4 and 5).

### **3.3.7 Differential scanning calorimetry (DSC)**

Differential scanning calorimetry was used to analyze the thermal behaviour (determine the melting and crystallisation temperatures) of the thermochromic dye composite on its own and inside electrospun fibres. A TA Instruments Q100 DSC, calibrated with indium metal according to standard procedures, was used. The samples were placed in a standard aluminium pan, weighed accurately and placed in the DSC chamber. All DSC measurements were conducted under a nitrogen atmosphere. All samples were heated to melt and homogenize the thermochromic composite throughout the core-shell fibres (i.e. to remove the thermal history). The samples were then cooled and heated again. Heating and cooling

rates were set at 1 °C/min or 5 °C/min depending on the sample. Data obtained during cooling was used to determine the crystallisation (solidification) temperatures and data obtained during the second heating step was used to determine the melting temperatures of the samples.

The temperatures at the highest points of the endothermic and exothermic peaks (on the plot of differential heat flow versus temperature) were used, respectively, as the melting and solidification points for dodecanol and for the thermochromic composite. These points were associated with and were compared to the thermochromic transition temperatures of the dyes and of the fibres.

### **3.3.8 Determination of thermochromic transition temperatures**

Bulk dyes were added to polytops and heated in an oil bath, on a heated stirrer. Photographs were taken at predetermined temperature intervals to indicate the colour of the dyes at these temperatures.

Thermochromic fibre mats as well as thermochromic dyes coated on paper were sealed in a plastic zip-lock bag and added to an ice bath that was cooled to  $\pm 2$  °C. Coated dye samples were prepared by dissolving the dye in chloroform, as it would be prior to coaxial electrospinning, and then coating it onto paper and leaving it to dry. At the starting temperature (2 °C) all the samples were in the coloured state. The ice bath was slowly heated, on heated stirrer equipped with a temperature probe. Photographs were taken at intervals as the temperature increased. The temperature at which each photograph was taken was recorded. This served as the visual method of determining the temperature of thermochromic colour loss for thermochromic fibres and thermochromic dye coatings.

### 3.4 References

1. Luthern, J. and Peredes, A., *Determination of the stoichiometry of a thermochromic color complex via Job's method*. Journal of Materials Science Letters, 2000, **19**:185-188.
2. Seeboth, A., Löttsch, D., Potechius, E. and Vetter, R., *Thermochromic effects of leuco dyes studied in polypropylene*. Chinese Journal of Polymer Science, 2006, **24**(4):363-368.
3. Burkinshaw, S.M., Griffiths, J. and Towns, A.D., *Reversibly thermochromic systems based on pH-sensitive spirolactone-derived functional dyes*. Journal of Materials Chemistry, 1998, **8**:2677-2683.
4. Khalaf, A., *Production of hollow fibers by co-electrospinning of cellulose acetate*. MSc Thesis, University of Stellenbosch: Stellenbosch, March 2009.
5. Teo, W.E. and Ramakrishna, S., *A review on electrospinning design and nanofibre assemblies*. Nanotechnology, 2006, **17**:R89-R106.

## **Chapter 4**

### **Results and Discussion – Part 1**

#### *Determination of Optimal Core and Shell Materials and Spinning Liquid Compositions*

##### **4.1 Introduction**

This chapter describes the initial thermochromic dye composition, the experiments that were performed to determine the ideal shell polymer–solvent combination and the additional solvent required in the core spinning liquid to enable solvent facilitated coaxial electrospinning of the core materials. This is followed by discussions of experiments in which the thermochromic dye composition was changed in attempts to improve the coaxial electrospinning process and the thermochromic transition of the composite. Thermal (DSC and TGA) and microscopic (SEM and TEM) analyses are included.

##### **4.2 Initial thermochromic dye composition and core spinning liquid**

This section describes the composition and thermochromic transition of the initial thermochromic dye composite that was used in the majority of coaxial electrospinning experiments with the shell polymer solutions discussed in Section 4.3. To enable processing of the thermochromic dye as core spinning liquid in coaxial electrospinning, the composite had to be either melted, or dissolved in a suitable solvent. The determination of the best method and of the facilitating solvent for the core spinning liquid is briefly discussed in this section. More details follow in Section 4.3 because the determination of the best method and correct facilitating solvent was dependent on, and went hand in hand with the selection of the shell polymer and solvent combination.

###### **4.2.1 Thermochromic dye composite and evaluation of its thermochromic transition**

The thermochromic dye composite was produced with a molar ratio of 50:3:1 dodecanol:BPA:CVL. This ratio was based on information found in literature<sup>1-3</sup> (as described

in Chapter 3). The thermochromic effect of this dye composite was tested by visual evaluation of the colour and composition of the composite at different temperatures. The dye composite (contained in a flask) was heated in an oil bath, on a heated stirrer, from the ambient temperature of  $\pm 20$  °C up to a temperature of 90 °C. The flask, containing the dye composite, was photographed at 20 °C (prior to heating) to show the colour and the physical state of the composite. At 35 °C and 50 °C it was removed from the oil bath and immediately photographed to show the colours and the physical appearance of the liquids at these temperatures. These images are shown in Figure 4.1.

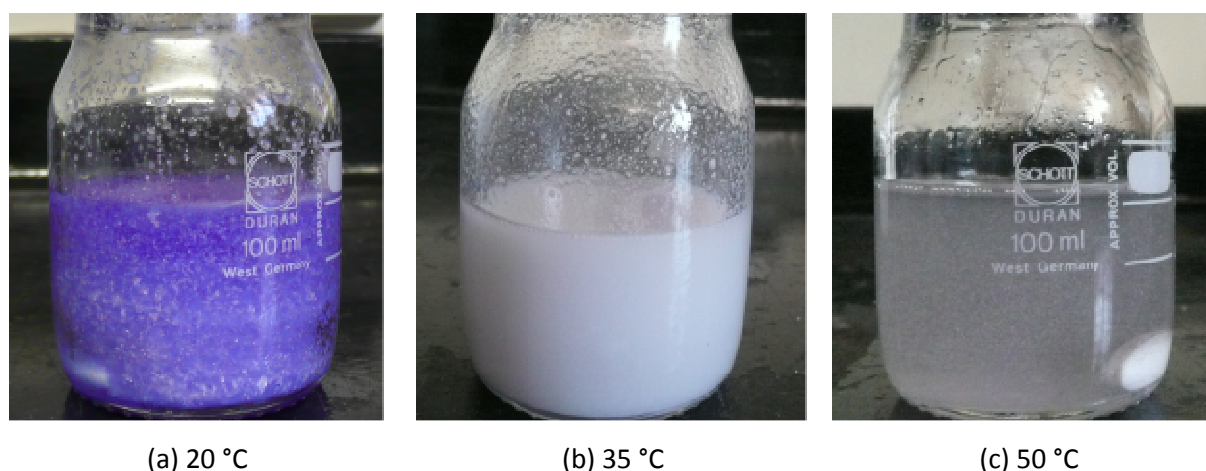


**Figure 4.1** Photographs showing the colour change of the 50:3:1 dodecanol:BPA:CVL (molar ratio) bulk thermochromic dye composite over a range of temperatures.

At 20 °C the composite was in the form of a blue solid. The composite started to melt and lose colour from 22–25 °C onwards. At 35 °C the composite was completely molten and had a white, milky colour and colloidal composition. At 50 °C the molten composite was colourless, with a colloidal composition. Full solubility and a homogeneous solution could only be obtained at temperatures of 80 °C and higher. Any lowering in the temperature led to the precipitation of particles and the reformation of the colloidal liquid.

The individual solubilities of CVL and BPA in molten dodecanol were evaluated. It was found that at the respective ratios used for the 50:3:1 composite (i.e. molar ratio of 50:1 dodecanol:CVL, and 50:3 dodecanol:BPA), BPA completely dissolved at temperatures of 24–35 °C (i.e. where the dodecanol was in the molten state) and CVL did not. Complete solubility of CVL in the molten dodecanol could only be attained when the mixture was

heated to temperatures of 80 °C and higher. Therefore the colloidal particles, shown in Figure 4.1 (b & c), were probably composed of CVL.

#### 4.2.2 Core spinning liquid formulation

The solid thermochromic dye composite had to be in liquid form in order to use it as core spinning liquid in coaxial electrospinning. Coaxial electrospinning experiments (as will be discussed in Section 4.3) were performed with molten and dissolved thermochromic composites.

##### 4.2.2.1 *Molten thermochromic composite as core spinning liquid*

An infrared lamp was used to heat the environment around the coaxial electrospinning setup to a temperature of  $\pm 30$  °C (the temperature was monitored with a thermometer). The dye composite was melted and transferred to this environment, where the molten state of the composite was expected to be maintained. This method of melt coaxial electrospinning was problematic due to the difficulties experienced in heating the whole system, including the environment and all components of the electrospinning setup that were in contact with the dye composite, to sufficiently high temperatures to avoid precipitation of any of the dye components. The spinneret openings, especially the core capillary, frequently became blocked due to dodecanol (i.e. dye composite) solidification. Another problem was that, during coaxial electrospinning with the molten dye composite, the molten dodecanol easily extracted the shell solvent, which led to the polymer precipitating at the spinneret exit and interfering with the electrospinning process.

##### 4.2.2.2 *Dissolved thermochromic composite as core spinning liquid*

Following the problems with melt coaxial electrospinning, the focus was shifted to the method of solvent facilitated coaxial electrospinning of the thermochromic composite. In order to determine suitable facilitating solvents, ethanol, DMF, acetone and chloroform were added, in separate experiments, to the 50:3:1 thermochromic composite in 1:1 v/v ratios. DMF, acetone and chloroform instantly dissolved all components and gave clear, homogeneous solutions. Ethanol also dissolved the composite but it took a few hours to fully



dissolve and the solution did not always remain homogeneous. Ethanol was therefore, not a suitable core-facilitating solvent.

In order to maximize the amount of thermochromic composite in the cores of the core-shell fibres after solvent evaporation; and to avoid the risk of residual solvent in the fibres, the smallest amount of acetone and chloroform (i.e. smallest solvent:composite ratio) that would still dissolve the thermochromic composite had to be determined. The solvent:composite ratios were lowered stepwise (1:1, 4:5, 3:5, 2:5, 1:5 v/v) in order to find these ratios. The smallest ratios at which a clear, homogeneous solutions could be obtained was 2:5–3:5 v/v for acetone:composite (depending on the ambient temperatures) and 2:5 v/v for chloroform:composite. The DMF was only tested in the 1:1 v/v ratio. The thermochromic transition of the dye composites could be reproduced following evaporation of these solvents from the composite.

The DMF:composite ratio of 1:1 v/v; the acetone:composite ratios of 2:5–3:5 v/v; and the chloroform:PMMA ratio of 2:5 v/v could be used for the solvent facilitated coaxial electrospinning experiments. At these ratios the thermochromic dye composite was in solution at room temperature. This would enable coaxial electrospinning without melting the core material during processing. The core facilitating solvent that was selected for coaxial electrospinning with each specific polymer–solvent combination is given with the different experiments, as discussed in Section 4.3.

### **4.3 Shell polymer solution composition and coaxial electrospinning**

This section includes the results and discussions of experiments that were performed to find suitable shell spinning solution compositions that could be used, together with the core spinning liquid (thermochromic dye composite, either molten or dissolved in a suitable solvent), for coaxial electrospinning to form thermochromic core-shell fibres. During coaxial electrospinning the core and shell solutions were in contact. It was therefore extremely important to take into account the possible interactions between the various core and shell components. The interactions of materials, especially solvent effects, limited the options in terms of shell solution compositions.

As previously mentioned, the addition of solvent to the thermochromic dye composite appeared to be more feasible than melting this material to facilitate coaxial electrospinning. There were several things to consider with the selection of this solvent. The selected shell spinning solution largely determined what the most appropriate core facilitating solvent would be. The following prerequisites guided the choices for core solvent and shell spinning solution composition:

- It was important that neither the core nor the shell spinning solution lead to immediate precipitation of any component in the other solution.
- The interfacial tension between core and shell solutions needed to be as low as possible. In other words, the surface tension of core and shell solutions had to be similar in order to enable a sufficient viscous dragging effect. Similar requirements have been identified in literature.<sup>4,5</sup>
- In some cases the creation of a low interfacial tension together with the inhibition of either solution precipitating the other inevitably lead to core and shell solution miscibility. Miscibility of the core and shell solutions could be expected to lead to less clearly defined boundaries between the core and the shell structures of the resulting fibres.<sup>6,7</sup> It was more important that the first two parameters were reached than the latter breached.

Five different polymers were evaluated for the shell solution: Nylon 6,6, PVOH, PAN, CA and PMMA. When considering the three prerequisites above, only CA and PMMA exhibited satisfactory results to allow their possible use as polymer for the shell solution during coaxial electrospinning with a thermochromic dye composite as core material.

#### **4.3.1 Summary of polymer and solvent combinations**

For each polymer, a range of suitable solvents were selected. For each solvent system (combined or single solvent), in which the polymer dissolved to form a homogeneous solution, a range of solutions with different polymer weight percentages (wt%) were made. These solutions were tested for spinnability by conventional electrospinning. Solutions that resulted in fibres were examined under the SEM to check for beads and to examine the

morphology. Only solutions that formed bead free and smooth fibres were used in experiments for coaxial electrospinning.

Table 4.1 provides a summary of notable results from the Nylon 6,6, PVOH and PAN polymer and solvent systems that were evaluated. This is followed by more detailed results and discussions of the CA and PMMA polymer solvent combinations and their evaluation. Although the main focus of this section is on the choice of polymer and solvent for the shell spinning solution, frequent references are made to the core spinning solution to point out how the interdependence of these two solutions influenced the choices that were made.

**Table 4.1**

**Summary of notable results for the selected polymer–solvent systems**

Polymer & Solvent(s)	Results
<p><b>Nylon 6,6</b> in formic acid</p>	<ul style="list-style-type: none"> <li>▪ Successful single solution electrospinning</li> <li>▪ Below 20 wt% - no fibres, only electrospaying</li> <li>▪ 20 wt% - severely beaded fibres</li> <li>▪ 30–40 wt% - smooth, uniform fibres with average diameters of 390 nm and 1140 nm respectively for 30 wt% and 40 wt% (refer to Figure B1, Appendix B)</li> <li>▪ Once a sufficiently high concentration (30–40 wt%), providing enough polymer chain entanglements to produce uniform fibres, was reached, the polymer solution had become highly viscous and resistant to flow. This was difficult to work with and caused blocking of the spinneret orifice.</li> <li>▪ The problem of high resistance to flow, in combination with the harshness of the solvent, and problems with solution creeping out of the spinneret opening made this option unsuitable for coaxial electrospinning experiments.</li> </ul>
<p><b>PVOH</b> in H<sub>2</sub>O and H<sub>2</sub>O:ethanol</p>	<ul style="list-style-type: none"> <li>▪ Single electrospinning: 8–12 wt% formed bead free and uniform fibres; 11–17 cm spinning distance and 10 kV voltage gave the best results (refer to, Figure B2, Appendix B for SEM images of these fibres)</li> <li>▪ Coaxial electrospinning: only performed with a molten core; could not find a suitable core solvent (all options precipitated PVOH from the shell solution) for solvent facilitated coaxial electrospinning</li> <li>▪ Viscous dragging forces of the shell solution on the core composite were insufficient to facilitate core-shell electrospinning and entrain the core material. This was probably due to the high interfacial tension between the PVOH solution (in water (H<sub>2</sub>O)) and the molten thermochromic dye composite as core liquid (the surface tension of H<sub>2</sub>O is</li> </ul>

	<p>70 mN/m (at 20 °C), and that of molten dodecanol is <math>\pm 30</math> mN/m. The surface tension of a polymer solution is very similar to the surface tension of the solvent(s) used to make the solution. The PVOH shell solutions (in water) and molten thermochromic dye composites were immiscible.</p> <ul style="list-style-type: none"> <li>▪ Addition of a surfactant, to lower the surface tension of the water-based shell solution, did not lead to the production of core-shell fibres either. The core material still simply accumulated at the spinneret exit until it broke through the shell layer and was electrospayed onto the collector.</li> <li>▪ Addition of ethanol to the water-based PVOH shell solution proved to lower the interfacial tension because it resulted in some degree of dragging of the core liquid (surface tension of ethanol is 23 mN/m at 20 °C).</li> <li>▪ Ethanol addition rendered the core and shell solutions slightly miscible, enabling dodecanol from the core to extract ethanol from the shell solution. This resulted in such a degree of precipitation from the PVOH solution that needle blockage and the subsequent interruption of the electrospinning process became a problem.</li> </ul>
<p><b>PAN in DMF</b></p>	<ul style="list-style-type: none"> <li>▪ Single electrospinning: 8 wt% solutions produced bead free, uniform fibres (refer to Figure B3, Appendix B)</li> <li>▪ Coaxial electrospinning: DMF has a surface tension of 37 mN/m (at 20 °C). This surface tension is much closer, compared to previous polymer–solvent combinations, to that of molten dodecanol (the major core component). The similar shell and core liquid surface tensions, which could be expected for these experiments, facilitated the viscous dragging effect to the extent that small amounts of core material were entrained during some of the experiments (especially when the core dye composite was mixed 1:1 v/v with DMF).</li> <li>▪ Fibres were non-uniform with rough surfaces and despite numerous attempts, using a range of parameters; a stable process could not be achieved.</li> <li>▪ Molten dodecanol resulted in precipitation of the shell solution and easy blockage of the spinneret opening. Addition of DMF to the core spinning solution did not enhance core-shell spinning sufficiently; precipitation was still a problem.</li> <li>▪ Interfacial tension between the PAN solution (in DMF) and the thermochromic composite (molten or dissolved in DMF) was apparently still too high for effective viscous dragging.</li> <li>▪ Surfactant addition did not produce satisfactory results either.</li> <li>▪ No other compatible solvent, which could be added to the core spinning solution to help facilitate coaxial electrospinning (without interfering with or precipitating the polymer from the shell solution), could be found. Coaxial electrospinning was not effective with PAN as shell forming polymer.</li> </ul>

### 4.3.2 Evaluation of cellulose acetate as possible shell forming polymer

It was known from previous studies in our group that a 14 wt% solution of CA in a solvent combination of acetone–dioxane in a 2:1 v/v ratio could be used to produce bead free core-shell fibres when using a core liquid of mineral oil.<sup>8</sup> A different core spinning liquid would be used in the current study and this would have different interactions with the shell polymer solution and therefore the coaxial electrospinning results were not expected to be the same.

#### 4.3.2.1 CA concentration and acetone:dioxane solvent ratio studies

The 14 wt% CA (2:1 v/v acetone:dioxane) shell composition was used as starting point for the current study. Polymer concentration and solvent ratio studies were performed to evaluate the suitability of the different compositions for solvent facilitated coaxial electrospinning of thermochromic core-shell fibres.

#### Concentration study - single electrospinning

In order to evaluate the possibility of using higher and lower concentrations of CA in 2:1 v/v acetone:dioxane for the current study (i.e. to be used as shell spinning solution in the coaxial electrospinning of thermochromic fibres), single electrospinning experiments were performed with 11 wt% and 17 wt% CA (2:1 v/v acetone:dioxane) solutions.

Single electrospinning of 11 wt% and 17 wt% CA solutions in 2:1 acetone:dioxane were successfully used to produce relatively uniform fibres. The 11 wt% CA (2:1 acetone:dioxane) solution resulted in fibres with a few beads, whereas smooth fibres were produced from the 17 wt% CA (2:1 acetone:dioxane) solution. Figure 4.2 shows the SEM images of these fibres.

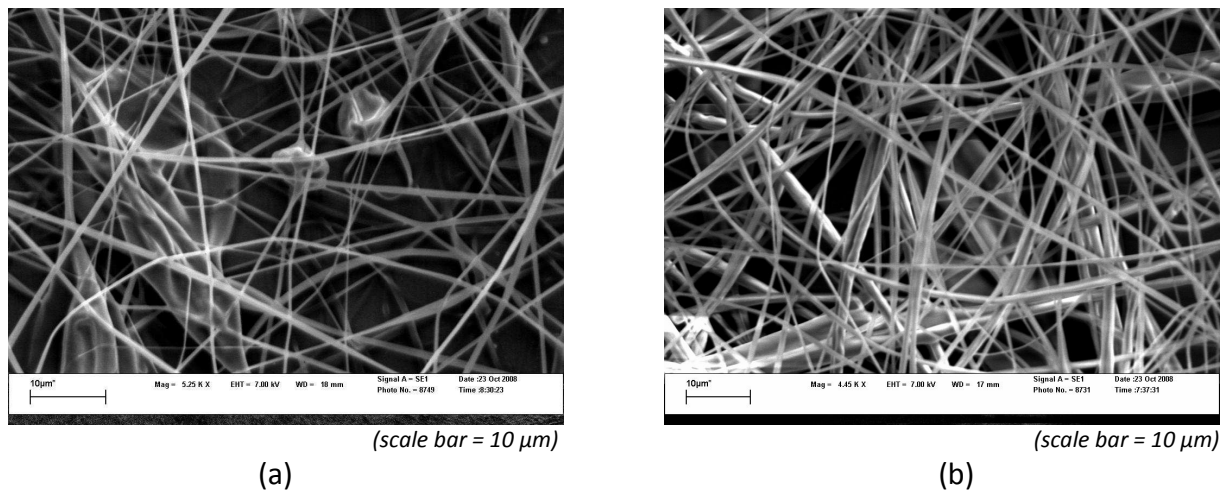


**Figure 4.2** SEM images of fibres produced by single electrospinning from a) 11 wt% CA in acetone:dioxane (2:1 v/v) solution; and b) 17 wt% CA in acetone:dioxane (2:1 v/v) solution.

\* Coaxial electrospinning conditions for both experiments: 19 °C; 45% rH; 16 kV; 11 cm tip-to-collector distance; feed rate of 4 mL/h.

#### Concentration study - coaxial electrospinning

Coaxial electrospinning experiments were performed using 11 wt%, 14 wt% and 17 wt% CA solutions in 2:1 v/v acetone:dioxane as shell spinning solutions. The 50:3:1 (molar ratio dodecanol:BPA:CVL) thermochromic composite was dissolved 5:2 or 5:3 v/v in acetone and used as the core spinning liquid for all these experiments. All of the CA concentrations (i.e. 11–17 wt% in 2:1 v/v acetone:dioxane) could be used to produce fibres with the coaxial electrospinning process.

Figures 4.3 & 4.4 show SEM images of these fibres. In Figure 4.4 cross-section images are given. These cross-sections were revealed by freeze fracturing fibre mats that were twisted into yarns or rolled up. Some fibres (highlighted in yellow blocks) appeared to have hollow structures, which was an indication that core-shell fibres were possibly formed.

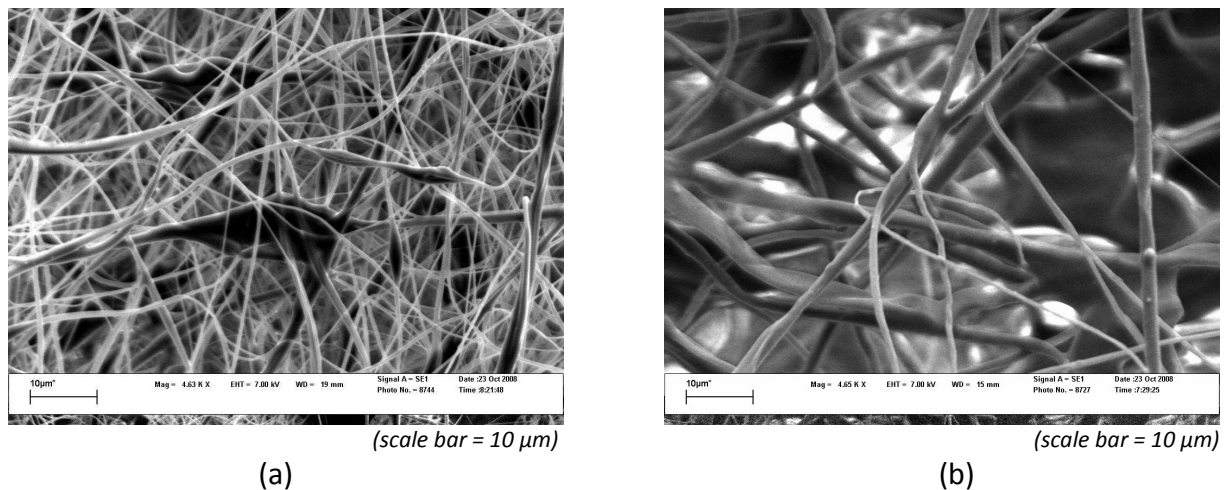


**Figure 4.3** SEM images of fibres produced by coaxial electrospinning using a) <sup>\*1</sup> a shell spinning solution of 11 wt% CA in 2:1 v/v acetone:dioxane; and b) <sup>\*2</sup> a shell spinning solution of 17 wt% CA in 2:1 v/v acetone:dioxane. The core spinning solution, in both cases, consisted of a 50:3:1 (molar ratio dodecanol:BPA:CVL) thermochromic composite dissolved 5:2 v/v in acetone.

<sup>\*1</sup> Coaxial electrospinning conditions: 19 °C; 45% rH; 16 kV; 11 cm tip-to-collector distance; core flow rate of 0.2 mL/h; and shell flow rate of 4 mL/h.

<sup>\*2</sup> Coaxial electrospinning conditions: 19 °C; 44% rH; 16 kV; 11 cm tip-to-collector distance; core flow rate of 0.2 mL/h; and shell flow rate of 4 mL/h.

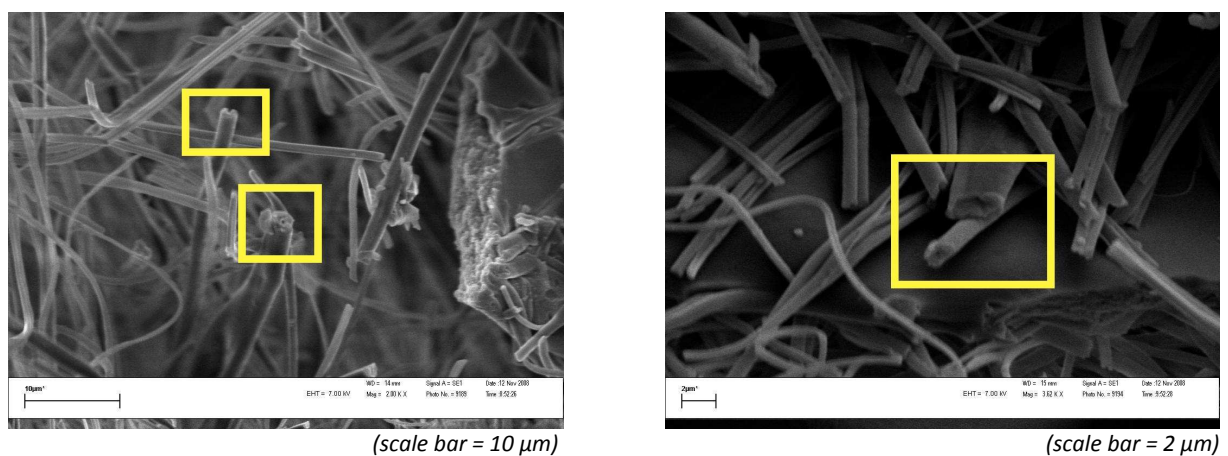


**Figure 4.4** SEM images indicating core-shell morphology in fibres produced by coaxial electrospinning\* using a shell spinning solution of 14 wt% CA in 2:1 v/v acetone:dioxane, and a core spinning solution of thermochromic dye composite (50:3:1 molar ratio dodecanol:BPA:CVL) in acetone (5:3 v/v).

\*Coaxial electrospinning conditions: 20 °C; 56% rH; 16 kV; 8 cm tip-to-collector distance; core flow rate of 0.1 mL/h; and shell flow rate of 2 mL/h.

All of the fibre mats shown above had a pale blue colour, but no thermochromic transition could be observed. The 14 wt% CA in 2:1 v/v acetone:dioxane gave the most uniform fibres and the most stable process.

### Solvent ratio study for acetone:dioxane - coaxial electrospinning

In order to test the effects of different shell solvent volatilities on core-shell fibre formation during the coaxial electrospinning process, and on the stability of the process, the acetone:dioxane v/v ratios were varied (dioxane is less volatile than acetone) and the effects were evaluated. The solvent ratios, along with the CA concentration(s) tested with each of these, are summarized in Table 4.2. A 50:3:1 (molar ratio dodecanol:BPA:CVL) thermochromic composite, dissolved 5:2 v/v in acetone, was used as the core spinning liquid for these experiments. The important results are briefly summarized in Table 4.2.

**Table 4.2**

**The effects of different acetone:dioxane v/v ratios in coaxial electrospinning experiments**

Solvent composition (acetone:dioxane v/v)	CA concentration (wt%)	Results/Comments
3:1	14	Solutions dried rapidly and caused needle blockage due to higher shell solvent volatility (higher acetone content)
2:1	11	Most stable coaxial electrospinning process achieved with this solvent combination; 14 wt% CA solution preferred
	14	
	17	
1:1	12	Solvent volatility lowered further due to increased dioxane content; slower drying of shell polymer but process not stable; overall dielectric constant* now also lowered, which made electrospinning difficult: a lower dielectric constant lowers the ability of charges to effectively accumulate on the tip of the Taylor cone and this hinders electrospinning <sup>9</sup>
	15	
1:2	11	
	14	

\* Solvent properties were listed in Chapter 3, Table 3.2.

The 14 wt% CA solution in 2:1 v/v acetone:dioxane was confirmed as the most suitable CA shell spinning solution composition for solvent facilitated coaxial electrospinning experiments with a thermochromic dye composite as core material.



#### 4.3.2.2 *Proof of thermochromic composite entrainment and investigations into reasons for the absence of thermochromic transition*

No thermochromic transition could be observed for any of the fibre mats produced in any of the experiments discussed up to this point. The only indication that core material might have been entrained in the fibres was a pale blue colour that was observed for some fibre mats. Therefore the following experiments were performed to investigate and possibly confirm entrainment of thermochromic composite and the formation of a core-shell structure, and also to find an explanation for the absence of thermochromic transition.

##### Fibre diameter study

The SEM images from the 11 wt% and 17 wt% CA in 2:1 v/v acetone:dioxane single and coaxial electrospinning experiments (as previously discussed) were used to investigate the effect of shell concentration on fibre diameter; as well as to indicate core entrainment (by possibly showing a difference in diameters of single as opposed to core-shell fibres that were electrospun under the same conditions). The single solution CA fibres were also produced through the coaxial spinneret to eliminate spinneret needle diameter effects on the size of the fibres. This was done by stopping the core feed and electrospinning the CA solutions from the outer coaxial capillary. Parameters including spinning distances, core and shell feed rates, applied voltages and spinneret orifice diameters were similar for all experiments used to compare fibre diameters. The shell solution concentration and the presence or absence of core spinning solution were the only variables.

Table 4.3 gives a summary of the average fibre diameters for 11 wt% CA and 17 wt% CA single and core-shell fibres. An increase in the CA concentration of the shell spinning solution gave an increase in the average diameters of fibres electrospun from such solutions. The coaxially electrospun fibres generally had larger average fibre diameters than the single CA fibres that were electrospun from shell solutions of corresponding concentrations. The inclusion of core material was the most likely explanation for the increased average fibre diameters.

**Table 4.3**

**Comparison of average fibre diameters for single and core-shell fibres according to polymer concentration**

Description	Concentration (wt%)	Average total fibre diameter (nm)
Core-shell	11	653
Shell only (single solution)	11	570
Core-shell	17	1705
Shell only (single solution)	17	1040

#### Immersing the fibre mats in oil

One hypothesis to explain the lack of colour visibility for the core-shell fibres was that the colour was masked by light scattering effects.<sup>10,11</sup> Coaxial electrospinning with CA as shell material typically resulted in fibres with diameters (i.e. 400–900 nm) in the range of the wavelength of visible light (i.e. 400–800 nm). To test this hypothesis, yarns were rolled from fibre mats and immersed in clear silicon oil to form a thin transparent layer of oil around the fibres and in so doing reduce the scattering effect (i.e. increase the visibility of any blue colour from the core material).

The hypothesis was confirmed when the blue colour of the core material became more clearly visible after immersion of the pale blue or white fibres in the oil (see Figure 4.5 below). Although the blue colour was now clearly visible, thermochromic transition was still not observed for these fibres (the blue colour was permanent).



**Figure 4.5** Yarn of coaxially electrospun dye composite CA core-shell fibres.

*\*The part on the right was immersed in oil, which made the blue colour of the thermochromic composite (core material) more visible.*

The small diameters of the CA core-shell fibres (and the associated light scattering) were proven to be a likely contributing factor to the low colour visibility (white or pale blue) of the fibre mats at temperatures below the colour switching temperature. A similar effect was experienced by Li et al.<sup>10</sup> when producing thermochromic fibres by melt coaxial electrospinning. The colour was not visible and they attributed this to Mie light scattering due the small core diameters (200–400 nm) and shell thicknesses (200–500 nm) of the fibres. A study by Pedicini and Ferris<sup>11</sup> showed that fibres that contained carbon black particles, and had diameters of 500 nm, appeared white. They explained that because a porous mat of high surface area was formed by electrospinning the polymer, the degree of light scattering produced by the mat effectively masked the appearance of the carbon black particles contained within the fibres.

#### Dissolving (gelling) the shell polymer to expose the core

An experiment was done, where a pale blue fibre mat was immersed in DCM. The CA shell of the coaxially electrospun fibres gelled (partially dissolved) instantly, leaving behind a substance that revealed the bright blue core material (Figure 4.6). This was another indication that the thermochromic composite was entrained in the fibres. Again, no thermochromic transition was observed for these gelled blue fibres.



**Figure 4.6** Core-shell fibres with thermochromic dye composite as core material (CA shell), before and after immersion in DCM.

#### Transmission electron microscopy (TEM) analysis

TEM analysis was used in attempts to prove and examine the core-shell structures of the coaxially electrospun CA fibres. Figure 4.7 shows TEM images of fibres with clear core-shell

structures, as well as of a solid CA fibre (without core). The solid fibre could have been formed during a period of unstable coaxial electrospinning; or it could have been formed due to the low viscosity of the core spinning liquid (when dissolved in the facilitating solvent), which meant that the core might not have been continuously entrained along the length of the fibre.<sup>12,13</sup>

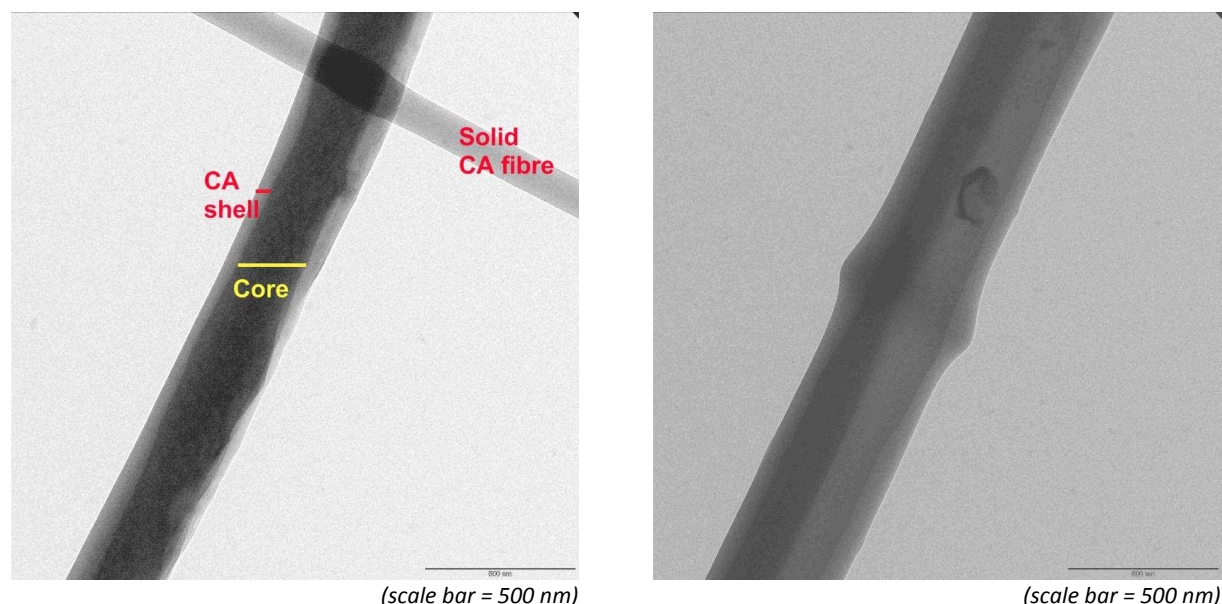


**Figure 4.7** TEM images revealing the core-shell structures of fibres produced by coaxial electrospinning\* using a shell spinning solution of 14 wt% CA in 2:1 v/v acetone:dioxane; and a core solution of thermochromic dye composite (100:3:1 molar ratio dodecanol:BPA:CVL) dissolved in acetone (5:3 v/v).

\* Coaxial electrospinning conditions: 23.4 °C; 51% rH; 15–16 kV; 7.5 cm tip-to-collector distance; core flow rate of 0.2 mL/h; and shell flow rate of 2 mL/h.

### Thermogravimetric analysis (TGA)

TGA was used to determine whether or not all three components of the thermochromic dye composite were entrained in the coaxial electrospun fibres. The presence of the CVL component (in its ring-opened, colour developed state) within the fibres was confirmed by previous experiments, but the reason for the absence of thermochromism was still unclear.

TGA was first performed on CVL, BPA, dodecanol and CA individually to determine the temperature range over which each compound was lost. Table 4.4 summarizes the onset temperatures for each component.

**Table 4.4****Approximate temperatures for onset of decomposition of core-shell fibre components**

Component	Onset temperature (°C)
Dodecanol	92
BPA	175–180
CVL	287
CA	303

TGA was then performed on the core-shell fibres by using a continuous, steady heating rate as well as a varied heating rate that included isothermal steps (as set out in Table 4.5). The latter was used in an attempt to eliminate any overlapping of the decomposition peaks and to separate all components for quantitative analysis of the coaxially electrospun fibres.

**Table 4.5****TGA heating profile for compositional analysis of electrospun core-shell fibres**

Temperature range (°C)	Heating rate	Compound lost
Ambient–90	5 °C/min	
90–150	2 °C/min	Dodecanol
150	10 min isothermal	Dodecanol
150–210	5 °C/min	BPA
210	20 min isothermal	BPA
210–250	5 °C/min	CVL
250–275	2 °C/min	CVL
275	30 min isothermal	CVL (could lose minute amounts of CA)
275–400	2 °C/min	CA (could still include some CVL)

The decomposition temperature ranges (i.e. peak areas) of CVL, BPA and CA overlapped. This is shown in Figure A1, Appendix A where the TGA thermograms (derivatives of weight percentages on y-axis) for each of the components are overlaid with the TGA thermograms of core-shell fibres heated continuously, as well as according to a heating profile with isothermal steps. Even when isothermal steps were used (as for Figure 4.8) it was not possible to completely separate and quantify each component accurately. Figure 4.8 shows that there was some weight loss between the initial dodecanol mass loss (90–150 °C) and the final CA mass loss. This indicated the presence of the BPA and CVL.

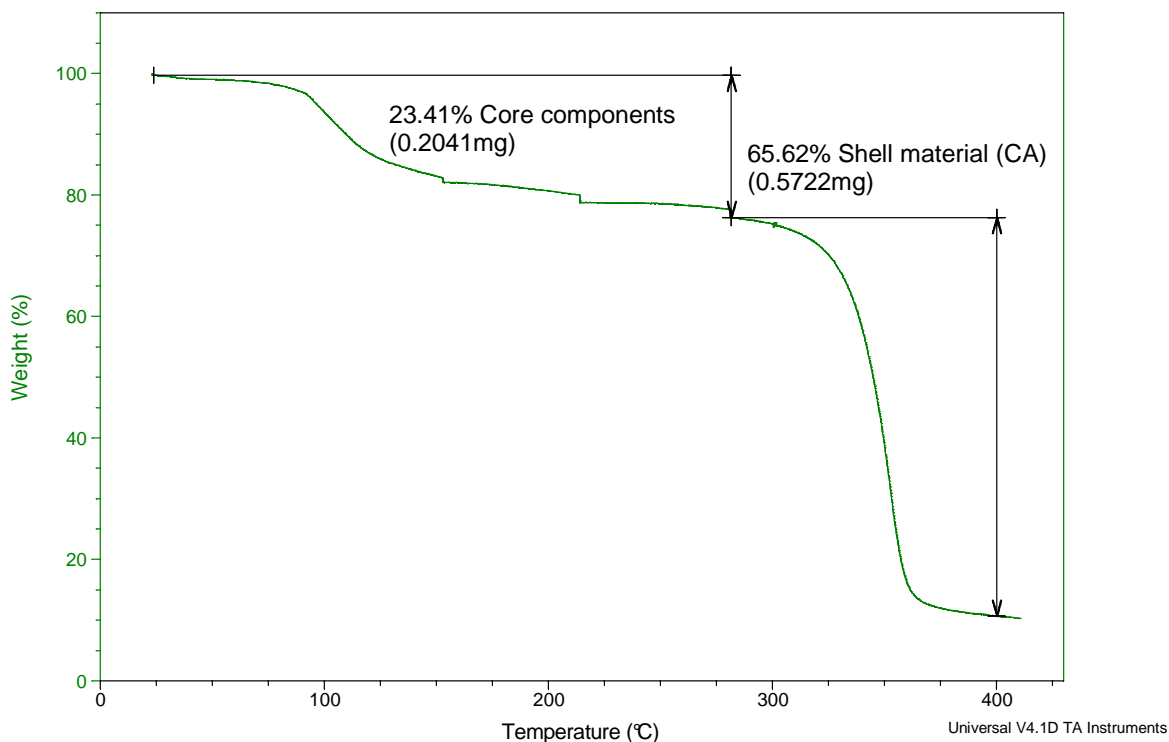


**Figure 4.8** TGA thermogram for compositional analysis of dye composite core-shell fibres (core electrospinning solution: 50:3:1 dodecanol:BPA:CVL thermochromic composite dissolved 5:3 v/v in acetone; shell electrospinning solution: 14 wt% CA in 2:1 v/v dioxane:acetone).

The results therefore showed that all three thermochromic dye components were present within the fibres and that the coaxial electrospinning process, to a large extent, was successful. This meant that some other factor(s), and not the absence of any of the components of the thermochromic composite, was inhibiting and/or altering the thermochromic transition of the core-shell fibres.

The relative weight percentage of core material compared to polymer shell material could be approximated from the TGA thermograms, because the cores were largely composed of dodecanol and this mass loss could be clearly separated from that of the shell material. Analysis of the thermogram (Figure 4.8) indicated that approximately 66% of the total fibre weight consisted of polymer shell and only about 23% of thermochromic dye composite. The low colour visibility and absence of thermochromic transition in the CA core-shell fibres could therefore also have been due to the relatively small core in comparison to the shell.

Differential scanning calorimetry (DSC)

The pale blue base colour, exhibited by the fibre mats, was irreversible. It persisted even when the surrounding temperature was 30–35 °C. At these temperatures the corresponding bulk thermochromic dye composite was colourless. It was known at this point that the thermochromic composite (dodecanol, BPA and CVL) was undoubtedly entrained within the fibres. DSC analysis was therefore used to investigate the effect of encapsulation (within a submicron diameter fibre shell) on the thermal transitions of dodecanol, and also on the thermal transitions of the thermochromic composite as a whole. In bulk, the thermal transitions were associated with thermochromic transitions (i.e. the molten composite was white or colourless and the solid composite was blue).

*DSC analysis of confinement effect on pure dodecanol inside CA fibres*

DSC analyses were performed in order to see what effect the confinement and reduction of volume, inside the fibres, would have on the melting and solidification of dodecanol. Core-shell fibres with pure dodecanol as core material were produced, and analyzed with DSC. Bulk dodecanol was also analyzed using DSC. Some background information on dodecanol is given in the next paragraph, after which discussions of the DSC results follow.

Dodecanol is classified as a phase change material. This means that it can absorb a large amount of energy while being exposed to heat, before it melts completely and the temperature starts increasing again. When the dodecanol solidifies upon cooling, the stored energy is released in the form of heat. This effect should give the thermochromic fibres temperature regulating properties as well.<sup>14</sup> Due to the time required for energy absorption and release during melting (and associated colour loss) and solidification (and associated colour formation) of dodecanol and of the thermochromic dye composite, the rates of melting and solidification and the corresponding colour changes for the bulk materials were slow. The temperature of the dodecanol or a thermochromic dye composite that contains dodecanol will only increase or decrease further once all the dodecanol has been melted or solidified.

DSC results (Figure 4.9) showed a small melt enthalpy peak for dodecanol entrained in core-shell fibres and a larger melt enthalpy peak for the bulk dodecanol. This possibly reflected the fact that less energy was required to melt the smaller volume of dodecanol inside the core-shell fibres than to melt the bulk dodecanol (when compared on total weight, the core-shell fibre sample in the DSC pan contained a smaller weight fraction of dodecanol than the sample pan with bulk dodecanol).

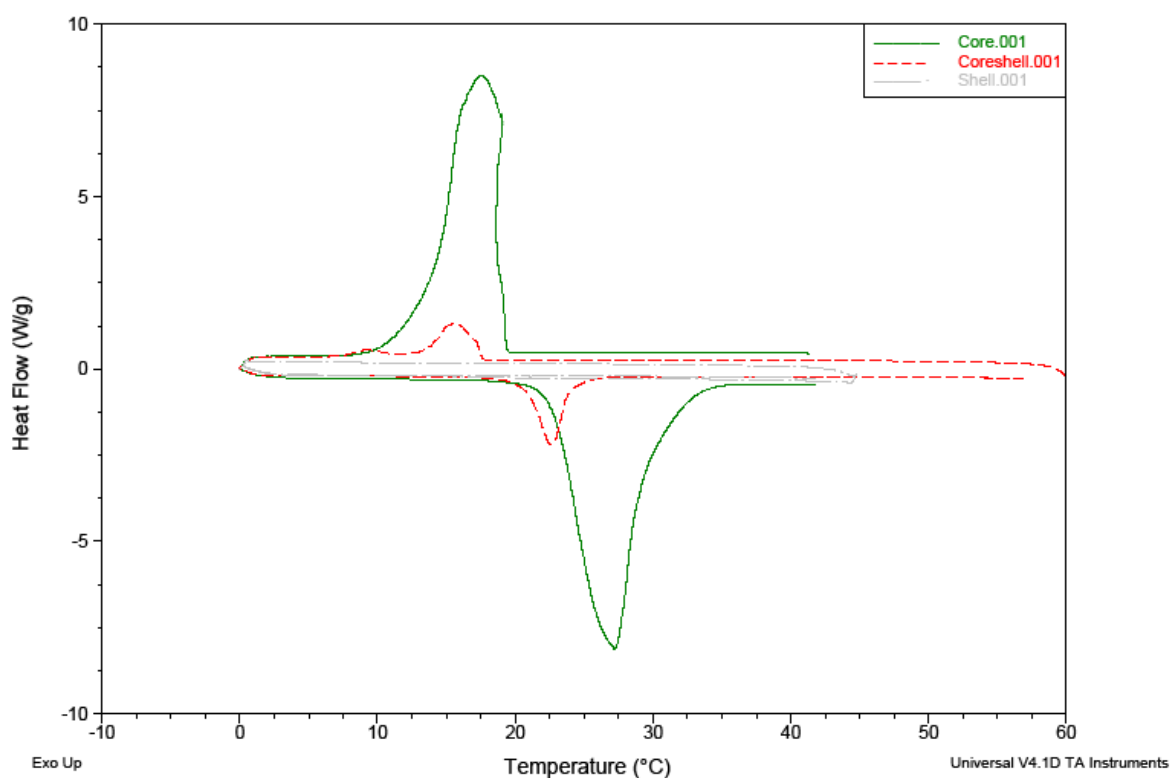


**Figure 4.9** DSC analysis of dodecanol (—); dodecanol CA core-shell fibres (- - -) and pure CA fibres (- - - -).

The difference in the amount of energy and time required for melting the bulk dodecanol, compared to the amount of energy and time required to melt the dodecanol inside the core-shell fibres could be expected to be reflected in the rate of colour change of the reversible thermochromic dye composites in bulk and inside fibres. The bulk thermochromic composite, similar to bulk dodecanol, would melt from the outside in. Therefore, even when the outer layer had melted and lost colour, the inner parts would still be crystalline and coloured. Thus, the colour switching rate for bulk thermochromic dyes were gradual. The thermochromic composite entrained in the fibres, on the other hand, should lose colour just as quickly as it melts (due to its small volume). At this stage of the study however, no thermochromic transition had been observed for the fibres.



The temperatures for the onset of melting and the onset of solidification were more or less the same and this point was around 20 °C for both the bulk and the entrained dodecanol. There was however, a difference of more than 10 °C between the temperatures at peak maxima for the heating and cooling DSC curves of the bulk dodecanol (Figure 4.9). The effect was slightly less significant for the dodecanol entrained in core-shell fibres. A difference between the heating and cooling colour switching temperatures, corresponding to the difference between the melting and solidification peak maxima, could therefore be expected for the thermochromic dye composite in bulk compared to within the fibres.

*DSC analysis of confinement effect on thermochromic composite inside CA fibres*

DSC analysis was used to compare the melting and solidification temperatures of the bulk 50:3:1 thermochromic composite to that of coaxially electrospun fibres containing the same thermochromic composite. Figures 4.10 & 4.11 show the results.

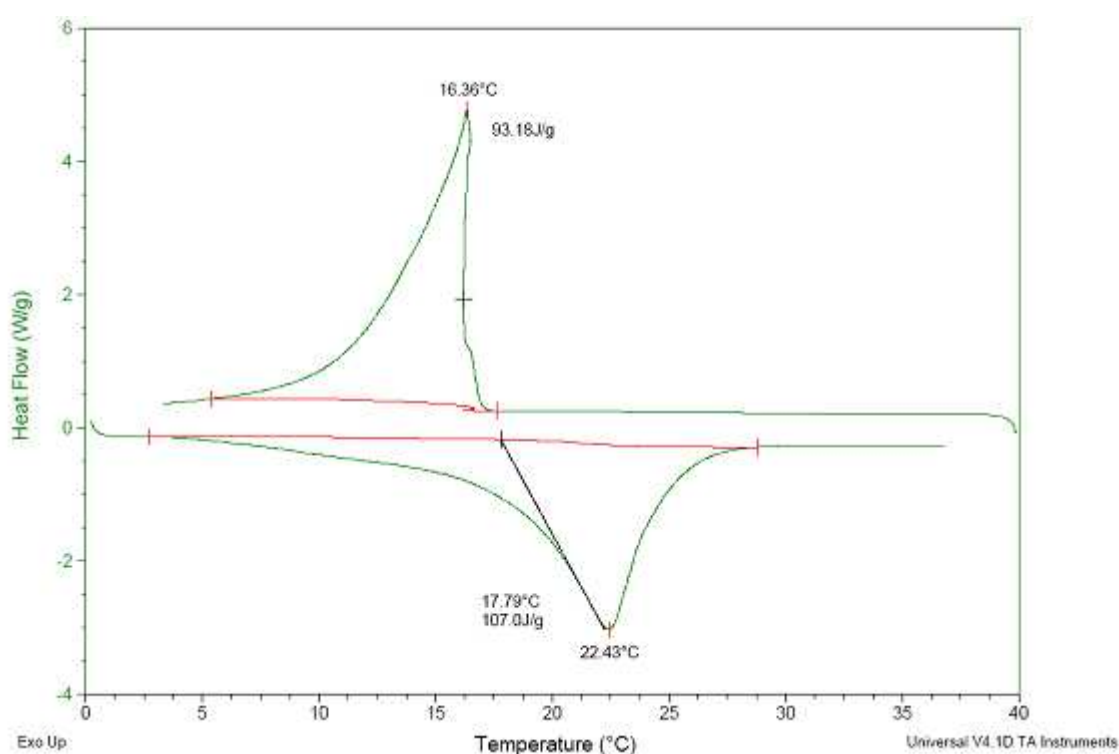


**Figure 4.10** DSC plot of 50:3:1 dodecanol:BPA:CVL bulk thermochromic dye composite.

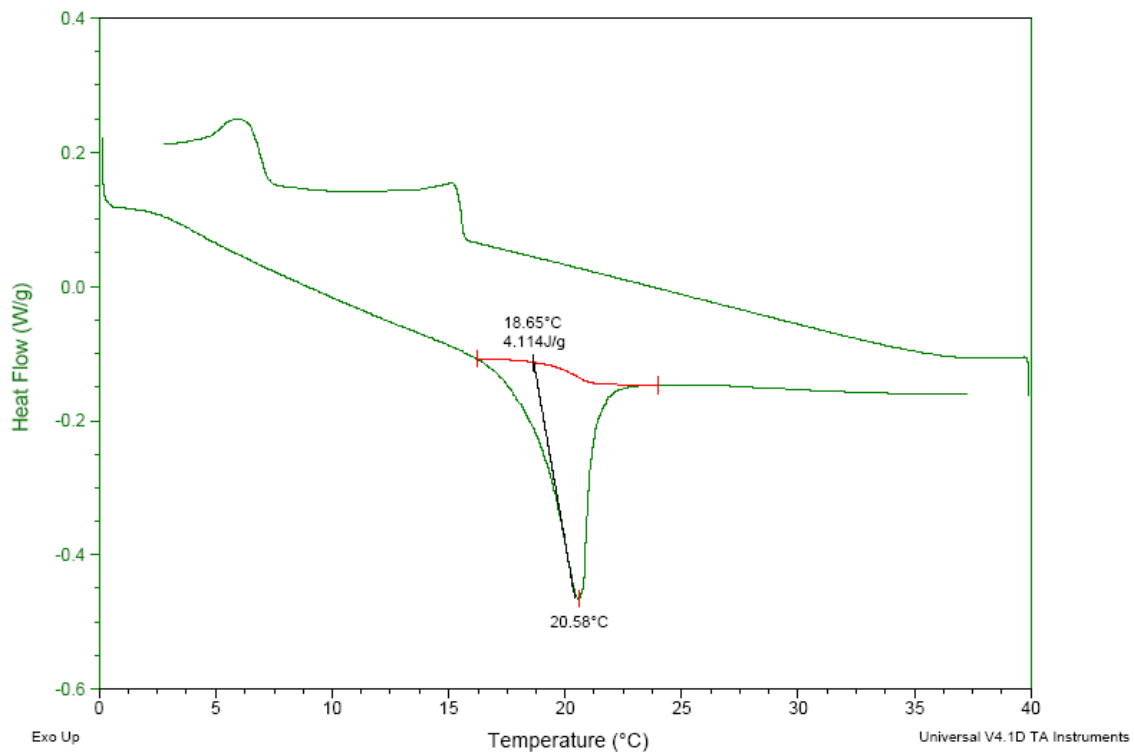


**Figure 4.11 DSC plot of dye composite CA core-shell fibres electrospun using a thermochromic composite with a molar ratio of 50:3:1 dodecanol:BPA:CVL.**

DSC analysis of the bulk 50:3:1 thermochromic composite (Figure 4.10) showed a melting peak maximum at 22.4 °C and solidification peak maximum at 16.4 °C. The dye composite core-shell fibres (Figure 4.11) had a melting peak maximum of  $\pm 20.6$  °C, but no clear solidification peak. Instead there were two ill-defined smaller peaks around the temperatures of 15 °C and 5 °C. The composite seemed to solidify in parts and not completely, as compared to the single solidification peak of the bulk thermochromic composite when cooled at the same heating rate. Dodecanol, on the other hand, when entrained alone inside the fibres did not show this double solidification peak effect.

The solidification temperature of the dodecanol as part of the thermochromic composite in the thermochromic fibres was a concern. Not all the dodecanol solidified at the desired temperature and temperatures near 0 °C were required for complete solidification (Figure 4.11). This would be expected to lower the thermochromic transition temperature but instead a pale blue base colour, which did not become darker upon cooling to  $\pm 6$  °C in the freezer (or when placing the fibres in liquid nitrogen), was permanently visible for all CA core-shell fibre mats produced up to this point.

A hypothesis was formulated that an insufficient amount of dodecanol was entrained inside the fibres to allow full dissociation of CVL and BPA to facilitate thermochromic transition to the colourless form. To test this hypothesis, experiments were done with dye compositions containing varying amounts of dodecanol in order to increase the final dodecanol fraction inside the fibres and possibly enable thermochromic transition.

#### Increasing the dodecanol fraction in the thermochromic composite to possibly enable thermochromic transition of the core-shell fibres

Solvent facilitated coaxial electrospinning experiments were performed with 14 wt% CA solutions in 2:1 v/v acetone:dioxane and thermochromic dye composites composed of 100:3:1, 200:3:1 and 250:3:1 dodecanol:BPA:CVL molar ratios. The dye composites were dissolved 5:2 v/v in acetone to form the core spinning liquids. Fibres were formed in all experiments, but still no thermochromic transition was observed.

DSC analysis was performed on the core-shell fibres with the 100:3:1 molar ratio thermochromic composite to evaluate the thermal transition of the core material (there was no visible difference in thermochromic transition amongst the fibres containing the 100:3:1, 200:3:1 and 250:3:1 composites, hence DSC was only performed on the 100:3:1 sample). The thermal transitions are shown in Figure 4.12. The exothermic peaks for the thermochromic composite in the fibres were more clearly defined than that of the 50:3:1 dye composite core-shell fibres (as previously shown in Figure 11). Solidification again took place in two steps, as identified by the two exothermic peaks. The temperatures at the two solidification (exothermic) peak maxima were 15.6 °C and 4.2 °C.

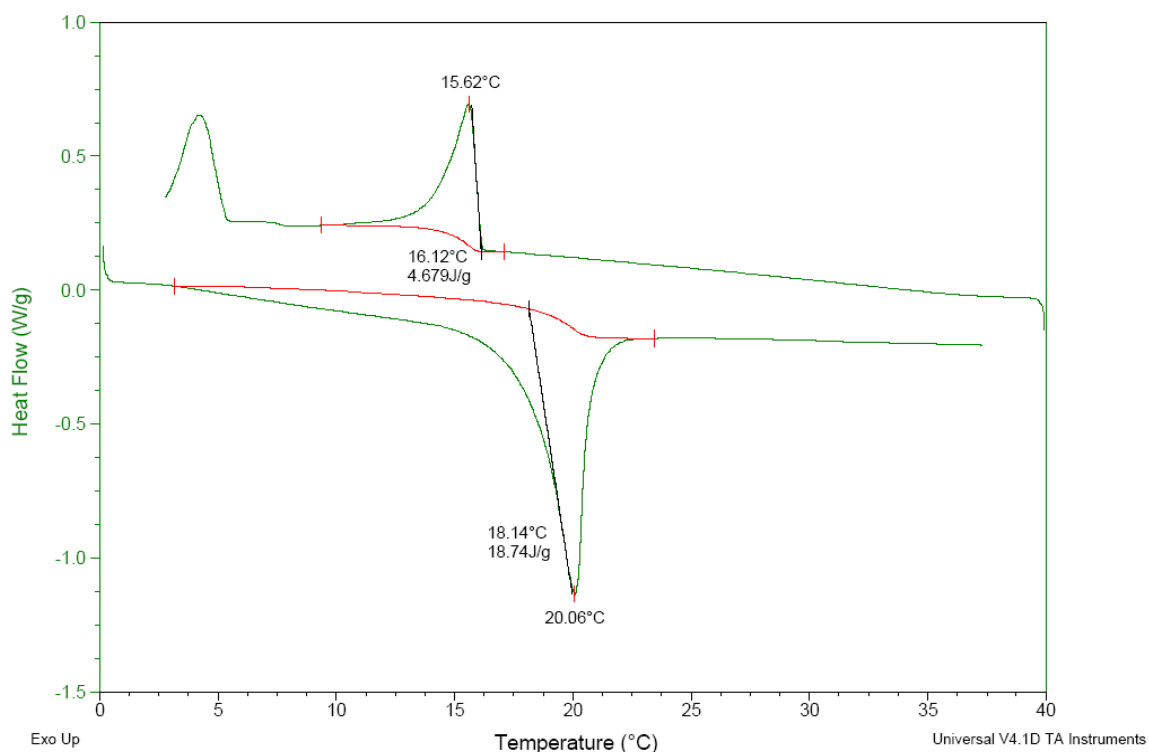


**Figure 4.12** DSC plot of dye composite CA core-shell fibres electrospun using a thermochromic composite with a molar ratio of 100:3:1 dodecanol:BPA:CVL.

The core-shell fibre mats, containing these different thermochromic compositions, all exhibited the pale blue base colour. The 200:3:1 and 250:3:1 bulk dyes were not intensely coloured and quickly lost all colour once the dodecanol began to melt. Even though a large excess of dodecanol was used for the thermochromic composites entrained in all these experiments, and the dodecanol in the composites was melting and solidifying inside the fibres (as seen in the DSC results: Figure 4.12), the pale blue colour was still irreversible. It was concluded that a shortage of dodecanol in the core was probably not the explanation for the irreversible pale blue colour, because increasing the fraction of dodecanol did not result in thermochromic transition.

At this point the difficulties in achieving continuous core entrapment, as well as the poor colour visibility and absence of thermochromic transition over the ranges of variables and parameters tested, indicated that CA was not necessarily the best option for the shell polymer. The study was continued with PMMA as an alternative shell forming polymer.

### 4.3.3 Evaluation of poly(methyl methacrylate) as possible shell forming polymer

PMMA is an optically clear polymer and the PMMA used in this study had a higher molar mass than the CA (350 000 g/mol compared to  $\pm 163\ 000$  g/mol). Higher molar masses generally lead to larger fibre diameters<sup>15-17</sup> but the effect can not necessarily be compared between different polymers. PMMA with a high molar mass was however selected, and the solution concentration chosen such that it might result in fibres with higher fibre diameters than those that were obtained during the CA study. Larger fibre diameters were required to minimize the light scattering effect that was experienced for the submicron CA core-shell fibres.

PMMA is soluble in a large variety of solvents. Experiments with PMMA as shell forming polymer were performed using various solvent combinations of acetone, dioxane, DMF, THF, MEK and chloroform. The combinations that were used and the overall results are briefly summarised in Table C1, Appendix C. SEM images for some of the experiments are included in Appendix B (Figures B4–B19). Many combinations did not result in stable coaxial electrospinning processes and did not form thermochromic fibres. Only experiments that provided insightful results (with regard to the production of thermochromic fibres), or resulted in the production of thermochromic fibres are discussed below (these experiments are highlighted in Table C1, Appendix C).

#### 4.3.3.1 PMMA concentration and solvent ratio studies

##### Concentration study for PMMA solutions in 2:1 v/v acetone:dioxane - coaxial electrospinning

PMMA easily dissolved in 2:1 v/v acetone:dioxane and because this solvent system previously gave stable electrospinning of CA, its suitability to coaxial electrospinning with PMMA as shell polymer was evaluated. PMMA solutions of 8 wt%, 10 wt%, 12 wt% and 15 wt% (in 2:1 v/v acetone:dioxane) were coaxially electrospun with core spinning solutions of 50:3:1 (dodecanol:BPA:CVL molar ratio) thermochromic composites dissolved 5:3 v/v in acetone.

All of the PMMA solutions, i.e. 8–15 wt% in 2:1 v/v acetone:dioxane, allowed the production of core-shell fibres when coaxially electrospun with the given core spinning solution. The spinning process was relatively easy to maintain and relatively large amounts of fibres could be collected in small time frames. The jets dried out relatively quickly during the spinning process and this resulted in process instability during some experiments. Figure 4.13 shows SEM images of these fibres.

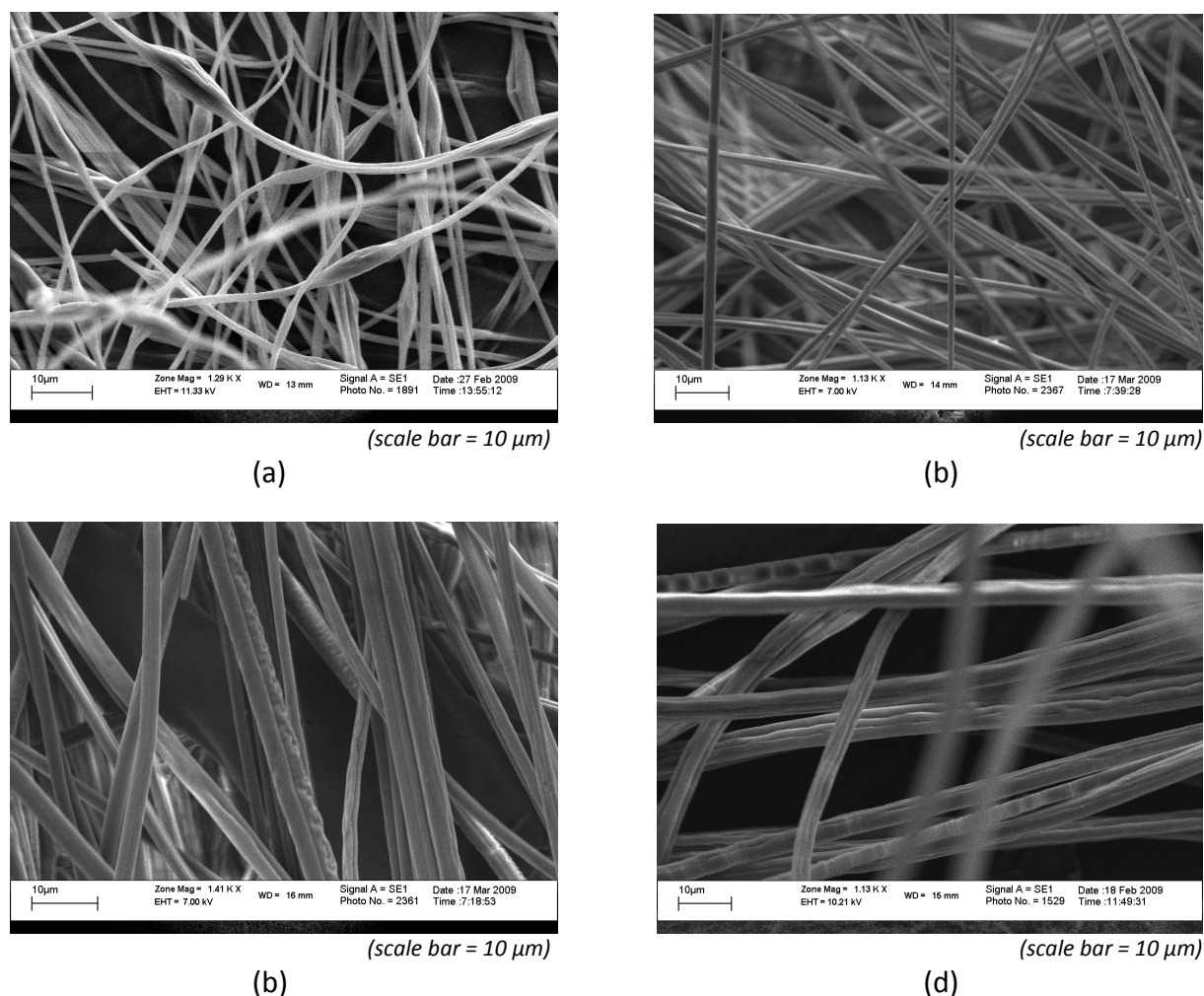


**Figure 4.13** SEM images showing the surface morphology of core-shell fibres coaxially electrospun using shell solutions of different concentrations of PMMA in 2:1 v/v acetone:dioxane solutions: a) 8 wt%; b) 10 wt%; c) 12 wt%; d) 15 wt%.

\* See Table C2, Appendix C for electrospinning conditions.

The lowest concentration (in 2:1 v/v acetone:dioxane) that could still be used to produce fibres was 8 wt% PMMA. Below this, the viscosity was too low and the polymer chain entanglements became too few to inhibit varicous breakup of the shell solution during electrospinning. Figure 4.13 (a) shows that for 8 wt% PMMA (2:1 v/v acetone:dioxane)

solutions, spindle-like beads were seen. The low viscosity of these solutions (see Table 4.6 below) resulted in beading. Although there were enough chain entanglements to allow fibre formation, Raleigh instability was not completely eliminated and beads were still formed. At higher concentrations fibres were smooth and bead-free (Figure 4.13 (b–d)). The 15 wt% PMMA (2:1 v/v acetone:dioxane) solution tended to dry out very quickly. The stable jet region became longer and electrospinning and whipping less achievable. This sudden change in process stability could be attributed to the comparatively sharp increase in viscosity seen between the 12 wt% and 15 wt% PMMA (2:1 v/v acetone:dioxane) solutions (see Table 4.6 and Figure 4.14). The 10 wt% and 12 wt% PMMA (2:1 v/v acetone:dioxane) solutions, with viscosities of 25.5 mPa/s and 55.5 mPa/s respectively, resulted in the most stable electrospinning processes.

Table 4.6

Solution properties for a range of PMMA concentrations in 2:1 v/v acetone:dioxane

Weight percentage (wt%)	Surface tension at $\pm 20$ °C (mN/m)	Conductivity ( $\mu\text{S}/\text{cm}$ )	Viscosity at 20 °C (mPa/s)
8	24.2	11.7	15.5
10	24.9	11.1	27.5
12	26.2	9.85	55.5
15	25.9	9.62	165

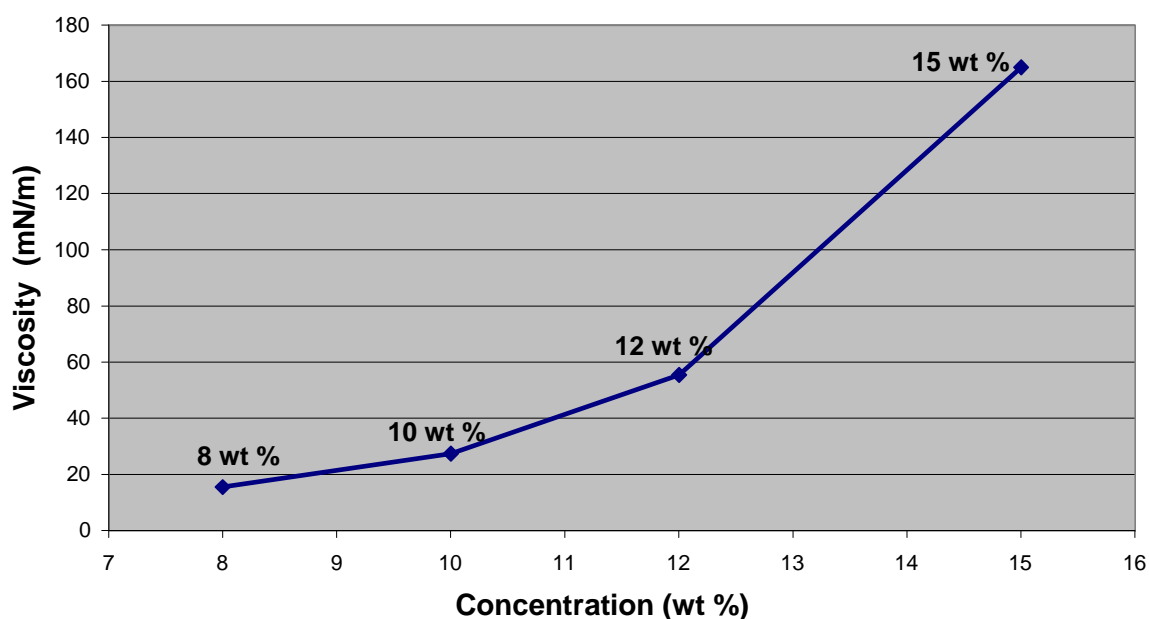
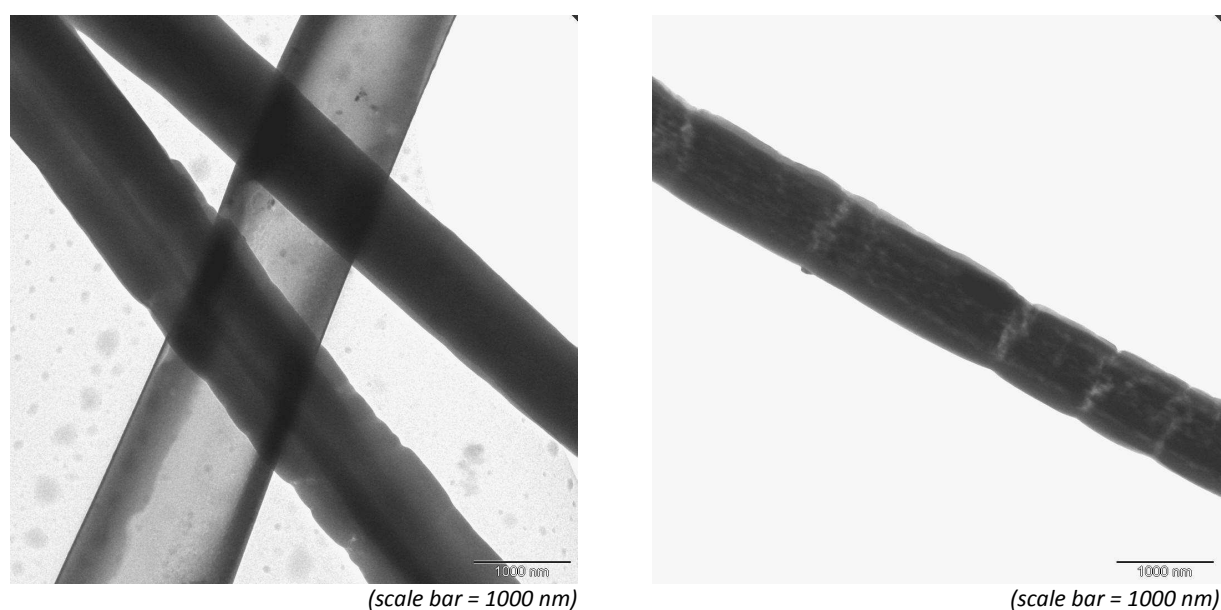


Figure 4.14 Graph showing the increase in solution viscosity corresponding to increased polymer concentrations for PMMA solutions in 2:1 v/v acetone:dioxane.

TEM images of core-shell fibres, produced using PMMA as shell forming polymer, are shown in Figure 4.15. Fibres with diameters above 1  $\mu\text{m}$  are typically too thick for electron beams to penetrate. PMMA core-shell fibres were on average larger than 3  $\mu\text{m}$  and therefore it was mostly not possible to view the internal structures of these fibres when using TEM. As the PMMA concentration was increased, the fibres became larger and more difficult to view. The images in Figure 4.18 were recorded for very thin fibres (from the 8 wt% PMMA in 2:1 v/v acetone:dioxane solution) that were the exception within typical PMMA coaxially electrospun mats.



**Figure 4.15** TEM images revealing the core-shell structures of fibres produced by coaxial electrospinning using a shell solution of 8 wt% PMMA in 2:1 v/v acetone:dioxane; and a core solution of thermochromic dye composite (50:3:1 molar ratio dodecanol:BPA:CVL) dissolved in acetone (5:3 v/v).

\* See Table C2, Appendix C for electrospinning conditions.

Compared to the experiments with CA (as discussed in Section 4.3.2), very short whipping regions were seen in coaxial electrospinning experiments with PMMA solutions in 2:1 v/v acetone:dioxane (1–2 cm as opposed to the typical 5–10 cm for CA). In these PMMA experiments, fibres exited the whipping region and formed fluffy columnar networks of fibres, resembling garlands,<sup>18</sup> before travelling onto the collector.

Garland formation (i.e. long, slow moving networks of electrically charged fibres) was first observed during the electrospinning of polycaprolactone solutions in acetone by



Reneker et al.<sup>18</sup> They showed that garlands were formed when the open loops of the jet came into contact just after the onset of bending instability and formed closed loops. The closed loops then merged and constrained the motion to form a fluffy network that stretched and became a long, roughly cylindrical column a few millimetres in diameter. The garlands, which were electrically charged, developed a path of large open loops that were characteristic of a large scale bending instability.<sup>18</sup>

In the current study, using PMMA solutions in acetone–dioxane combined solvents, the stable jet region was approximately 1 cm long (it often fluctuated) and was followed by a region of normal bending instability that had about the same length. Out of this area the garland was formed and the fibres were collected approximately 2–5 cm after garland formation, while the garland was still travelling in a straight path. This was especially suited to and aided fibre collection onto a rotating wire drum.

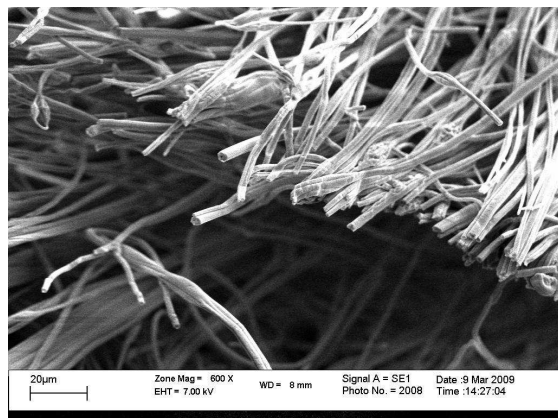
When using the highly conductive (compared to other solutions used in this project) 2:1 v/v acetone:dioxane shell solution combinations, the process often became unstable (conductivities were given in Table 4.6). The effect was worse when the humidity was lower than 50% rH (Table C2, Appendix C contains the humidity values of these experiments). The low humidity enabled an even larger amount of charges to be built up on the surface of the fibres. When the humidity was below  $\pm 40\%$  rH the fibre mats became very brittle.

#### Solvent ratio study for acetone:dioxane - coaxial electrospinning

In attempts to improve process stability (and to better understand the effects of shell solvent composition on coaxial electrospinning), the ratio of acetone to dioxane was varied (1:1 and 3:2 v/v acetone:dioxane). Acetone is much more volatile, has a much higher dielectric constant and a slightly lower surface tension than dioxane (see Table 3.2, Chapter 3). Varying the solvent ratios would change the properties of the combined solvent system. The concentrations and electrospinning conditions used for these experiments are included in Table C2, Appendix C.

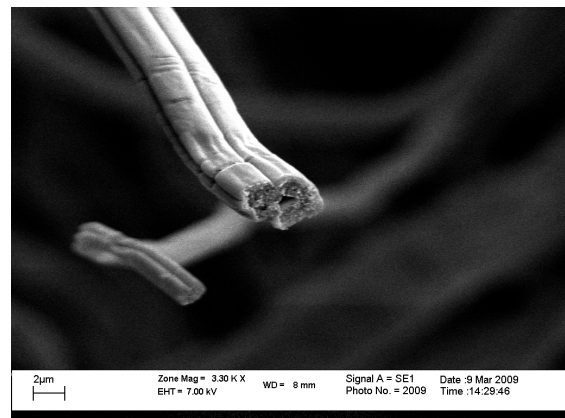
Core-shell fibres that were produced using PMMA dissolved in 1:1 v/v acetone:dioxane are shown in Figure 4.16. Fibres were freeze fractured to expose the inner morphology of the

core-shell fibres. Figure 4.16 (a) & (b) show cross-section views that reveal possible core-shell structures.



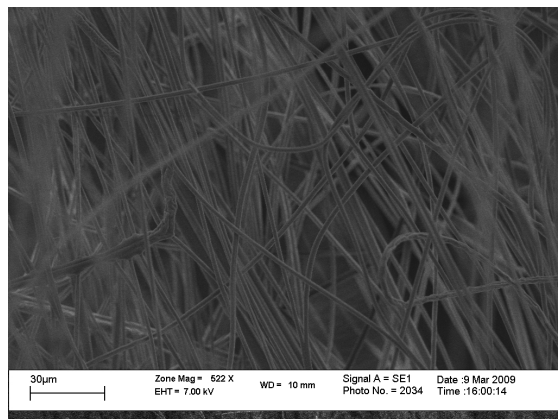
(scale bar = 20 μm)

(a)



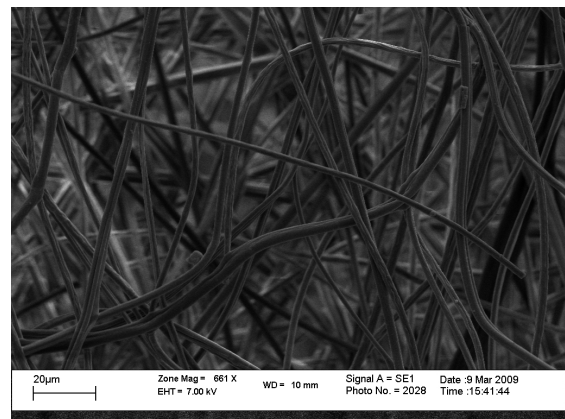
(scale bar = 2 μm)

(b)



(scale bar = 30 μm)

(c)



(scale bar = 20 μm)

(d)

**Figure 4.16** SEM images showing cross-sections and surface morphologies of core-shell fibres coaxially electrospun using shell solutions of different concentrations of PMMA in 1:1 v/v acetone:dioxane: a) 10 wt%; b) 10 wt% cross-section; c) 11 wt%; d) 12 wt%.

\* See Table C2, Appendix C for electrospinning conditions.

During coaxial electrospinning, using PMMA dissolved in 1:1 v/v acetone:dioxane as shell solution, the fibres dried out even more quickly than when shell solutions with 2:1 v/v acetone:dioxane solvent ratios (as experienced during the PMMA concentration study) were used. The length of the stable jet region and the length of the whipping region were seen to fluctuate during electrospinning. The effects observed for the 3:2 v/v acetone:dioxane combination were intermediate between the effects seen for the 2:1 v/v and the 1:1 v/v combinations. The significant difference between the rates of drying (of fibres) when the 1:1 v/v compared to the 2:1 v/v acetone:dioxane solvent combination was used, could be

due to the increase of the dioxane fraction in the combined (1:1 v/v) solvent. A possible explanation for these effects follows.

Acetone is a much better solvent for PMMA than dioxane is.<sup>19</sup> With the 1:1 v/v ratio there was less acetone and more dioxane than for the 2:1 v/v ratio, making the PMMA less soluble in the mixed solvent and causing it to precipitate faster and subsequently decrease the process stability. A more volatile solvent would evaporate before a less volatile one. Therefore, when the combined solvent volatility was lowered by dioxane addition, the solvent components still evaporated separately from each other during electrospinning. During coaxial electrospinning the acetone would have evaporated rapidly, leaving behind the less volatile dioxane. This increased the problem of rapid polymer solution precipitation. As soon as the acetone started evaporating, the stable jet region (i.e. before the onset of whipping) began to fluctuate, probably due to the lowered solubility of the polymer in the remaining solvent.

Due to the differences in solvent volatilities, as discussed above, the dielectric constant of the solution would also have changed during electrospinning. The dielectric constants of acetone and dioxane are 20.7 and 2.2 respectively (at 25 °C). The dielectric constant of the solvents in a solution determines the charge density of the solution.<sup>20</sup> The assumed lowering, as a result of acetone evaporation, of the overall dielectric constant of the solution during jet and fibre formation could be the reason for the fluctuation of the stable jet and whipping regions.<sup>9</sup>

Thompson et al.<sup>21</sup> and Liu et al.<sup>22</sup> found similar instabilities while using high vapour pressure solvents (as in this study). They found that the high viscosity and low charge density brought on by the early evaporation of solvent, resulted in insufficient flow to maintain a fully developed drop for electrospinning.

The initial high dielectric constant of the PMMA solutions in acetone–dioxane, due to the presence of acetone, allowed for high build up of charges on the Taylor cone and initial jet surface<sup>9</sup> leading to increased repelling action. The conductivities of these solutions were also relatively high (given in Table 4.6). Due to the high charge densities and charge repulsions that were achieved, the use of these solutions often resulted in splitting of the jet into two

or even four different jets and whipping regions. This effect was more severe with higher acetone content and less severe with higher dioxane content, probably due to the different dielectric constants of these solvents.

The results of the PMMA experiments performed up to this point showed that 12 & 15 wt% PMMA solutions in 2:1 and 1:1 v/v acetone:dioxane gave the smoothest fibres (amongst these experiments). The fibres did not show the required thermochromic effect. Instead an irreversible pale blue colour was observed once again.

#### Solvent ratio study with THF - coaxial electrospinning

In attempts to improve the process stability and prevent the rapid drying that hindered electrospinning in the previous PMMA experiments THF was incorporated into the mixed solvent system. The purpose of THF addition was to lower the volatility, while aiming to retain similar values for most of the other properties, of the mixed solvent. The addition of THF to the mixed solvent systems, similar to dioxane, would also lower the overall dielectric constant of the combined solvent system. The aim was therefore also to test the effect of a lower dielectric constant on the stability of the process. The advantage of using THF, as opposed to increasing the dioxane content, lay in the higher solubility of PMMA in THF compared to in dioxane. THF also has a similar volatility to acetone and therefore the initial dielectric constant of the solution could be changed without making it fluctuate during the process. The solvent ratios and PMMA concentrations that were used for this study are given in Table C1, Appendix C.

THF addition resulted in more stable processes than the other PMMA experiments discussed thus far. The process instability, due to rapid precipitation of polymer, was lessened by the increased solubility of PMMA in these tri-component solvent systems. THF addition also increased the distance over which normal bending instability (prior to garland formation) occurred and more so as the relative THF content increased. The effect of jet splitting was also eliminated, probably due to the lowering of the overall dielectric constant.

Among the solvent combinations that included THF, the 1:1:1 and 2:1:2 v/v/v acetone:THF:dioxane systems with 12 wt% PMMA gave the best results. The electrospinning

conditions are given in Table C2, Appendix C. SEM images for the fibres produced during these experiments are shown in Figure 4.17 and Figure 4.18.

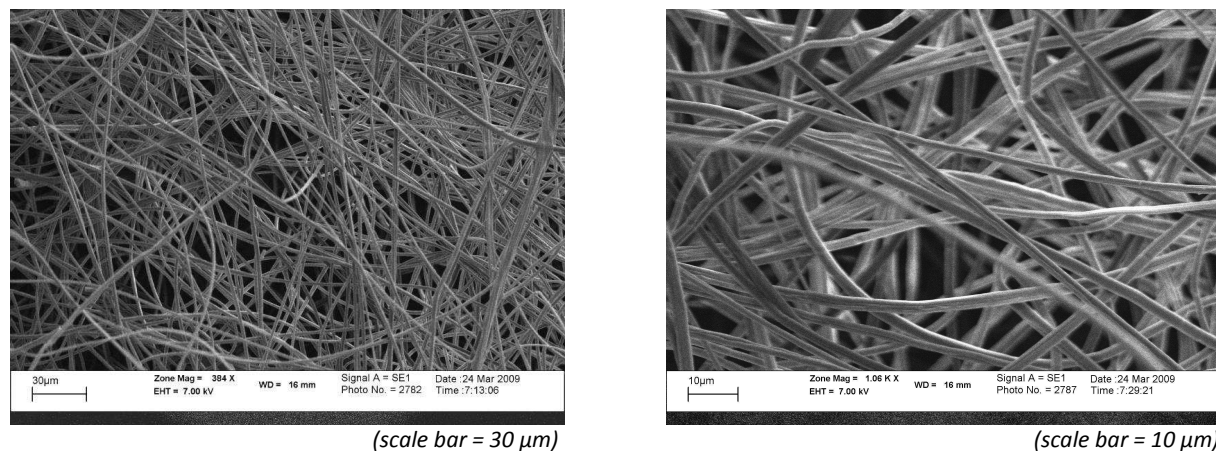


**Figure 4.17** SEM images showing the surface morphology of core-shell fibres coaxially electrospun using shell solutions of 12 wt% PMMA in 1:1:1 v/v/v acetone:THF:dioxane.

\* See Table C2, Appendix C for electrospinning conditions.

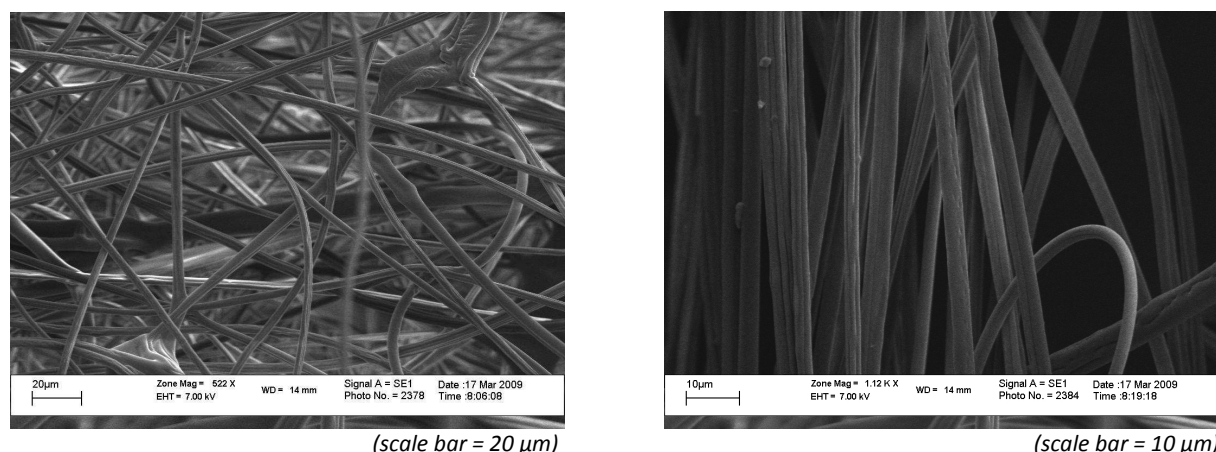


**Figure 4.18** SEM images showing the surface morphology of core-shell fibres coaxially electrospun using shell solutions of 12 wt% PMMA in 2:1:2 v/v/v acetone:THF:dioxane.

\* See Table C2, Appendix C for electrospinning conditions.

TEM images of core-shell fibres, produced using PMMA shell solutions in 2:1:2 and 1:1:1 v/v/v acetone:THF:dioxane solvents, are shown in Figure 4.19. As previously mentioned, the diameters of the PMMA fibres that were produced in this study were too large to allow viewing the internal structures with TEM. The images in Figure 4.19 were recorded for very thin fibres that were the exception within typical PMMA coaxially electrospun mats.

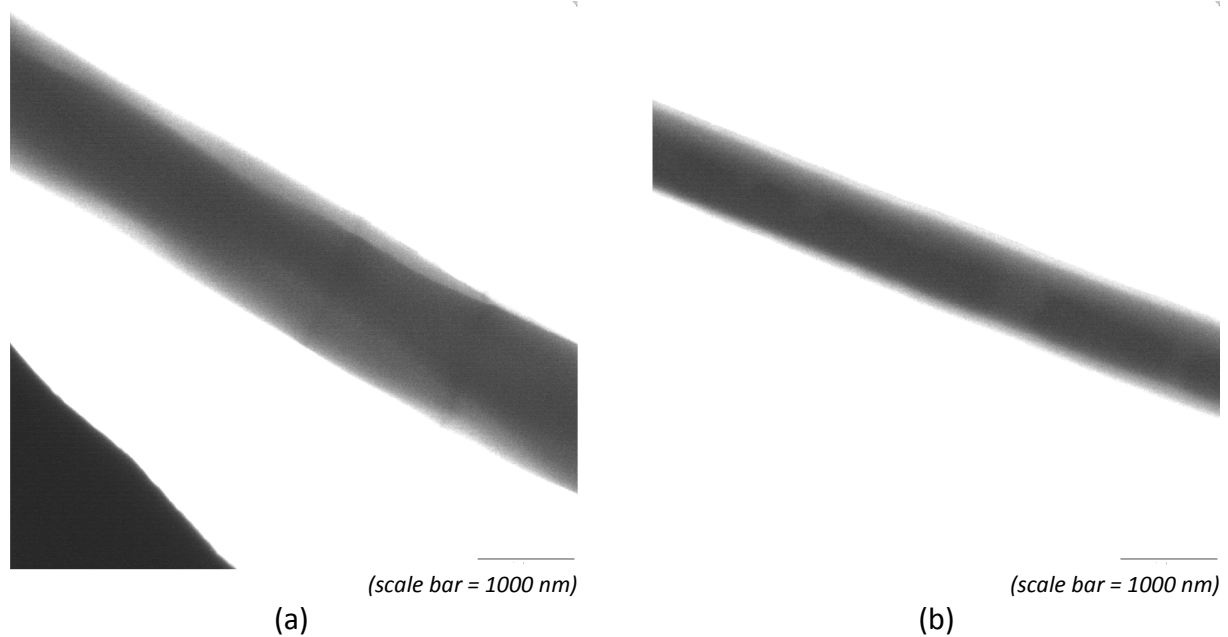


**Figure 4.19** TEM images revealing the core-shell structures of fibres produced by coaxial electrospinning using shell solutions of: a) 12 wt% PMMA in 2:1:2 v/v/v acetone:THF:dioxane, b) 12 wt% PMMA in 1:1:1 v/v/v acetone:THF:dioxane; and core solutions of thermochromic dye composite (50:3:1 molar ratio dodecanol:BPA:CVL) dissolved in acetone (5:3 v/v).

\* See Table C2, Appendix C for electrospinning conditions.

The permanent pale blue base colour, as observed for CA core-shell fibres, was observed for all PMMA experiments up to this point. For many CA samples, the irreversible blue colour could only be observed after coating the fibres with oil to eliminate the severe light scattering effect. In comparison, the irreversible blue colour was clearly visible for dry PMMA fibre mats.

In general, core-shell fibres with PMMA as shell material had larger overall diameters than those with CA shells spun from similar solution concentrations. The PMMA core-shell fibres typically ranged from 3–6  $\mu\text{m}$  while the CA fibres were on average smaller than 1  $\mu\text{m}$  in diameter (typically around 400–900 nm). The increased colour visibility for the PMMA fibre mats was probably due to the larger diameters of these fibres. The micron-scale PMMA fibres scattered light to a lesser extent than the submicron CA fibres and therefore looked less white than the CA fibres.

#### 4.3.3.2 Investigation and elimination of the pale blue base colour

##### Effect of shell solvents on CVL and thermochromic composite

The common shell solvents for all previously discussed experiments were acetone and dioxane. It is possible that the shell solvents could have mixed with the core solution, and might have had an inhibiting effect on the thermochromic transition of the composite, as they came into contact during coaxial electrospinning. It was previously shown (Section 4.2.2.2) that acetone dissolved the thermochromic composite and that after evaporation of the acetone, the thermochromic effect was fully regained. The hypothesis was, therefore, formulated that dioxane mixed into the core solution during coaxial electrospinning and had a ring-opening effect on the CVL in the thermochromic composite, which resulted in the pale blue colour of the core-shell fibres.

To test the hypothesis, the effects of dioxane on CVL and on the thermochromic composite were evaluated. Roughly 0.5 g of CVL powder was added to approximately 2 mL of dioxane in a small flask. CVL dissolved in the dioxane and the solution had a blue colour. In another small flask, approximately 1 mL of molten, colourless thermochromic composite was mixed with approximately 2 mL of dioxane. A blue solution was obtained. From these results it was concluded that dioxane causes colour development of CVL (CVL in its pure form and as part of the thermochromic composite). After dioxane was evaporated from the bulk dye composite, the thermochromic effect returned. The dye composite within the core-shell fibres, on the other hand, had a permanent blue colour and did not exhibit any thermochromic transition.

It was also shown that dioxane alone did not dissolve CA and that it was a weak solvent for PMMA. Entrapment of dioxane within core-shell fibres was therefore a possibility. Once acetone (used with dioxane in the mixed solvent) had evaporated and the CA or PMMA shell solidified, any dioxane that became mixed with the core material would probably no longer be able to escape from the core of the fibres. This trapped dioxane could therefore have caused the CVL (of the thermochromic composite) in the core to remain in its colour developed state, regardless of the temperature. Dioxane had to be eliminated from the

spinning solutions to get more extensive proof that it was the cause of the permanent blue colour of the fibres, and also to eliminate this problem.

#### Shell solvent systems that eliminate the use of dioxane

In attempts at finding a solvent system that did not contain dioxane, PMMA solutions in acetone–DMF, acetone–MEK, pure MEK, pure chloroform, pure THF, pure DMF, pure acetone, THF–DMF, MEK–THF, chloroform–acetone and chloroform–ethanol solvent combinations were tested in solvent facilitated coaxial electrospinning experiments (with dissolved thermochromic dye composites as core spinning liquids). All of these shell solution combinations and a brief summary of the results are included in Table C1, Appendix C.

None of the above mentioned solvent combinations, except chloroform–acetone and chloroform–ethanol (discussed in the following paragraphs), gave satisfactory results. The problems included unstable spinning processes, fibres that did not have the desired morphology, and lack of any thermochromic transition. The positive outcome of these otherwise unsuccessful experiments was that the absence of dioxane resulted in the elimination of the pale blue base colour. The fibres that were formed were white.

Coaxial electrospinning of PMMA solutions in chloroform–acetone solvents also resulted in the elimination of the irreversible pale blue base colour. A thermochromic transition was also seen for these core-shell fibres, but the fibres were either severely beaded or the core was (clearly) not uniformly entrained. The latter resulted in the uneven distribution of colour (across the fibre mat) in the coloured thermochromic state.

PMMA solutions of 12 wt%, 14 wt% and 16 wt% in either 3:1 or 3:2 v/v chloroform:ethanol solvent systems gave the most satisfactory results. Chloroform is a good solvent for PMMA but on its own it did not allow electrospinning of PMMA. A region of bending instability did not develop. This was possibly mainly due to the low conductivity (0.02  $\mu\text{S}/\text{cm}$ ) and the low dielectric constant (4.8 at 25 °C) of chloroform. Ethanol alone did not dissolve PMMA but as part of the combined solvent, it enabled coaxial electrospinning by creating bending instability and more so as the ethanol fraction in the combined solvent was increased. The main differences between ethanol and chloroform are that ethanol has a higher dielectric



constant (24 at 25 °C) and a lower vapour pressure (Table 3.2, Chapter 3 tabulates the solvent properties). Both solvents have low electrical conductivity. The selected mixtures of chloroform and ethanol fell within the solubility range of PMMA and produced electrospinnable polymer solutions. Coaxial electrospinning with these shell spinning solutions (with the thermochromic dye composite dissolved 5:2 v/v in chloroform) gave stable or semi-stable processes, which resulted in the formation of fibre mats with white base colours. Thermochromic transitions were observed for these fibre samples. An in depth discussion and further experimentation with regard to these shell spinning solutions follow in Chapter 5.

#### 4.4 Optimization of thermochromic dye composition

When the 50:3:1 (dodecanol:BPA:CVL molar ratio) composite was dissolved in a facilitating solvent, a homogeneous solution was obtained but the original bulk thermochromic composite had a colloidal composition (as discussed in Section 4.2.1). This was probably because the CVL content was above its solubility level in molten dodecanol at typical ambient temperatures of 24 °C and 35 °C. Experiments were performed in attempts to formulate a thermochromic composite that would not exhibit this problem and perhaps improve the thermochromic transition within the core-shell fibres.

In terms of the envisioned application of thermochromic fibres, the dye composite ideally had to meet two requirements:

- all components had to be completely dissolved in the molten state, i.e. the solution had to be homogenous, preferably at temperatures between 24 °C and 35 °C, and
- the dye composite had to exhibit a sharp colour contrast between the coloured and colourless states (below and above  $\pm 24$  °C).

##### Thermochromic dye composition with homogeneous molten state and sharp colour contrast

The dodecanol:CVL molar ratio was varied in a set of experiments, where the BPA:CVL ratio was kept at 3:1 (i.e. the same as in the original composition from literature). By doing this, inevitably, the dodecanol:BPA ratio was also varied. The aim was to find a dodecanol:CVL

ratio where full solubility of CVL (and BPA) was possible (without the need of raising the temperature above 35 °C); and to evaluate the contrast between the coloured and colourless states, as the dodecanol:CVL and dodecanol:BPA ratios changed across the range. Table 4.7 summarizes the results of these experiments and Figure 4.20 shows the different dye compositions in their coloured and colourless states, at selected temperatures.

**Table 4.7**

**Results of varying the dodecanol:CVL molar ratio of the thermochromic composite, while keeping the BPA:CVL molar ratio (3:1) constant**

Molar ratios of dye components			Colour at different temperatures (See Figure 4.20 for images)			Notes/comments
Dodecanol	BPA	CVL	≤22 °C	50 °C	80 °C	
10	3	1	Dark blue	Dark blue	Dark blue	CVL not fully soluble at 24–35 °C; insufficient molten dodecanol to associate with all BPA; excess BPA remained available to develop CVL ring-opened (blue) state at all temperatures
20	3	1	Dark blue	Medium blue	Medium blue	
30	3	1	Dark blue	Milky blue	Clear with blue tint	CVL not fully soluble at 24–35 °C
50	3	1	Dark blue	Milky (colloidal)	Clear & colourless	CVL not fully soluble at 24–35 °C
150	3	1	Light blue	Clear & colourless	Clear & colourless	Full solubility of CVL and BPA at 24–35 °C; pale coloured state due to reduction of BPA content compared to dodecanol*; insufficient BPA to associate with and fully develop the ring-opened, coloured state of CVL <sup>1</sup>

\* *Burkinshaw et al.*<sup>3</sup> also found that an increase in PCM-solvent to developer and colour former generally lowers the colour yield.

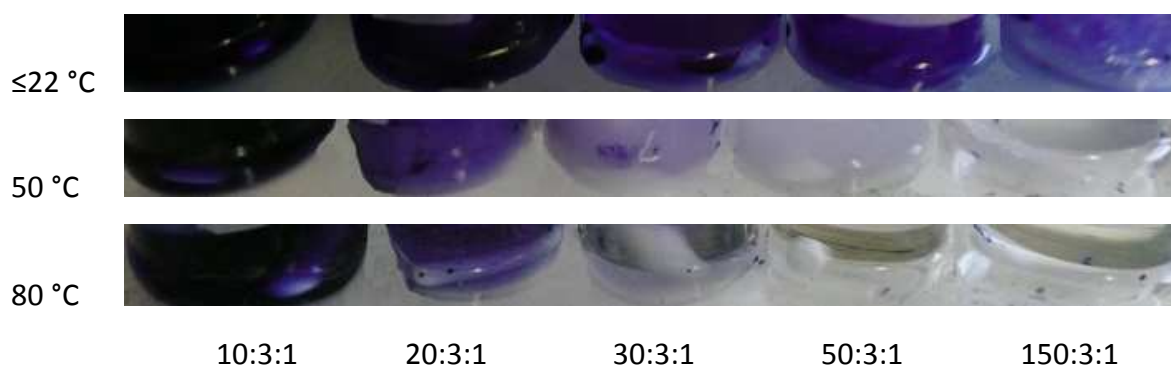


**Figure 4.20** Photographs showing the colour change of different bulk thermochromic dye composites (dodecanol:BPA:CVL molar ratio, with increasing dodecanol content) over a range of temperatures.

These experiments showed that a molar ratio of 150:1 dodecanol:CVL worked well in terms of CVL solvation, but the optimal dodecanol:BPA molar ratio was 50:3 and this was not maintained in the composite that had a 150:1 molar ratio of dodecanol:CVL.

A second set of experiments was performed to find a composite in which the dodecanol:BPA ratio could be kept at 50:3, while the dodecanol:CVL was increased to where CVL dissolved in the molten dodecanol at 24–35 °C. By varying the dodecanol:CVL ratio and keeping the dodecanol:BPA ratio constant, inevitably, the CVL:BPA ratio was also varied. It was important to evaluate how the variation (increase) in BPA:CVL content would affect the thermochromic effect. The results are summarized in Table 4.8.

**Table 4.8**

**Results of varying the dodecanol:CVL molar ratio of the thermochromic composite, while keeping the dodecanol:BPA molar ratio (50:3) constant**

Molar ratios of dye components			Colour at different temperatures		Notes/comments
Dodecanol	BPA	CVL	≤22 °C	≥25 °C	
50	3	1	Dark blue	Milky white	CVL not fully soluble at 24–35 °C
100	6	1	Dark blue	Colourless	Full solubility of CVL and BPA at ±35 °C
200	12	1	Dark blue	Colourless	Full solubility of CVL and BPA at ≥24 °C

In the ranges experimented with, a change in the BPA:CVL ratio did not have a significant effect in terms of the intensity of colour that was achieved for the bulk dyes. As long as the 50:3 dodecanol:BPA ratio was maintained, the BPA:CVL ratio could be increased (at least up to 12:1) as the dodecanol:CVL ratio was increased to gain full solubility of CVL and BPA in molten dodecanol at temperatures of 24–35 °C. The 100:6:1 was preferred above the 200:12:1 dodecanol:BPA:CVL molar ratio to avoid excessive dilution of CVL (the actual dye component) in the final core-shell fibres.

## 4.5 Summary

To summarize the results from this chapter, the optimal spinning solution formulations going forward were:

- shell: 14 wt% & 16 wt% PMMA solutions in 3:1 & 3:2 v/v chloroform:ethanol; and
- core: 100:6:1 molar ratio dodecanol:CVL:BPA, dissolved in 5:2 v/v in chloroform.

The next chapter describes analysis of the fibres coaxially electrospun when using these formulations.

## 4.6 References

1. Luthern, J. and Peredes, A., *Determination of the stoichiometry of a thermochromic color complex via Job's method*. Journal of Materials Science Letters, 2000, **19**:185-188.
2. Seeboth, A., Löttsch, D., Potechius, E. and Vetter, R., *Thermochromic effects of leuco dyes studied in polypropylene*. Chinese Journal of Polymer Science, 2006, **24**(4):363-368.
3. Burkinshaw, S.M., Griffiths, J. and Towns, A.D., *Reversibly thermochromic systems based on pH-sensitive spirolactone-derived functional dyes*. Journal of Materials Chemistry, 1998, **8**:2677-2683.
4. Diaz, J.E., Barrero, A., Marquez, M. and Loscertales, I.G., *Controlled encapsulation of hydrophobic liquids in hydrophilic polymer nanofibers by co-electrospinning*. Advanced Functional Materials, 2006, **16**(16):2110-2116.
5. Reznik, S.N., Yarin, A.L., Zussman, E. and Bercovici, L., *Evolution of a compound droplet attached to a core-shell nozzle under the action of a strong electric field*. Physics of Fluids, 2006, **18**:062101-062110.
6. Sun, Z., Zussman, E., Yarin, A.L., Wendorff, J.H. and Greiner, A., *Compound core-shell polymer nanofibers by co-electrospinning*. Advanced Materials, 2003, **15**(22):1929-1932.
7. Dror, Y., Salalha, W., Avrahami, R., Zussman, E., Yarin, A.L., Dersch, R., Greiner, A. and Wendorff, J.H., *One-step production of polymeric microtubes by co-electrospinning*. Small, 2007, **3**(6):1064-1073.
8. Khalaf, A., *Production of hollow fibers by co-electrospinning of cellulose acetate*. MSc Thesis, University of Stellenbosch: Stellenbosch, March 2009.
9. Ramakrishna, S., Fujihara, K., Teo, K.E., Lim, T.C. and Ma, Z., *An introduction to electrospinning and nanofibers*. 2005, World Scientific Publishing: Singapore.
10. Li, F., Zhao, Y., Wang, S., Han, D., Jiang, L. and Song, Y., *Thermochromic core-shell nanofibers fabricated by melt coaxial electrospinning*. Journal of Applied Polymer Science, 2009, **112**:269-274.
11. Pedicini, A. and Farris, R.J., *Thermally induced color change in electrospun fiber mats*. Journal of Polymer Science Part B: Polymer Physics, 2004, **42**(5):752-757.

12. Li, D. and Xia, Y., *Direct fabrication of composite and ceramic hollow nanofibers by electrospinning*. Nano Letters, 2004, **4**(5):933-938.
13. Sun, B., Duan, B. and Yuan, X., *Preparation of core/shell PVP/PLA ultrafine fibers by coaxial electrospinning*. Journal of Applied Polymer Science, 2006, **102**:39-45.
14. McCann, J.T., Marquez, M. and Xia, Y., *Melt coaxial electrospinning: A versatile method for encapsulation of solid materials and fabrication of phase change nanofibers*. Nano Letters, 2006, **6**(12):2868-2872.
15. Moghe, A.K. and Gupta, B.S., *Co-axial electrospinning for nanofiber structures: Preparation and applications*. Polymer Reviews, 2008, **48**(2):353-377.
16. Doshi, J. and Reneker, D.H., *Electrospinning process and applications of electrospun fibers*. Electrostatics, 1995, **35**:151-160.
17. Deitzel, J.M., Kleinmeyer, J., Harris, D. and Beck Tan, N.C., *The effect of processing variables on the morphology of electrospun nanofibers and textiles*. Polymer, 2001, **42**:261-272.
18. Reneker, D.H., Kataphinan, W., Theron, A., Zussman, E. and Yarin, A.L., *Nanofiber garlands of polycaprolactone by electrospinning*. Polymer, 2002, **43**:6785-6794.
19. Mark, J.E., *Polymer Data Handbook*, Second ed., Mark, J.E., Mark, J.E. 1999, Oxford University Press: New York.
20. Son, W.K., Youk, J.H., Lee, T.S. and Park, W.H., *The effects of solution properties and polyelectrolyte on electrospinning of ultrafine poly(ethylene oxide) fibers*. Polymer, 2004, **45**:2959-2966.
21. Thompson, C.J., Chase, G.G., Yarin, A.L. and Reneker, D.H., *Effects of parameters on nanofiber diameter determined from electrospinning model*. Polymer, 2007, **48**:6913-6922.
22. Liu, H. and Hsieh, Y.-L., *Ultrafine fibrous cellulose membranes from electrospinning of cellulose acetate*. Journal of Polymer Science, Part B: Polymer Physics, 2002, **40**:2119-2129.

## **Chapter 5**

### ***Results and Discussion – Part 2***

#### ***Production and Analysis of Thermochromic Core-Shell Fibres***

##### **5.1 Introduction**

The focus of this chapter is on coaxial electrospinning experiments involving the core and shell solutions that, as determined in the previous chapter, could be used to form thermochromic fibres. The experimental conditions that were used to produce core-shell fibres with reversible thermochromism from PMMA shell solutions (in chloroform–acetone combined solvents) are given. The stability of the coloured state and the reversibility of the thermochromic effect of the fibres were investigated by varying the molar ratios of the thermochromic dye composite (in terms of the BPA content). Analyses included TGA and DSC. SEM images that show the morphologies and cross-section structures of the thermochromic fibres are included.

##### **5.2 Coaxial electrospinning of thermochromic fibres**

The spinning solutions that gave the desired results in terms of producing thermochromic core-shell fibres, as summarized at the end of Chapter 4, were used as the starting point for the experiments in this section. In Chapter 4 the focus was on finding core and shell spinning solutions that could be used to produce thermochromic core-shell fibres by coaxial electrospinning. In this section the electrospinning conditions (in terms of flow rate, applied voltage, tip-to-collector distance, temperature and relative humidity) that resulted in stable processes are given. When it was found that the developed colour was not stable when the fibres were held at a temperature where the colour was initially visible, the effect was investigated by producing fibres with core materials of which the BPA content was varied. This was done in attempts to improve the stability of the colour developed state. The formulations and thermochromic transitions of these dyes, as well as the production of

thermochromic fibres using these dyes and the thermochromic transition of these fibres are discussed in this section.

### 5.2.1 Evaluation of PMMA concentration and chloroform:ethanol solvent ratio in shell solutions

The core and shell solutions that were used for these experiments are tabulated in Tables 5.1 & 5.2 below. These tables also contain the measured solution properties, as well as the surface morphologies of the resultant core-shell fibres. Differences between the results of these experiments are discussed in terms of solution properties.

**Table 5.1**

#### Thermochromic composite and core spinning solution composition and properties

Molar ratio (Dodecanol:BPA:CVL)	Melting / solidification temperature from DSC (°C)	Spinning solution (5:2 v/v dye:chloroform)		
		Surface tension at 20 °C (mN/m)	Conductivity	Viscosity at 20 °C (mPa/s)
100:6:1	22.2 / 17.4	23.1	Not conductive	6.5

**Table 5.2**

#### PMMA shell solution combinations, properties and resulting core-shell fibre morphologies

PMMA (wt%)	Solvent ratio (v/v chloroform:ethanol)	Surface tension at 20 °C (mN/m)	Conductivity ( $\mu$ S/cm)	Viscosity at 20 °C (mPa/s)	Morphology
14	3:1	23.7	0.56	303	Beaded
14	3:2	23.5	1.52	215	Minor beads
16	3:1	24.7	0.38	435	Some beads, wet
16	3:2	24.3	1.67	369	Smooth, no beads

The surface tension of the shell solutions varied slightly, but in essence the values were similar and also similar to the surface tension of the core spinning liquid (Table 5.1) that was used to produce the thermochromic core-shell fibres. The solvent combinations (to dissolve the core and shell) were specifically chosen to obtain such similar surface tensions. As described in Section 4.3 and also in the literature,<sup>1,2</sup> similar surface tensions for the core and



shell spinning solutions ensure low interfacial tension that leads to an enhanced viscous dragging effect<sup>1</sup> of the shell solution on the core solution. This enhanced viscous drag increases the likelihood of successful entrainment of the core in the shell during coaxial electrospinning.

Thermochromic core-shell fibres were produced using the 100:6:1 core composite dissolved in chloroform (described in Table 5.1) as the core spinning solution with each of the shell solutions in Table 5.2. The electrospinning process parameters and ambient conditions were relatively similar for all of these experiments and the conditions that worked best for each of the solutions are tabulated in Table 5.3. Depending on the shell solution, the settings of some parameters were adjusted slightly in order to improve the process stability or to improve the morphology of the resultant fibres. A brief discussion on the flow rates, humidity, capillary diameters and core-needle protrusion that were preferred for this set of experiments also follows.

**Table 5.3**

**Process parameters for coaxial electrospinning experiments\* with PMMA (chloroform:ethanol) shell solutions**

Shell solution		Flow rate (mL/h)		Voltage (kV)	Tip-to-collector distance (cm)	Temp (°C)	rH (%)
Concentration (wt%)	Solvent ratio (chloroform:ethanol v/v)	Shell	Core				
14	3:1	10	1.5	18	27	21	60
14	3:2	10	1.5	16–18	27	20.3	65
16	3:1	11	1.5	18	32	19.6	62
16	3:2	12	2	17	27	22.5	58

\* A 100:6:1 molar ratio dodecanol:BPA:CVL thermochromic composite (dissolved 5:2 v/v in chloroform) was used as core material.

In order to entrain the maximum amount of core material and to minimise shell thickness, the highest possible core to shell flow rate ratio,<sup>3</sup> at which the process remained stable, was used. The volume ratio of the core to shell flow rate was approximately 1:6 for all the above experiments.

Humidity had a significant effect on the stability of the process. When the humidity was too high a typically stable process easily ceased to work. The most suitable humidity for the current set of experiments was between 55% rH and 65% rH. When the humidity was below 60% rH it was much easier to maintain a stable process.

The inner diameter of the core capillary was set at 0.3 mm, but shell capillaries with large and small diameters (2.0 mm and 1.2 mm inner diameter) were tested. Both shell capillary options resulted in the formation of core-shell thermochromic fibres, but the larger capillary gave more repeatable results. This was because the larger shell capillary allowed for a larger initial jet radius<sup>4</sup> to be formed and this made more shell solution available to stabilize, confine and encourage the encapsulation of the core material<sup>5</sup> as it exited the spinneret and formed part of the compound Taylor cone and jet. The core needle was set to protrude out of the shell orifice by half the radius of the latter, as advised in literature.<sup>2,6</sup>

SEM images (Figures 5.1–5.4) of the thermochromic fibres that were produced show the surface morphologies and cross-section views of these fibres. The surface images exhibit the formation of smooth or beaded fibres. The cross-section views in Figures 5.1 & 5.4 reveal possible core-shell structures.

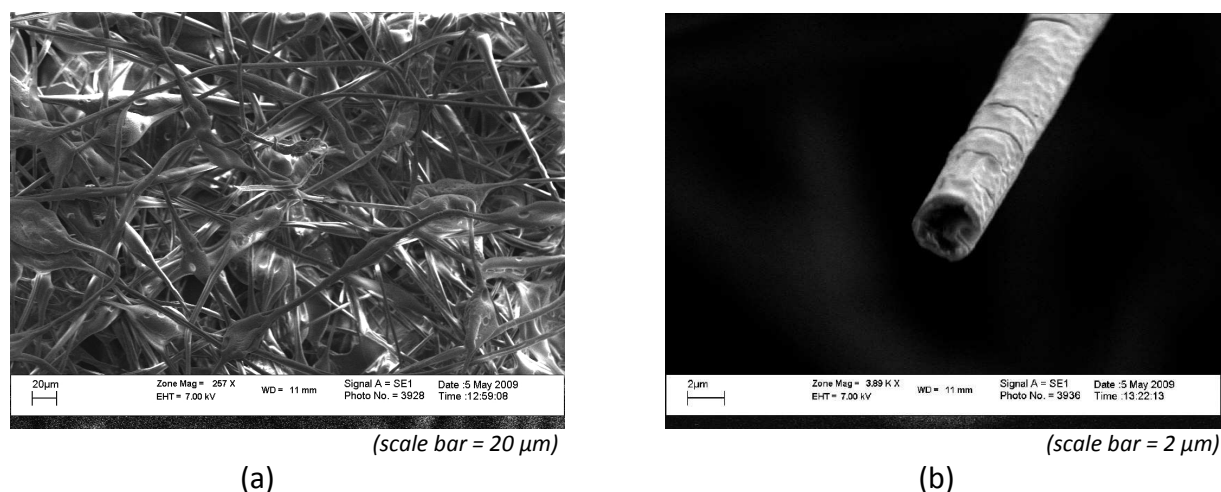


**Figure 5.1** SEM images showing (a) surface morphology (beaded) and (b) cross-section of thermochromic core-shell fibres (shell solution: 14 wt% PMMA, 3:1 v/v chloroform:ethanol; core liquid: 100:6:1 dodecanol:BPA:CVL, 5:2 v/v dye composite:chloroform).

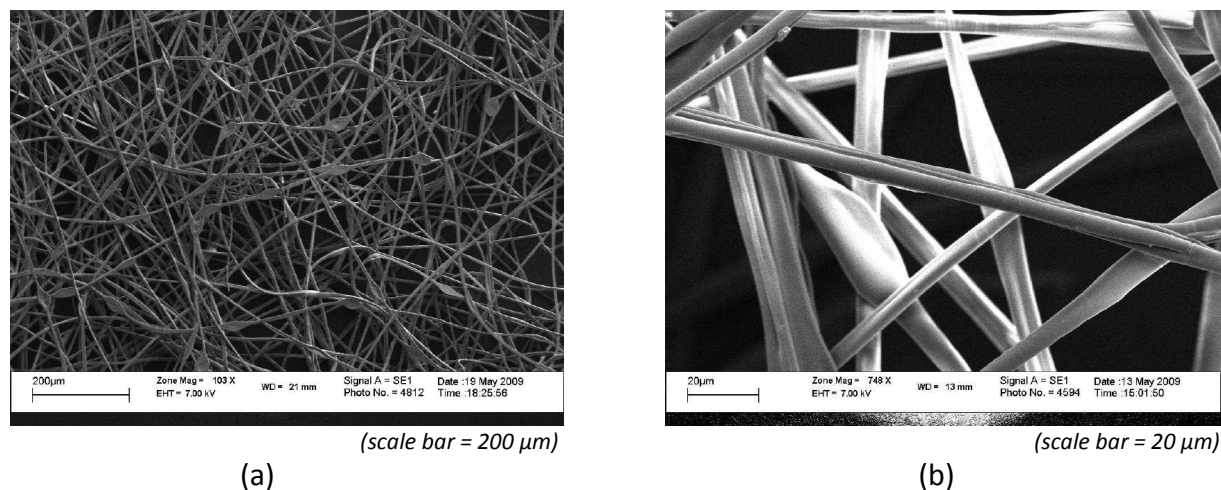


**Figure 5.2** SEM images showing (a) surface morphology and (b) surface morphology of thermochromic core-shell fibres (shell solution: 14 wt% PMMA, 3:2 v/v chloroform:ethanol; core liquid: 100:6:1 dodecanol:BPA:CVL, 5:2 v/v dye composite:chloroform).

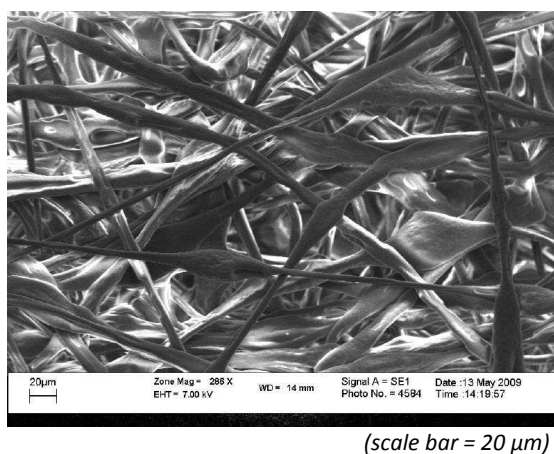


**Figure 5.3** SEM images showing surface morphology of thermochromic core-shell fibres (shell solution: 16 wt% PMMA, 3:1 v/v chloroform:ethanol; core liquid: 100:6:1 dodecanol:BPA:CVL, 5:2 v/v dye composite:chloroform).

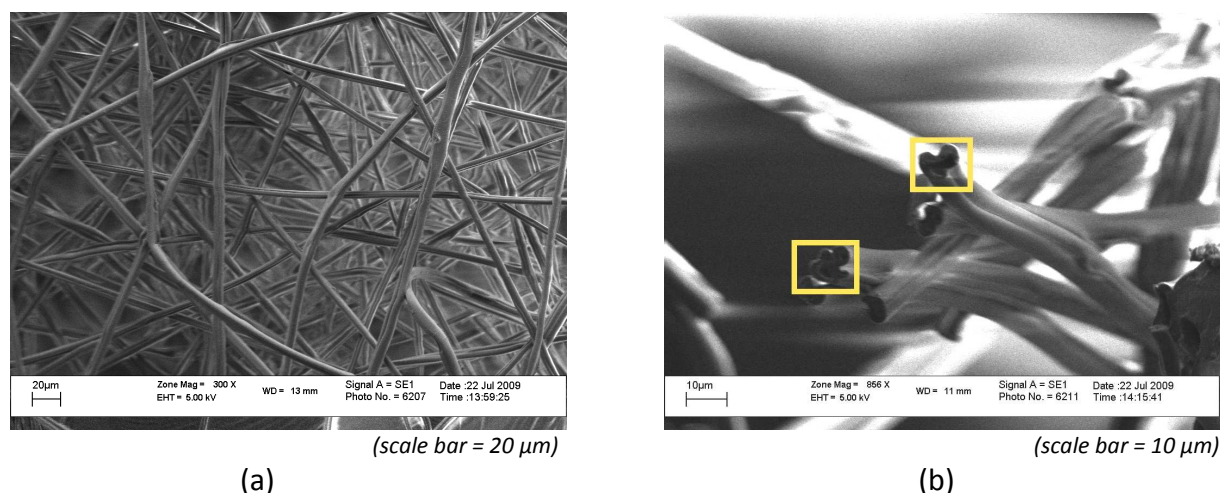


**Figure 5.4** SEM images showing (a) surface morphology and (b) cross-section of thermochromic core-shell fibres (shell solution: 16 wt% PMMA, 3:2 v/v chloroform:ethanol; core liquid: 100:6:1 dodecanol:BPA:CVL, 5:2 v/v dye composite:chloroform).

The core-shell fibres that were produced from the first three shell spinning solutions in Table 5.2 exhibited different extents of bead formation (see Figure 5.1–5.3). Bead formation depends primarily on the shell solution properties. The results of the current experiments are explained below.

Beading was most significant for the fibres produced from the 14 wt% solution in 3:1 v/v chloroform:ethanol. The viscosities of all solutions were high enough to prevent jet breakup<sup>7</sup> and allow fibre formation, but due to the low conductivity of the solutions, the surface tensions were often allowed to dominate.<sup>8</sup> This resulted in bead formation. The effect was the worst for the 14 wt% (3:1 v/v chloroform:ethanol) solution. This shell solution had a relatively low conductivity and, although not the lowest amongst the solutions, the lack of conductivity in combination with a low viscosity (lower viscosity than the 16 wt% in 3:1 v/v chloroform:ethanol solution, which had the lowest conductivity and highest surface tension) caused the surface tension to dominate and allow the most extensive bead formation. Experiments with the 16 wt% (3:1 v/v chloroform:ethanol) solution, which had the lowest conductivity, resulted in wet fibres. The extremely low conductivity of this solution inhibited the whipping action to such an extent that the fibres were not completely dried before reaching the collector and some beads were formed. The 14 wt% (3:2 v/v chloroform:ethanol) solution had the lowest viscosity, but this was compensated for by its slightly higher conductivity that could overcome the surface tension forces and allow the formation of fibres that only exhibited minor beads. This was not considered a major problem. The 16 wt% (3:2 v/v chloroform:ethanol) solution had the optimum combination of surface tension, conductivity and viscosity to produce smooth, bead free fibres. Of all the shell solutions that were tested during the course of this project, this shell solution gave the most stable process that most consistently produced thermochromic fibres with smooth, bead free morphologies.

Both the 14 wt% and 16 wt% PMMA (3:2 v/v chloroform:ethanol) solutions gave satisfactory results but the 16wt% PMMA (3:2 v/v chloroform:ethanol) shell solution was preferred for further analyses because it formed fibres with larger diameters than the 14 wt% PMMA (3:2 v/v chloroform:ethanol) solution (i.e. 6.5–10  $\mu\text{m}$  as opposed to 3.5–6.5 $\mu\text{m}$  for 14 wt% PMMA). Light scattering effects<sup>9,10</sup> could be minimized by the thickest fibres obtained.

Additionally, the experimental processes with 14 wt% PMMA (3:2 v/v chloroform:ethanol) solutions were observed to be more sensitive to slight variations in experimental parameter settings and when these variations occurred, thermochromic fibres were no longer produced. Although not investigated in more detail here, this was possibly caused by the lower viscosity of this shell solution, which failed to fully entrain the core material.

The fibre mats that were formed all exhibited a thermochromic effect. When the fibre mats were placed in the freezer ( $\pm 6$  °C), the blue colour developed. Upon exposure to ambient temperatures of  $\pm 16$ – $25$  °C the fibre mats rapidly lost colour and became white (the colour of a normal PMMA fibre mat). It was observed that the fibre mats did not always redevelop the colour when returned to the freezer. Fibres that were heated to above  $\pm 25$ – $30$  °C before being returned to the freezer redeveloped the blue colour. Those that were only heated to temperatures below  $\pm 20$  °C lost the colour but did not redevelop it upon being returned to the freezer. It was also observed that when fibre mats, which initially became blue when placed in the freezer, were stored in the freezer for more than a day became white even though these samples were held at the low temperature inside the freezer. When these fibres were removed from the freezer, heated to above  $\pm 25$ – $30$  °C and then cooled to  $\pm 6$  °C (in the freezer), the blue colour developed again. These observations were unexpected. The hypothesis was that there could possibly be some chemical or other interference with the BPA–CVL ring-opening reaction in the thermochromic composite in the fibres, which would prevent the development and retention of the coloured state. This interference could possibly be due to a competing interaction between BPA and the PMMA shell.

### 5.2.2 Evaluation of increased BPA content in thermochromic composition

In order to test for a possible competing PMMA–BPA interaction, the BPA content of the thermochromic composite was increased (from 100:6:1 to 100:20:1 and 100:30:1 molar ratios of dodecanol:BPA:CVL) so that there would be an excess of BPA in the core-shell fibres and a CVL–BPA ring-opening reaction would still be possible after some of the BPA had associated with the PMMA shell. If the developed colour became more stable with an increase in BPA, the hypothesis would be supported. The effects that the increased BPA content had on the thermochromic functioning (or lack thereof) of the bulk dyes were evaluated in this section. Coaxial electrospinning experiments, using these dye composites

(dissolved 5:2 v/v in acetone) as core spinning liquids, are also discussed in this section. The thermochromic transition and stability of the colour developed state of the resultant fibres, as well as the differences in the thermochromic transitions of these fibres and the corresponding bulk dyes are discussed and further analyzed in Section 5.3.

The photographs in Figure 5.5 show the thermochromic colour change or lack thereof for the three different dye composites in bulk, at different temperatures. The 100:6:1 ratio gave a fully reversible colour change between colourless and blue as the temperature was raised and lowered above and below the colour switching temperature of approximately 17–24 °C. The 100:20:1 and 100:30:1 molar ratio compositions did not exhibit a clear thermochromic transition. The blue colour became slightly lighter as the temperature was increased, but even at 80 °C both these bulk dye composites retained the blue colour.

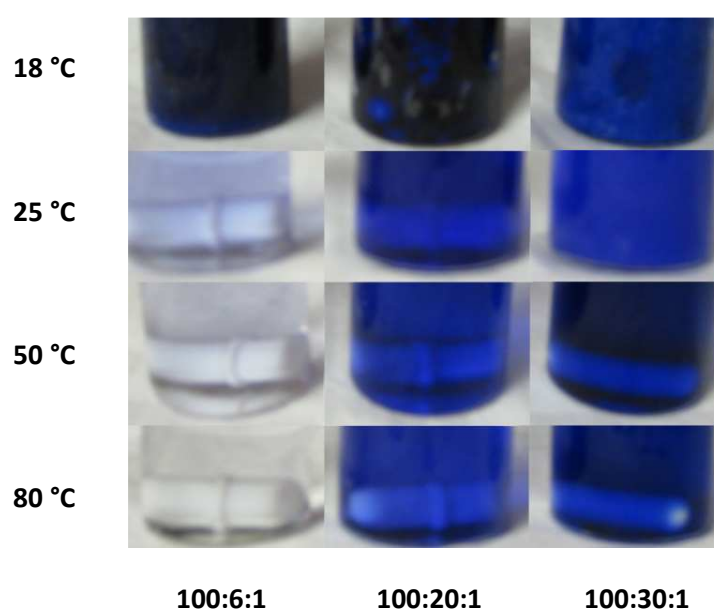


**Figure 5.5** Photographs indicating the colour of the different dye compositions (dodecanol:BPA:CVL molar ratio) in bulk, over a range of temperatures.

This inhibition of the thermochromic transition was caused by the excess BPA that was present in the 100:20:1 and 100:30:1 (molar ratio dodecanol:BPA:CVL) compositions. Above the dodecanol melting temperature, the competing interaction between dodecanol and BPA stopped some of the BPA from developing the ring-opened, coloured state of CVL. At dodecanol:BPA molar ratios of 100:20 and 100:30 however, the molten dodecanol became saturated with BPA and the excess BPA was still available to develop the ring-opened, coloured state of CVL.

As mentioned, the dye composites were dissolved 5:2 v/v in chloroform to be used as core spinning solutions in the production of thermochromic core-shell fibres. The solution properties are given in Table 5.4. The 100:30:1 (molar ratio dodecanol:BPA:CVL) composite did not dissolve completely in the chloroform. During coaxial electrospinning, dispersed particles (probably BPA) settled to the base of the solution vessel (syringe and tubing). The actual input formulation would therefore not have been 100:30:1 (molar ratio) dodecanol:BPA:CVL as it was originally mixed.

**Table 5.4****Thermochromic dye compositions and spinning solution properties**

Molar ratio (Dodecanol:BPA:CVL)	Spinning solution (5:2 v/v dye:chloroform)		
	Conductivity	Viscosity at 20 °C (mPa/s)	Surface tension at 20 °C (mN/m)
100:6:1	Not conductive	6.5	23.1
100:20:1		10	24.2
100:30:1*		11.5	24.9

\* This dye composite was not homogeneous in its molten or dissolved state.

The measured resistivities for the core spinning solutions were infinite (above the scale of the range of the multimeter used). The core solutions were therefore classified as non-conductive. This was mainly due to the low conductivity of chloroform (0.02  $\mu\text{S}/\text{cm}$ ), which formed a large part of these core spinning solutions. The conductivity of the core liquid does not have any impact on core-shell formation,<sup>2</sup> because all electric charges quickly accumulate on the outer surface of the shell solution at the tip of the Taylor cone. Therefore the lack of core solution conductivity did not result in any difficulties during coaxial electrospinning of thermochromic core-shell fibres.

The viscosity of the core liquids was very low. It increased slightly as the amount of BPA in the compositions was increased. It is known from literature that at a very low core solution viscosity (10x less than the shell viscosity), successful core-shell formation can become less likely under certain experimental conditions.<sup>2</sup> This effect was not experienced during coaxial electrospinning of core-shell thermochromic fibres in the current study. It is likely that low

interfacial tension (similar surface tensions) was the main contributing factor to successful core-shell formation in this project.

Coaxial electrospinning experiments with the different thermochromic dye composites were only performed in combination with the 16 wt% PMMA (3:2 v/v chloroform:ethanol) shell solution. The specifications and process parameters of the experiments are given in Table 5.5.

**Table 5.5**

**Process parameters for coaxial electrospinning experiments\* with thermochromic composites of increasing BPA content**

Core composition (v/v)		Flow rate (mL/h)		Voltage (kV)	Tip-to-collector distance (cm)	Temp (°C)	rH (%)
Dodecanol:BPA:CVL	Dye:Chloroform	Shell	Core				
100:6:1	5:2	12	2	17	27	22.5	58
100:20:1	5:2	12	2	17	27	21.4	55
100:30:1	5:2	12	2	17	27	22.9	62

\* A 16 wt% PMMA (3:2 v/v chloroform:ethanol) shell solution was used as shell spinning solution.

Thermochromic core-shell fibres were produced using all three variations of the thermochromic composite. The colour developed state of the 100:20:1 and 100:30:1 dye composite containing fibres, as opposed to the 100:6:1 dye composite containing fibres, was stable (did not disappear after a day or even after 4 months) as long as it was kept in the freezer at  $\pm 6$  °C.

SEM images that show the surface morphologies and cross-section views of these fibres (with 100:20:1 and 100:30:1 thermochromic composite) are given in Figures 5.6 & 5.7 below. The thermochromic fibres produced from the 16 wt% PMMA (3:2 v/v chloroform:ethanol) shell solution and the 100:6:1 thermochromic composite was previously shown in Figure 5.4.



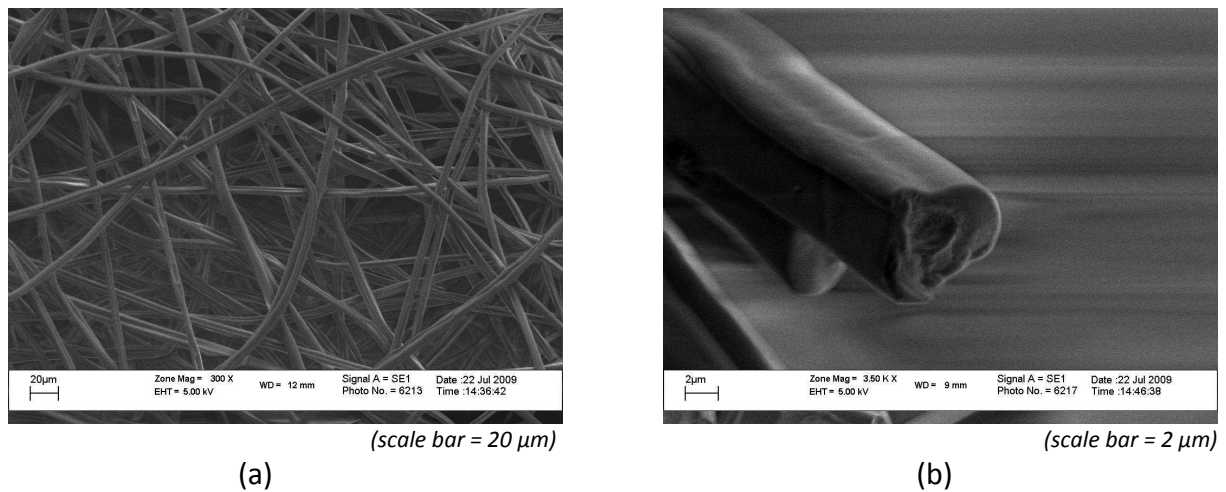


**Figure 5.6** SEM images showing (a) surface morphology and (b) cross-section of thermochromic core-shell fibres (shell solution: 16 wt% PMMA, 3:2 v/v chloroform:ethanol; core liquid: 100:20:1 dodecanol:BPA:CVL, 5:2 v/v dye composite:chloroform).

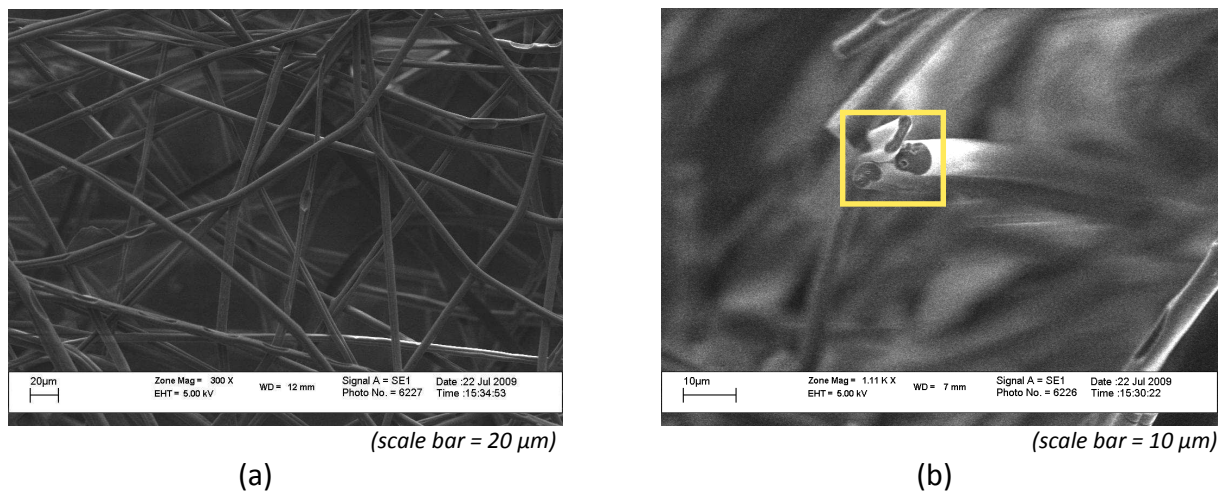


**Figure 5.7** SEM images showing (a) surface morphology and (b) cross-section of thermochromic core-shell fibres (shell solution: 16 wt% PMMA, 3:2 v/v chloroform:ethanol; core liquid: 100:30:1 dodecanol:BPA:CVL, 5:2 v/v dye composite:chloroform).

### 5.3 Analytical investigation of thermochromic transition

This section includes results from TGA, photographic determination of thermochromic transition temperatures and DSC that were used to analyze and explain the thermochromic transitioning of the PMMA thermochromic core-shell fibres (produced using 16 wt% PMMA (3:2 v/v chloroform:ethanol) shell solutions and 100:6:1, 100:20:1 and 100:30:1 thermochromic composites, as discussed in Section 5.2.2). TGA was used to confirm entrainment of all components of the thermochromic dye composite and to evaluate the